

Helicopter Aeroelastic Analysis with Tandem Rotor Blades - Implication on Safety and Operation

Author: Bishnujee Singh, Post Doctor DSc in Engineering Management
Azteca University (Universidad Azteca), Mexico, North America

ABSTRACT

An improvement in energy efficiency and weight reduction in helicopters and the necessity to analyze flexible structural systems that function in a fluid environment necessitates the study of Aeroelasticity. As a result, the study and design process for all aircraft, especially when it comes to reliability and safety standards, is greatly facilitated. This is even though there is a dearth of publicly available research on tandem-rotor helicopters. As part of this study, an aeroelastic extrapolation model for helicopters is constructed using dampers and springs to interconnect various masses. As a result, they can be used to simulate the dynamic properties of a helicopter with tandem-rotor blades. Also, in this work, the mathematical theorem takes into account both applied and intermediate aerodynamic loads. Includes the type of variation that they have. The stick control for the longitudinal cyclic pitch provides the most effective hover performance capabilities in terms of scope for the control augmentation categories studied in this research. Combined with conformist roll control, this allows for a system of velocity control primarily within the horizontal axes to be implemented effectively. Because of the inertial velocity response technology, the pilot's workload and ratings are enhanced. Though it should be mentioned that systems of this sort tend to be susceptible to turbulence. When subjected to turbulence, their overall position holding abilities will deteriorate as the turbulence level increases. A positive position for the command system will be attained by strengthening the system of velocity control, especially for missions involving the exact hover hold. As a whole, the findings of the directed test system evaluation for the drift execution task confirm the validity of the insightful technique for characterizing diverse control expansion modes. RMS (or standard deviation of the pair rotor helicopter's position error) forecasts well the best pilot execution ability for a given increasing framework, according to the inquiry. On the test system, a genuine pilot will reach this level of performance with enough training. Rather than aiming for the "optimal" position, it appears that the pilot chooses a place where the aggregate (pilot-airplane) framework damping level is nearly constant with the pilot acquisition (characterized by 0.35 damping proportion at least position blunder).

Keywords: Helicopter Aeroelastic Analysis Tandem Rotor Blades Safety Operation

1. INTRODUCTION

Due to an increased search for energy-efficient and weight-optimized helicopters as well as the need for an analysis of the flexible structural systems which operate within a fluid setting, the area of Aeroelasticity is unavoidable. It is essential because it facilitates the analysis as well as the design process for all aircraft especially when it comes to both reliability and safety criteria. That is despite the scarcity of adequate research material on tandem-rotor helicopters accessible to the public domain. As far as aircraft faster or sonic speeds are concerned, the focus is put on the model order decrease particularly for the nonlinear and computational aeroelasticity. That involves the use of the Computational Fluid Dynamics (CFD) framework whose embedded boundary is within several computational tools. It is embedded within tools like NX Nastran software. This tool makes it possible to facilitate the failure criteria chiefly the flutter to be appropriately respected as a Limit Cycle Oscillation (LCO). Aeroelasticity encompasses the modeling, the analysis as well as the study of the airplane's external aerodynamic loads. It also involves the study of the nature of their variation and the structural mass and damping characteristics associated with the aircraft (Brown and Line, 2005). Additionally, by engaging relevant research studies that are well beyond this study's material scope, it will be possible for the researchers to undertake further investigations within this exciting aeroelasticity field. The present topics of the research study are highly diversified. Given the enhanced sophistication of the technology applied regarding the systems control, it is quite more common to attack aeroelasticity-related problems through active response control instruments for the relevant flight-control exteriors.

Unlike other rotor-craft and aerofoil shaped aircraft that are famous for civil airborne service applications and thus have got a lot of research material about them much more easily accessible to the public domain, the tandem-rotor helicopter model has got scarcely any material especially about their aeroelastic behavior published in the public domain due to its famous military airborne service applications; which makes the investigation about the precious aeroelastic behavior of the tandem-rotor helicopters very challenging. Finally, the discourses the active Aeroservoelastic solutions as the most reliable and effective remedies to the aircraft's failure behaviors that are associated with aeroelasticity. However, unlike winged aircraft that have specialized control surfaces such as ailerons as functional remedies to their popular divergence, fluttering, and control reversal aeroelastic failure behavior, there are no such functional control surfaces on the tandem-rotor helicopter, thus in this study, we use the appropriately manipulated swash plate actuation to actively counter any failure behavior associated with the aeroelasticity of the tandem-rotor helicopter. Optimal structural configurations of the tandem-rotor helicopter's three body segments for the minimal structural aeroelastic failure were also analyzed and established as aeronautic design preventative remedies for the aeroelastic principle structural failure problem of the tandem-rotor helicopter.

1.1 BACKGROUND

The aeroelastic extrapolation considered within this study entails the derivation of a mathematical model for the helicopter in the form of various masses inter-connected through dampers and springs (Alpman et al., 2004). These are usually applicably manipulated to be able to imitate the dynamic features associated with the structure of a helicopter entailing tandem-rotor blades. In the same manner, the mathematical theorem applicable within this study includes the details relating to the applied as well as interim aerodynamic loads. It also includes the nature or form of their variation. These variations are essential especially when it comes to the prediction of the safety and failure criteria of the helicopter (Light, 1993). This for instance includes the flutter margin as well as their conforming solution fixes like the appropriate determination and implementation of changes to the local structural stiffness and the mass distribution of the helicopter. For that matter, this study will consequently provide a comprehensive discussion of the ideal of the Static Aeroelasticity for the helicopter's mild-speed process range and the concept of the Dynamic Aeroelasticity for harsh-humid meteorological conditions operation and top speed (Bendat & Piersol, 2011). The harsh-humid meteorological conditions considered for this study are the kind where the shockwaves within the atmosphere are highly substantial that it is impossible not to experience nonlinearity (Harris, 2014). In the same manner, this study involves an analytical examination of the related problems for both the Dynamic Aeroelastic scientific and Static Aeroelastic models regarding a helicopter that has tandem-rotor blades (Cao et al., 2004). Some of these elements will include divergence and control reversal as well as flutter for control surfaces correspondingly. It will also include a determination of their analytical solutions like the proper adjustment of the stiffness, the mass as well as Helicopter aerodynamics. This is to be achieved through Aero-servoelasticity procedures as well as through the applicable placement of the mass balances attached on the control surfaces to contain their flutter. The study will finally provide a detailed discussion of the modeling as well as the implementation of the Automatic closed-loop mechanisms for feedback control. These will be explored as potential remedies not just controlling but also potentially fully overwhelming the associated aeroelasticity problems like divergence, buffeting, control reversal as well as fluttering. That is essential since it would help or aid the achievement of the preferred weight-improved as well as energy-efficient airplane designs. All of this would be possible through the optimum containment of the Helicopter parts premature failure.

1.2 CONTEXT

Unlike aerofoil-shaped aircrafts such as fighter jets or aircraft with aerofoil parts such as wings that use aerofoils lift force for flight and most importantly have a lot of research material about their aeroelastic behavior easily accessible in the public domain, the tandem-rotor helicopter uniquely relies entirely on its rotor blades for lift force during flight and most importantly has got hardly any trace of research material about its aeroelastic behavior in the public domain. This study thus aims to analytically model and establish a relation between the nature and variation of the external aerodynamic environment of a helicopter with tandem-rotor blades and its internal structural dynamics characteristics which would be modeled as a series of masses connected by springs and dampers. This will in turn enable the prediction and thus anticipation, through analytic modelling and estimation of acting loads and changes of stiffness and deformation of the sections in and across the helicopter; of aerodynamic safety and failure criteria such as the pitching velocity margin, rolling velocity margin and the margin of the safe payload eccentricity in the fuselage and also enable suggest possible test fixes during the modelling and analysis of the aeroelasticity of the helicopter. The study also aims to analyze the effect of the variation of the structural flexibility of the segments of the tandem-rotor helicopter and the distribution of loads in the body structure of the helicopter. This study will thus contribute to the rare research material about the aeroelastic behavior of tandem-rotor helicopters accessible to the public domain.

1.3 PURPOSES

- To model and relate the nature and variation of the external aerodynamic environment of a helicopter with tandem-rotor blades and its internal dynamics characteristics.
- To establish the safety and failure criteria of the helicopter with tandem-rotor blades such as divergence margin, flutter margin and also suggest their possible fixes.
- To perform numerical model simulations and Computational Fluid Dynamics (CFD) Finite Element Model simulation of the aeroelasticity of the helicopter with tandem-rotor blades and also make comparisons of the results and analyses of the two predictive methods.
- To numerically illustrate how, the possible solutions to aeroelastic failure criteria can be applied by appropriate adjustment of the on-board masses and sections stiffness.
- To critically determine the modelling as well as the application of optimal automated closed-loop mechanisms of feedback control as potential techniques for the achievement of the desired energy efficient and weight-optimized helicopter designs.
- To analyze the effect of the variation of the structural flexibility of the segments of the tandem-rotor helicopter and the distribution of loads in the body structure of the helicopter.

2. LITERATURE REVIEW

The tandem-rotor designs are highly in most cases applicable in cases of heavy-lift helicopters. This is attributed to the fact that, just like the coaxial design, it is possible to use all of the rotor power when undertaking a useful lift. It should however be mentioned that just like the coaxial design, the power that is induced by the partially overlapping tandem-rotor s is usually higher when compared to the power generated by two isolated rotors. That could be attributed to the fact that one of the rotors is required to operate within the slipstream for the other. Such an operation creates a situation where there is an inducement of much higher power for the thrust of the same magnitude. When undertaking a literature research review of the tandem-rotor blades, it is significant to consider several historical and equally important facts. It should be noted that the Wright brothers did fly in 1903 while Sikorsky did build and pioneered the flying of the very first operative helicopter, (R-4) in the year 1942. This particular Helicopter was three-bladed and included 11.6 m in terms of the rotor diameter. The Helicopter was powered by an engine of 185-hp. To that end, there is an initial gap extending to nearly forty years between the rotary wing and the fixed-wing technologies. It is henceforth hardly surprising that various problems relating to rotary-wings and more specifically those which concern unstable aerodynamics are not yet appropriately understood (Wachspress, and Quackenbush, 2006). Moreover, the above situation is complicated further by the sophistication of the vehicle especially in comparison to the fixed-wing aircraft. The field of

Rotor Blades has been one of the most progressive as far the concept of aeroelasticity is concerned. That has especially been the case over the past more than thirty years. Such a dynamic research undertaking has been able to generate a significant amount of literature published in an attempt to appropriately understand Aeroelasticity in Tandem-rotor Blades. The review papers do provide a historical viewpoint particularly in light of the amount of evolution that continues to be experienced within the field (13). Loewy (11) is accredited for being one of the first scholars to provide a substantial review of the aeroelastic problems especially concerning the rotary-wing dynamic. He did provide a considerable and detailed review regarding a huge range of dynamic problems. Dat (2) did equally provide a review although limited in nature placing further emphasis on unsteady aerodynamics role as well as the problems of vibration that raise during forwarding flight. Friedmann did also provide another comprehensive review concerning rotary-wing aeroelasticity. In his review, he did provide a rather comprehensive discussion concerning the flap-lag as well as coupled flap-lag-torsion concerns. The review did focus on both the problems associated with forwarding flight and in hover. Much emphasis was placed on the intrinsically nonlinear form of the stability problem concerning the hingeless-blade aeroelasticity. The nonlinearities under consideration included the geometrical nonlinearities and that was because moderate blade deflections were involved or given due consideration. In the same manner, the investigation included an analysis of the role played by unsteady aerodynamics (Wieslaw, et al. 2004). This analysis further included the dynamic stall and an examination of the management of problems of nonlinear aeroelasticity within the forward flight. The review also included Rotary-Wing Aeroelasticity finite element solutions to the associated problems. It also included an analysis of the management of the coupled rotor-fuselage associated problems. In the same manner, Ormiston (12) engaged in the discussion of the concept of aeroelasticity for the bearingless and hingeless rotors within the hover and this he did from both the theoretical and experimental perspective.

As much as there is no doubting the role played by aeroelastic stability especially when it comes to the design rotor systems, there is an even more critical role played by the aeroelastic response problem and the dynamic loads' prediction. Subsequently, Loewy and Reichert did also provide an exclusive review of the vibration as well as the control mechanisms within the rotorcraft. These papers were mainly focused on the vibrations associated with the rotor's aeroelastic response. They did put particular emphasis on the several passive, active as well as semi-active devices for the control of the vibrations of such nature. Johnson undertook the publication of a broad review paper focused on both aspects of vibration and aeroelastic stability problems associated with the more advanced rotor systems. In a follow-up to his previously reviewed papers, Friedman did undertake the discussion of the fundamental developments which occurred in the period between 1983 and 1987 where the emphasis was put on new methods used in the formulation of aeroelastic problems. It also included an emphasis on the advancement in the handling of the problems of aeroelasticity, especially within the forward flight. In the same manner, the discussion included an analysis of the coupled rotor-fuselage, the modeling of the structural blade, structural optimization as well as the application of active control to reduce vibration and also for stability augmentation. Ormiston, Warmbrodt, Hodges, and Peters did prepare an all-inclusive report containing a detailed review of the experimental and theoretical development relating to the aeromechanical and aeroelastic stability of helicopters as well as the tilt-rotor helicopter between the 1967 and 1987 period. Rather later, important developments and ideas across four specific areas including geometric nonlinearities role in RWA, composite blades structural modeling, coupled rotor-fuselage aeromechanical problems and their active control, as well as higher harmonic control (HHC) for vibration reduction in rotorcraft, were rendered consideration by Friedman. In the same manner, Chopra did undertake a review concerning the technological advancements concerning helicopter aeromechanical stability. For this review, major emphasis was put on the pitch-flap, coupled flap-lag-torsion, flap-lag, air as well as ground resonance (Yagiz and Asian, 2004). In the same manner, this detailed paper did also include the advancements within the field of aeromechanical analysis of composite rotors, bearingless as well as circulation control. On top of the several papers focused on the subject of this particular review, the topic has also been rendered further discussion in several books. The most notable of these books is Johnson's 1980 monumental exposition on the concept of helicopter theory. The book entails an extensive, comprehensive, and equally essential material on the concepts of aerodynamic, dynamic as well as mathematical facets concerning dynamics, aeroelasticity as well as rotary wing aerodynamics. In the same manner, Leishman, (2000) did devote a huge effort to his book explaining the elements of helicopter aerodynamics. This book includes a discussion regarding the appropriate treatment of the unsteady aerodynamics, the dynamic stall as well as the rotor wake models.

Kunz and Johnson did compile a brief history of the concept of comprehensive rotor codes. They also devoted time towards an investigation of their development across a given period. They assert that Finite Element (FE) systems use beam elements as well as the endless one-dimensional beam model in the development of the structural models for various codes. It was highlighted that second-generation inclusive codes make use of the lifting line aerodynamics theory. The models above included the use of a two-dimensional lookup tabletop for aerofoil features. The calculation of the rotor inflow was done through the use of a free wake model. This particular model evolves over a given period and eventually captures the interaction taking place between varying vortices. Such types of inflow models are computationally costly and usually necessitate initialization from linear or uniform inflow models as well as models of the prescribed wake nature. Even though there is a need for the initialization, it is asserted that the expense devoted for computational purposes continues to be so exorbitant for some simulations like the aeroelastic stability examination where there are need models of lower fidelity inflow.

Park and Kee did undertake a direct code to code assessment regarding the CAMRAD II and DYMORE II stability when modeling a rotor in downward flight. Regardless of CAMRAD II's more ostentatious structural as well as aerodynamic models, it could only be able to offer irregular and marginal performance enhancements. The majority of these were simply down to the fact that MORE II was not able to model the Blade Vortex Interaction (BVI) effects. This can be explained by the fact that the BVI rate of recurrence is usually too high especially for the elastic vibrations to sensitively respond to them. It had been projected that CAMRAD II's ability to be in a position of capturing such a phenomenon would instigate only small or insignificant changes in the overall results. Even though several efforts were made by the comprehensive rotor codes in an attempt to capture the entire physical occurrences the rotor experienced, they don't always present appropriate alternatives within an environment of the research environment. Because of the characteristic novelty related to various research aspects, it is not always possible for the comprehensive rotor codes to capture the impacts of the concept under investigation. Stepniewski, (1955) provides an extensive discussion of the tandem-rotor problem. The ideas associated with the overlapping areas usually provide a basis through which to analyze overlapping rotors, particularly when using the momentum theory perspective. It is assumed that the rotors do not have any vertical spacing and this is shown in Case 1. In the figure below, it is illustrated that the use of the geometry of the problem, the following can be attained;

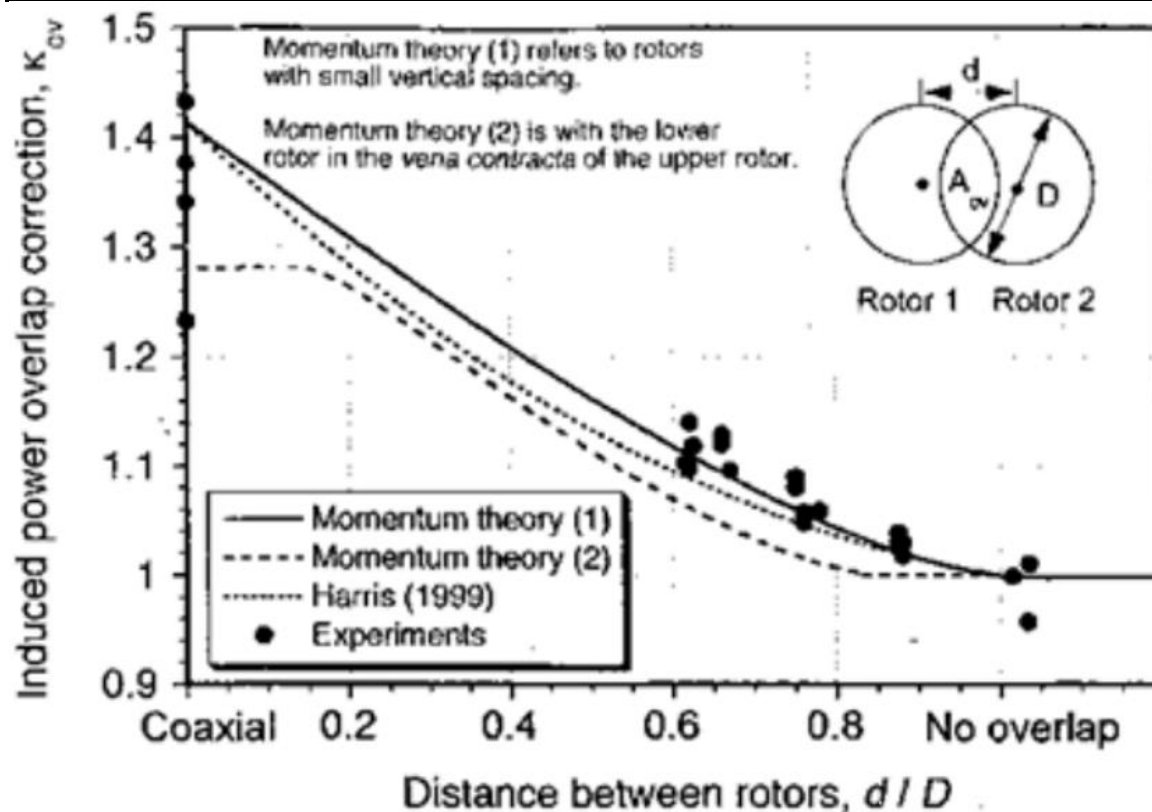


Figure 1: the use of the geometry of the problem

There is a relative scarcity of relevant data concerning tandem-rotor systems, especially when compared to data concerned with a single rotor. Although, the obtainable results were collected by Stepniewski & Keys, (1984). They collected the data from a variety of sources and some of these included results relating to Sweet, (1960) as well as Boeing-Vertol experimentations. It is noted from the data collected that designs of the tandem-rotor nature like the CH-46 as well as CH-47 models have an approximate distance of 0.65 between rotors (d/D). Such a distance allows for an induced correction of the power overlap (K/cov) amounting to nearly 1.13. In terms of the forward flight though, it is observed that the tandem and coaxial systems look as if to act very much in the same manner as two single rotors though with one of the rotors operating in the fully advanced downwash of the other rotor.

A. PRIORITIZING HOVER FLIGHT FOR AEROELASTIC ANALYSIS

Some of the possible applications associated with huge helicopters and especially those fitted with external load capabilities include container stacking on ships or trucks, the modular construction of houses as well as placement of a bridge. There is a requirement for a high degree of precision particularly from the helicopter if operations of this nature would stand any chance of being performed in a manner that is both safe and timely. The capacity of a helicopter to be able to hover precisely in line with a fixed point of reference is majorly dependent on the inertial as well as aerodynamic features possessed by the aircraft. It's also dependent on the overall design of the control system for the automatic flight as well as the rotor response as well as the system from flight control. In the present times, there hasn't been any particular experience involving huge helicopters 1 (80,000 pounds and larger gross weights). In the event of the existence of such an experience, it would be possible to ascertain their overall potential and the limitations in terms of their capabilities throughout the precise hover hold assignments. With an increase in the size of the helicopter so does the size of the rotors required since their operational rpm is required to be lower. Such an operational arrangement ensures that there are lower, rotor-based frequencies. This has the notable potential of altering the basic responses which are usually experienced within the current medium-gross weight helicopters. Wholesome extrapolation to a size that is quite bigger must keep into consideration that there is a whole lot of unknown factors having an impact on the flying capabilities (Whittle, 2015). That, therefore, makes it essential that there should be a much closer analytical as well as simulator evaluation for the performance of an aircraft of such nature, particularly when undertaking the accurate hover hold undertakings. Questions regarding the size of the aircraft do significantly impact the ability of the pilot to undertake the performance of such missions. It is henceforth essential that they are subjected to appropriate investigation, especially during the analysis and simulations. The pilot-assist requirements of the control system and the automatic hover hold functions must not just be evaluated but also synthesized (Benjamin et al., 2012). There should also be an establishment of the sensitivity of such helicopters to the levels of turbulence to ensure that the all-weather operational proficiency is ascertained. There should also be a relevant investigation of the acceleration environment, especially at the crew station. Such an operation is essential because the cockpit position in line with the center of gravity of the aircraft will increase in correspondence with the size of the helicopter size. Moreover, huge levels of acceleration will cause interference in the accuracy of the piloting task. The weather and geographic conditions could determine the properties of atmospheric turbulence. It is notable though that the correlation functions associated with atmospheric turbulence in several conditions are, except for a constant multiplier, extraordinarily comparable to one other. There only difference is basically in terms of intensity.

B. AEROELASTIC DESIGN CRITERIA FOR TANDEM-ROTOR BLADE HELICOPTER

It is possible to compute the possible amount of times that the dynamic stresses within the structure could indeed exceed a particular level of stress. Information of such nature is highly useful especially in the design of the aircraft in consideration of the service life as well as the levels of fatigue. To be in a position of obtaining thorough information concerning the dynamic stresses probability distribution, there would be a need to undertake a computation for higher-order correlation functions (Elan, 2015). Calculations of such nature are in most cases quite elaborate (Mazelsky). In the practical sense though, it is always possible to obtain ideas concerning the probability distribution through experimental means (Ramaswamy, et al., 2007). They can also be obtained through knowledge regarding the mean value as well as the root mean square deviation associated with the random variable. These have always proved to be sufficient enough especially in the world of engineering. It should also be noted that the notion of statistical treatment is hardly a new one. Lord Rayleigh is accredited with having pioneered the application of the theory of statistics to the concept of dynamics. It is his work that forms the foundations upon which Taylor and von Karman's turbulence theory is based. It is this work that forms the groundwork for the Brownian motion theory of noise within the acoustical and electric systems and some of the aspects of astrophysics. The other theory is the stationary time series mathematical theory formulated by Wiener and Kintchine. This particular theory is concerned with the form of analysis first developed by Lin. In the same manner, theory's application to aeroelastic complications was unearthed by Liepmann. The functions of the major concern in this study are major time-based and mainly depend on chance. These kinds of functions are known as stochastic processes. A stochastic procedure is quite similar to a definite function where it is asserted that a random variable hardly possesses a definite number. While an ensemble of a random variable could be deemed to be a result of observation for an unplanned experiment, an ensemble relating to a stochastic procedure must be defined as a huge number of experimentations undertaken within conditions of the same nature which each of the experiments does provide a time function (Goulos et al., 2012). The use of the stochastic process theory to problems of dynamic nature raises several fundamental concerns regarding the structural design philosophy (Loewy, 1984). It is noted though that it has been successfully applied in the fields of engineering seismology, gust quantifications, 8-41~8-43 fatigue-life research, landing-impact loads, 870 as well as rough-water operations for seaplanes, 8-74~8-78, etc. In the majority of such applications, the possibility of considering the random procedure as stationary is nonexistent.

The tandem-rotor helicopters are associated with two huge horizontally assembled rotors. These are mounted in front of one another. In the current times, such a form of configuration has majorly been used or applied for the helicopters used in the transportation of huge cargo. The tandem-rotor designs have been known to attain yaw through the application of opposite right and left cyclic to every single rotor. That, therefore, does effectively pull the helicopters both ends in the opposite directions. To be in a position of achieving pitch, there is an application of the reverse collective to each of the rotors. That consequently leads to a decrease in the lift generated at one of the ends while it causes an increase in the lift for the opposite end. That therefore successfully tilts the helicopter back and forward. It is essential to also note that Tandem-rotor helicopters do however make use of counter-rotating rotors where each of them can cancel out each other's torque. In that sense, therefore, all the energy or power generated from the engines can be applicable at the point of the lift. On the other hand, a helicopter that makes use of a single rotor makes use of some of the engine power to be in a position of countering the torque. The best alternative for that is to undertake a mounting of two rotors in what can be described as a coaxial configuration. A transmission that ensures that the two rotors are linked is used and it should be done in such a way that there is a synchronization of the rotors. It should be done in such a manner that they should not hit each other even in the event of failure of the engine. Nicolas Florin was the first person to undertake a successful development or construction of a tandem-rotor helicopter and this was accomplished in 1927. A tandem-rotor structure or system is advantageous in the sense that it is associated with a larger range in terms of the center of gravity (Cribbs et al.). Equally, it is also known to have a good longitudinal steadiness which makes it possible for it to support or hold bigger weight with shorter blades. This is possible because they are usually two sets. It is important to note though that the rear rotor does work in the front rotor's aerodynamic shadow which diminishes its efficiency. To minimize this kind of loss, there would be a need to the extent or increase the distance existing between the system's two-rotor hubs and through the elevation of the hubs over each other. It is also known that tandem-rotor helicopters do not usually require much power to hover and attain low speed in terms of flight especially in comparison to single rotor helicopters. Notably, though, both of these configurations characteristically necessitate the same amount of power to be in a position of achieving flights of high speed. In terms of some of the problems associated with the tandem-rotor system, it has been noted that they have a complex transmission system and that usually requires two large rotors. The other shortcoming is their tendency to be associated with a lower disk load which is usually not the case with single rotor helicopters.

The tandem-rotor helicopters are associated with two huge horizontally assembled rotors. These are mounted in front of one another. In the current times, such a form of configuration has majorly been used or applied for the helicopters used in the transportation of huge cargo. The tandem-rotor designs have been known to attain yaw through the application of opposite right and left cyclic to every single rotor. That, therefore, does effectively pull the helicopters both ends in the opposite directions. To be in a position of achieving pitch, there is an application of the reverse collective to each of the rotors. That consequently leads to a decrease in the lift generated at one of the ends while it causes an increase in the lift for the opposite end. That therefore successfully tilts the helicopter back and forward. It is essential to also note that Tandem-rotor helicopters do however make use of counter-rotating rotors where each of them can cancel out each other's torque. In that sense, therefore, all the energy or power generated from the engines can be applicable at the point of the lift. On the other hand, a helicopter that makes use of a single rotor makes use of some of the engine power to be in a position of countering the torque. The best alternative for that is to undertake a mounting of two rotors in what can be described as a coaxial configuration. A transmission that ensures that the two rotors are linked is used and it should be done in such a way that there is a synchronization of the rotors. It should be done in such a manner that they should not hit each other even in the event of failure of the engine. Nicolas Florin was the first person to undertake a successful development or construction of a tandem-rotor helicopter and this was accomplished in 1927. A tandem-rotor structure or system is advantageous in the sense that it is associated with a larger range in terms of the center of gravity (Cribbs et al.). Equally, it is also known to have a good longitudinal steadiness which makes it possible for it to support or hold bigger weight with shorter blades. This is possible because they are usually two sets. It is important to note though that the rear rotor does work in the front rotor's aerodynamic shadow which diminishes its efficiency. To minimize this kind of loss, there would be a need to extent or increase the distance existing between the system's two-rotor hubs and through the elevation of the hubs over each other. It is also known that tandem-rotor helicopters do not usually require much power to hover and attain low speed in terms of flight especially in comparison to single rotor helicopters. Notably, though, both of these configurations characteristically necessitate the same amount of power to be in a position of achieving flights of high speed. In terms of some of the problems associated with the tandem-rotor system, it has been noted

that they have a complex transmission system and that usually requires two large rotors. The other shortcoming is their tendency to be associated with a lower disk load which is usually not the case with single rotor helicopters.



Figure 2: A tandem-rotor helicopter

The majority of the most recent advances have their basis on the most current comprehension of such subjects as limit cycle oscillations. This is attributed to the fact there is an involvement of structural nonlinearities such as free play as well as fluid nonlinearities related to unsteady separated flow. For that matter, this study is focused on the discourses of the interaction that exists between forces generated from the aerodynamic flow as well as an elastic structure deformation within the aeroelastic model for the tandem-rotor airplane. These forces are associated with the production of deformation although the structural deformation does, in turn, change the aerodynamic forces. The kind of response attained from deformation and force causes a series of dynamic responses of the structure and fluid such as flutter, chaos, and limit cycle oscillations.

i. Aeroelasticity in tandem-rotor helicopters

The term aeroelasticity is used to designate a study field focused on the interaction existing between the distortion of an elastic assembly within the air stream and the consequent aerodynamic force. Relating to the above, the concept of structural dynamics can be defined as entailing the study of dynamic properties associated with continuous elastic alignments. It is such configurations that provide a means through which to analytically represent the deformed shape of a flight vehicle at any given moment in time (Smith, et al., 1996). To put it differently, it is associated with the vibration as well as the dynamic feedbacks attributed to the structural elements (Mestrinho, et al. 2011). It can henceforth be considered to be a component of aeroelasticity which is a field of investigation that focuses on the interaction that takes place between the distortion of the elastic structure within the air stream and the resultant aerodynamic force. The structural dynamics field is focused on addressing the dynamic deformation comportment of the continuous structural alignments (Hahn et al., 2007). Generally, it is worth noting that these load-deflection connections are nonlinear and that the deflections do not necessarily need to be small. For this particular section of the study, our attention shall be restricted to linearly elastic classifications experiencing small deflections. That shall be the case to facilitate tractable and equally analytical solutions. It is believed that such classifications provide the best alternative because they epitomize most of the operations related to flight flight-vehicle. It is important though to ensure that a certain level of geometrically nonlinear models are incorporated. This is essential because it would help to facilitate the generation of linear equations for the membranes, strings, helicopter blades, and turbine blades as well as flexible rods within rotational spacecraft. It is indeed not possible to attain linear motion equations for the free string vibration. That is particularly not possible without undertaking the initial consideration as well as the consequent careful exclusion of nonlinearities. It is important to state that both aeroelasticity and structural dynamics are constructed on the foundation's structural mechanics and dynamics. The interdisciplinary form of the field is most suitably illustrated in the figure below.

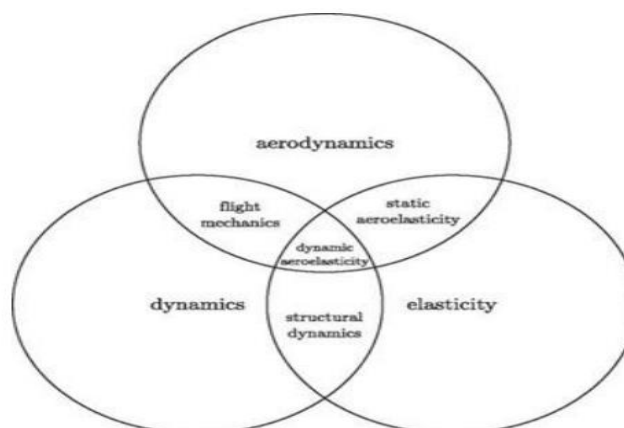


Figure 3: Schematic of the interdisciplinary of the field of aeroelasticity

The figure above has its origins from the 1940's work of Professor A. R. Collar. The triangle is a depiction of the interactions occurring amongst the three areas of aerodynamics, elasticity, and dynamics. It is provided for by the classical aerodynamic models that it is possible to predict the forces taking action on a body assuming a specific form. By using elasticity, it is possible to predict an elastic body's shape especially when it is subjected to a specific load. Dynamics do introduce the impact resulting from the inertial forces. By acquiring knowledge regarding elementary aerodynamics, elasticity, and dynamics, it is possible for students to ably investigate problems where there is an interaction of two or extra phenomena of that nature. In the same manner, the flight mechanics field is concerned with the interaction that takes place between dynamics and aerodynamics. Given their importance in the systems of aerospace design, these disciplines are also highly relevant for aeronautics or aeronautical studies. It is within the field of aeroelasticity that one can figure out the loads are dependent on the deformation while the deformation is dependent on the loads. For that matter, an erstwhile study concerning the three principal disciplines must be undertaken before engaging in an aeroelasticity investigation. Furthermore, it is important to undertake a study in structural dynamics to aid the process of developing concepts that are essential in the resolution of problems relating to aeroelasticity like modal depiction. It is important to keep into consideration the phenomena of aeroelastic has historically significant importance in the field of powered flight.

Formerly in 1903, Samuel Langley attempted to attain powered flight from a houseboat top located on the Potomac River. It is notable though that his efforts did not end well given he failed with his experiment catastrophically. The wings failed and this was attributed to their being overloaded and being overly flexible. It is was common for the occurrence of such aeroelastic phenomena and this also included torsional divergence. These were principal elements especially as far the biplane design predominance was concerned at least until the early years of the 1930s. Their predominance ceased with the introduction of the "stressed-skin" metal structural alignments. Their introduction was meant to provide sufficient torsional toughness for the monoplanes. The phenomenon of Aeroelastic is always evident in the day-to-day operations of nature. It can be observed in the day-to-day natural occurrences like the oscillation of trees during windy conditions, the vibrating sound made by the Venetian blinds also in the windy conditions. Dynamics make up some of the broadest aeroelastic phenomena also it should be noted that static aeroelastic occurrences are equally fundamental (Seddon and Newman, 2011). It is possible for aeroelastic as well as structural-dynamic occurrences to result in what can easily be hazardous static as well as dynamic instabilities and deformations. It is for that reason that their importance in terms of the applicable consequences with major aspects of technology can hardly be ignored. This is more so when the concern extends to the design of modern space vehicles and aircraft especially when both of them are associated with the demand for structures of extremely lightweight nature. To solve majority of the structural aeroelasticity and dynamics necessitates simple and basic requirements which include the attainment of operationally consistent and physically prime systems. In the same manner, Aeroelastic phenomena is of significance importance especially in terms of the role it plays when it comes to turbo machinery, converters of wind-energy and civil-engineering structures. It is also highly useful especially when it comes to the musical instruments' sound generation process. The classification of the Aeroelastic problems could be done on the basis of stability as well as the categorical responses. Even if nonlinear equations do attempt to provide a representation of the reality, it is evidently clear that the analytical results associated with the nonlinear calculations are substantially problematical.

While aerospace automobiles are being designed, the remarkable aeroelastic feature can cause a complete band of conduct from being gentle to disastrous. In proximity to the gentle part of the band, the pilot and the passenger do not feel comfortable. The microscopic level of the aircraft is spoilt as one progresses from the gentle end proximity to the steady-state as well as the fleeting vibrations. At the disastrous end of the band, the aeroelastic variabilities can swiftly spoil the aircraft causing the death of people instantly. The aerospace engineers ought to work on the aeroelastic challenges that are static, that is to say, challenges in which the inertia forces do not have a substantial impact. However, the aerospace challenges faced can also be caused by the inertia forces. Small-deformation concepts can be applied in the process of evaluating some of the remarkable aerospace problems by engineers. Aeroelastic phenomena may however greatly impact the efficiency of the aircraft, either negatively, or positively. The phenomena can as well define the efficiency of the control surfaces installed by the engineers to determine whether they carry out the functions for which they were installed. Therefore, these studies play a vital role in aerospace technology in various ways.

While space cars and aircraft are being designed today, emphasis is put on the need for the final product to be light in weight. When a lightweight vehicle is achieved, various aerospace problems are solved as the main target is obtaining a system that has high reliability in its operation and is structurally functional. Other fields in which aeroelastic phenomena are applicable and considered to be of great importance are conversion of wind energy, generating sound from music equipment, and generation of electricity in turbo machinery. The biggest challenge faced in the aerospace industry is the instability of aircraft. Given that the structural members of the aircraft have the elastic modulus that aerodynamic forces strongly rely on, these forces can easily subdue the elastic re-establishing forces in the aircraft. In this circumstance, if the inertial forces pose no or less effect, the situation is called divergence or a static-aeroelastic instability. However, if the inertia forces have an impact, it causes a dynamic instability in the aircraft, that is to say, a flutter. Flutters are not frequent challenges, especially in the tandem-rotor jet.

Studying the response of the aircraft during a flight is done in other areas of aeroelasticity. In static-aeroelasticity, feedback challenges of the aircraft comprise of a particular occurrence in which the forces of inertia don't affect its movement. One therefore ought to anticipate the lift caused by the aircraft which has a specific conformation at a particular angle of attack. One can also examine the greatest load factor that can be maintained by the aircraft. All these challenges can be solved by applying linear analysis. During the analysis of the linear challenges faced in aeroelastic feedback of the aircraft, the challenges are considered complementary in mathematics. Thus variability can be anticipated during the examinations in which standardized equations have significant solutions. However, feedback challenges in aircraft are mainly founded on the solution of non-homogeneous equations. At the point when the aircraft system turns into unstable, non-homogenous equation solutions terminate their existence. The homogenous equivalences and the surface circumstances related to a steady configuration create an ignorable solution.

ii. The ground and flight test validation tools in Aero elasticity as used in Aircraft

Experiments have been conducted specifically to equip the ability to denote the real time experiments and measurement in regards to the quantity of fuel, the speed of plane, number of mach, factors in regards to the load, altitude and control of deflections on the surface. The

Airplane is made with accelerators, vibration test at the ground and the strain gage. And the elevators with ailerons are ran by unique actuators that are have its special purpose to operate over varying frequency range. Before, identification of relevant modes is done by running actuation frequency, and measurement of impulses of command to mitigate response to step.

iii. Taxi/ Ground roll measurements

The Taxi measurement validates the beginning insight to into a tandem-rotor . A sparingly rough runway excites the plane; the flight is covered at the lowest speed in a relatively low attitude. Before measurement on the turbulence of the air is conducted, analysis on the PSD and the FFT must be done. The results must match with the prediction analysis and then the speed is tested . If the result match with the analysis then the actuators could be started following the frequency of the flutter then PSD and the FFT analysis is then conducted in regards to the response(Nirmitt, 2014). If the theoretical predictions are matching with the damping measurement, actuators are activated for the command. After the step up command, the response is analyzed if it is in line with the measurement. When successful the data is collected and stored in ou – g-g diagram form. Then you can go ahead to conduct to logically conduct work tandem-rotor on the outlook deformation of the aircraft. Note that this only done if the aero elastic behavior is at zero speeds, if it doesn't the test is stopped and adjusted until fully correct or even use the computational model until an agreement is reached. So finally if your results are harmonized to an agreement, then the aircraft is free to fly.

iv. Flight Testing

In the flight test, the helicopter is taken off and flew in a very low speed in a place of low altitude while leveling the fight. In the test the flight rotor and the turbulence of the air with internal load structure is measured. Still also the PSD analysis and FFD analysis is conducted. Determination on whether the results are matching with the prediction analyses of the test speed. The actuators can be activated to command the impulses, only if the prediction is matching with the analyses. After we correlate the existence of sufficient damping. If the results match with the analyzed information, then the next step would be activation of the actuators of the tandem-rotor of the aircrafts body on deformation frequency and also conduct both the PSD with FFT analyses on responses . And now when the measurements on damping are corresponding with the predictions of the developed theory, then the next step would be activating the actuators to command speed, and hence determining if the responses are matching with the analyzed information. After doing these then the data is collected and stored in the U- g –g' form diagram. Note that these stages can only be reached only if there is a reasonable agreement between the analyzed information and thence you can go ahead to conduct Manoeuvre following correlating load factors in the same speed and altitude. In every maneuver, activation of the actuators for command of specified impulses to check if sufficient damping is present; and if it does exist, we can get on to add its load factor until the specified setoff load factors are completed and test the flight envelope.

When the predictions are computed and come in harmony with the results arrived from each stage, then the speed of the flight can be increased but on the same altitude, since it is safe to go in a high speed for example can be increased by 25 knots. On reaching the particular stage, all the steps described above can repeated and still data is collected and stored u-g-g form diagram. The speed is cautiously and increased systematically until its maximum is reached, while observing each increment critically so as to validate each knot increment. Still on the same way, the altitude can be raised systematically until the maximum is reached and then re-do regimen. You can stop reducing the speed and observe the 1st speed that is safer if any of the following three things occurs:

- a) If there is a decrease in the middle damping co-efficiency lower than the recommended value i.e in civil planes it's 5%.
- b) Divergence of oscillations in any measurement (at least one divergence) and increases over the recommended limit.
- c) And finally if the coefficient that is dominant changes from the estimated value.

It has been witnessed that the tandem-rotor helicopter's body structural deformation analyses highly look at the studies developed theoretically. Therefore, theory plays a key role in the analyses and ground testing of a helicopter.

A theoretical framework is a key tool for making analyses and affirming a decision in regards to the condition of the flight and the configuration. Experiments on Ground vibration is a tool developed to tune the dynamic structure analyses to develop very correct modal structures, and an experiment on wind tunnels is used to adjust aerodynamic codes that are not accurate. According to civil analyses, aero-elasticity flight trials have proven to be very dangerous. The actual measurement (Real-time) with the different techniques of actuating aids in estimating the damping in the tandem-rotor of aircraft at different speeds, altitude with the load factor of the limit, and shifting its position following a lot of cautions. Experiments on the ground, analysis, with flight testing always work correspondingly to conclude a perfect clearance for the aircraft flight without any failure circumstances on aeroelasticity; the three factors of experiments and analyses are key to a successful flight during testing.

v. Ground Vibration testing

The major reason for conducting experimental dynamic testing at ground is to determine the correct frequency and shape structure of a clear tandem-rotor Helicopter with massive strain gauges with accelerometers at the borders in the tip of the end, nose body segments, and fuselage. Tandem-rotor aircraft is put under a soft support to support the aircrafts structural dynamic freely. The shakers (Vertical actuators) are utilized at the tip of the vertical end and its nose. Several methods of signal analyses are performed to identify the natural frequency, modal shape, and damping structure in the measurement. The actuators generally have bandwidth reaching 30 Hz, with an actuation frequency first conducted starting with 0.1 Hz up to 30 Hz to find its symmetric mode at the verified range. High techniques are employed in spectral analyses for elastically deformed signals to point out the dynamic response; some examples of the common techniques employed include fast Fourier transformation (FFT) with the power spectral density (PSD). In this stage, studying the response in dynamics has to continue in the natural bend with the torsion frequency which is the major aim for the tandem structural body deformation failure of the helicopter and the phenomenon of aero-elasticity. Every mode covers each of the following phenomena:

1. Quantify the response and start induction on the Oscillatory movement on mode at a specific frequency, and do a Fast Fourier Transformation analysis to find the frequency resonance and the damping structure on this particular mode.
2. Induction of the step function command from the moving oscillation to zero, and do measurements on the rate of decay, and inference is done damping structure in this mode.

3. Finally, startup function impulses, and estimate the rate of decay and thence inferring the structure of damping in the mode.

After the above Phenomenon, the person is set to draw a comparison on the frequencies that are measured experimentally with the shape of modes and details of predictions of finite elements. Using perfectly set techniques with the structure of the engineering equipment in aeronautic, the finite element can be adjusted to develop frequencies and shape of the mode which are in line with test data on the ground vibration. Therefore, with the introduction of the theoretical methods, there is great relevance of using them in particular applications in the dynamic structure analyses and aero-elastic phenomena. It should be noted that in each airplane, very many combinations of fuel with payloads are first checked to verify if they are stable in the flight envelope of the aircraft before the flying clearance is concluded. The relevance of maximizing the computed results is very important since testing each fuel combination with the fuselage and its hardware up to the wings which include the fuel containers/tanks, storage parts, and the armaments. The computed data will be the main tool of work in making the right decision on whether to go or not go while making a test on the flight and coming up with a fully certified flight. For these particular tasks to continue, the most critical status combination has to be identified first; the combinations are mainly those that have very low payloads. It is encouraged that a comparison can be made from the previous experiences and results if possible when it comes to computing and testing then flight. If the key critical configuration is found, it's specially set aside to be used in wind- tunneling with testing flights. Specifically, there is relevance to extrapolate the tandem-rotor helicopters body structural failure mode and shape which cover the frequency of vibration, looks at the failure associated with flight testing, and the bending motions with torsional moments, the calculated payloads in accordance with the structural failures i.e. if the helicopter's body divisions fail in the internal segments or the boundary segments. Knowing the major four applications helps the experts to differentiate between varying phenomena with a comparison on the shape of the failure mode structure, with the former experience to find a suitable decision to take on during flight and ground testing to verify the data and calculations with the flight clearance.

C. FLIGHT AND GROUND TEST AS AIRCRAFT AEROELASTICITY VALIDATION TOOLS

Ground tests are very crucial for evaluating the accuracy and reliability of the closed-looped feedback controllers that are implemented in the Aeroservoelastic control system of the tandem-rotor helicopter. In the case of the tandem-rotor helicopter in particular, the ground tests are outstanding for revealing the actual structural response of the helicopter's body structure to various load transitions – across its three separate body segments; which in turn enables appropriate corrective calibrations and or modifications to be cheaply implemented on the Aeroservoelastic controller of the tandem-rotor helicopter model configuration under test. During the ground vibration tests, vibration loads are generated by the vibrations actuators and fed the specimen tandem-rotor helicopter's body structure through sophisticated attachments. Moment loads due to the rolling and pitching effects that result from the actuation of the swashplate on the tandem-rotor blades can be simulated by unbalanced sideward vibration loads applied to the cockpit and the tail segments so as to mimic the swash plate actuation effects on the tandem-rotor helicopter model specimen. The flight test involved exposing the specimen tandem-rotor helicopter modeled to the “worst-case scenario” flight environments such as; designed or maximum payload lift flights where the helicopter is loaded with its maximum payload, maximum pitching, rolling, and yawing rates transition; so as to investigate the potential maximum dynamic nonlinear forces and moments loads setup within and across the three structural segments of the helicopter as well as the closed-looped feedback controller's accuracy of response to the flight modes change. However, both ground and flight tests are very expensive and hazardous for investigation of the aeroelasticity of the tandem-rotor helicopter and thus need a very precautionary environment. The dynamic tests enable the evaluation of the specimen tandem-rotor helicopter model configuration's active aeroservoelastic capabilities.

A special experimental aircraft is equipped with the capability of making real-time measurements of the amount of fuel, airspeed, Mach number, altitude, load factors, and control surface deflections. The aircraft is also instrumented as in the ground-vibration tests with strain gauges and accelerometers. Special actuators are included to operate the ailerons and elevators over a range of frequencies. A sweep of actuation frequencies is first conducted to identify important modes. In addition, at certain frequencies, responses to step and impulse commands are measured.

i. Ground Roll (Taxi) Measurements

Aircraft ground roll (taxi) provides the first insight into a tandem-rotor helicopter's aeroelastic response. The relatively rough runway excites the tandem helicopter's structural modes. In addition, here we conduct a sweep of frequencies and FFT-PSD analyses of measurements and determine whether results match with analysis predictions of aeroelastic behavior at near-zero speeds. If they do not, we must stop the test to correct and/or adjust the computational model until an agreement is found, and then tandem-rotor helicopter's body structural deformation predictions are re-evaluated. Only when results do agree, may we then proceed to take off.

ii. Flight Tests

In this step, we take off and fly at the lowest speed at low altitude and in level flight. We measure the tandem-rotor helicopter's response to air turbulence and internal structural loads and conduct FFT and PSD analyses. We determine whether these results match our analytical predictions for the tested speed. If they do not, we must again stop the test to correct and/or adjust the computational model until we find agreement. When they do agree, we then may proceed to activate the actuators for an impulse command. Next, we determine whether there is sufficient damping. If there is, we conduct a sweep of frequencies and conduct FFT and PSD analyses of frequencies and damping. If these results match the analysis, then we may (cautiously!) activate actuators at the calculated tandem-rotor helicopter's body structural deformation frequency and conduct FFT and PSD analyses of the response. When the damping measurements match theoretical predictions, then we activate actuators for a step command. Next, we determine whether the response matches the analysis. When it does, we then collect and store data in the form of U-g-g diagrams. Only if and when there is reasonable agreement with analyses we proceed cautiously to perform maneuvers at various load factors at the same speed and altitude. During each maneuver, we activate the actuators for an impulse command to see whether there is sufficient damping. If there is, we move on to increase the load factor until the complete set of specified load factors within the flight envelope is tested.

If our computed predictions are in agreement with the results obtained at any stage, only then is it safe to go to a higher speed (e. g., 25 knots faster) at the same altitude. At this point we repeat all of the steps, collecting and storing data in the form of U-g-g diagrams. We systematically and cautiously increase the speed up to its maximum, checking at every increment to ensure that our analysis is valid.

Similarly, we systematically increase altitude to its maximum and repeat the regimen. We stop (that is, reduce speed to the previous safe speed) immediately whenever any one of the following happens:

1. A modal damping coefficient g decreases below the level of damping required by regulations (5% in a civil aircraft).
2. Oscillations in at least one measurement diverge and grow beyond pre-approved limits.
3. The dominant frequency deviates from its predicted value.

Thus, it is observed that the analysis of tandem-rotor helicopter's body structural deformation is strongly based on theoretical studies.

The theory is the work tool for analysis and decisions about critical configurations and flight conditions. Ground vibration experiments are used to tune the structural dynamics analysis to yield accurate structural modes, and wind tunnel experiments to tune the unsteady aerodynamics code (Vassberg, et al., 2005). Aeroelasticity flight tests are extremely dangerous. Real-time measurements and various actuation techniques are used to estimate the damping of the tandem-rotor helicopter at various flight altitudes, speeds, and load factors and move from one point to another with much caution (Alpman and Lyle, 2004). Analysis, ground experiments, and flight tests always go together to provide full clearance for flight without aeroelastic failure problems.

iii. Ground vibration tests

The purpose of structural dynamics experiments on the ground is to validate the frequencies and mode shapes of a clean tandem-rotor helicopter or important configurations of the tandem-rotor helicopter. The ground vibration tests also provide an essential insight into the possible modes of body structural deformation of the tandem-rotor helicopter. To accomplish this, the tandem-rotor helicopter is equipped with strain gauges and accelerometers at the boundaries of the tail, fuselage, and nose body segments. The tandem-rotor helicopter is placed on soft supports to mimic the airplanes free-free structural dynamics. Vertical actuators (that is, the shakers) are used at the tips of the nose and tail; both vertical and side shakers may be used at the tips of the nose and vertical tail. There is a variety of signal analysis methods to identify natural frequencies, mode shapes, and structural damping from the measurements. Generally, the actuators have a bandwidth up to 30 Hz, and a sweep of actuation frequencies is first conducted from 0.1 to 30 Hz to identify the symmetric and asymmetric modes in this range. Classical techniques, such as Fast Fourier Transformation (FFT) and Power Spectral Density (PSD), are used for spectral analysis of unsteady elastic deformation signals to identify the natural frequencies. At this point, we must continue to study details of the dynamic response at the natural bending and torsional frequencies of interest for the tandem helicopter's body structural deformation failure or other aeroelastic phenomena. For each mode, this entails the following:

1. Induce oscillatory motion of the mode at a certain natural frequency, measure the response, and perform an FFT analysis to identify the resonance frequency and structural damping of that mode.
2. Induce a step-function command from oscillatory motion to zero, measure the decay rate, and infer the structural damping of that mode.
3. Induce an impulsive function, measure the decay rate, and infer structural damping of the mode.

Now we are ready to compare experimentally measured frequencies and mode shapes with detailed finite-element predictions. Using well-established techniques and state-of-the-art aeronautic engineering tools, we tune our finite element model to yield frequencies and mode shapes that fit the ground vibration test data. So, with all of this background on theoretical methods, it is important to apply in some ways, aeroelasticity and structural dynamics analyses of the tandem-rotor helicopter. We must recall that for every aircraft, there may be dozens to several hundred combinations of fuel and payloads that must be verified as stable within the aircraft's flight envelope before clearance for flight is given. The use of computational results is crucial because we cannot possibly test every combination of fuel and hardware mounted on the fuselage and wings (such as stores, armaments, and fuel tanks). Computational results then become our main work tool for every go/no-go decision making in flight-testing and ultimate aircraft certification for flight (Shinoda, et al., 2002). To proceed with this monumental set of tasks, we first need to identify the most critical combinations (that is, those with the lowest failure payloads). If possible, these should be compared with previous experience in terms of computation and flight testing. Once the most critical configurations are identified, we set them aside for special wind tunnel and flight tests. In particular, we need to ascertain the tandem-rotor helicopter's body structural failure mode's shape; the vibration frequency, stresses associated with the failure, and the torsional and bending moments, all evaluated at the payload associated with the structural failure (that is, where any of the helicopter's body segments fails either internally or at its boundary with another segment). Identification of all four items allows us to distinguish between various cases with comparable structural failure mode shapes and, together with previous experience, to decide about further needed ground and flight tests to verify computations and flight clearance.

D. MATHEMATICAL MODELING OF THE AIRCRAFT AERO- ELASTIC DYNAMICS

The subject of structural dynamics is a relatively wide subject that covers the natural frequency determination and shape modes commonly known as the free- Vibration problem, responses pertaining to the initial status/condition, time domains mainly from the forced response, with responses on frequency. The following discussions deal with modeling the dynamic structure of the tandem rotor of the helicopter. In the problems associated with response, loading is an item in the aerodynamic history, and then the issue can be identified as an aero-elastic problem. Generally, loading in aerodynamics stands on the structure deformation, and the condition will solely rely on the loading aerodynamically. Also, the rest of the important combinations like the limit-cycle oscillation in carrying surfaces up, have to be subjected to the methodology of the non-linear oscillation. These phenomena's however are out of the study coverage on this particular text. The measure of structural dynamics is the capability to deliver a way of describing quantitatively the pattern of deformation at any abrupt time in a continuing structure system in line with loading externally. There could be numerous methods in estimating the pattern of structure deformation, of which most of them are globally employed by several aerodynamic users/ experts but the major one is the Model Representation only if the underlying structure is in linear oscillation. The major aim for learning this chapter is to ensure that a mathematical representation of the model in the tandem-rotor aircraft is developed, and is used to state the dynamic structure of the continuous aero-elastic structure. It should also be known that the Galerkin and Ritz model is a technique have a similar set of function, and both come up with simple solutions in a simple way and both the methods are closely related to the finite element model, the finite element method is a wide estimation methodology which gives an accurate analysis of the tandem-rotor helicopter on realistic structural configuration.

When we choose to use Newton's laws of linear motion on system particles we need to ensure that we carefully use the forces in the system. We also find an advantage in the Lagrangean equation form on the motion which derives a herein and ignore any force that could not be of use in the calculation, for example, frictionless pin force, point of rolling force, frictionless guide force, and the inextensible connection force. For the cases of a conservative system, (that is to say, a system in which its total energy stays constant), this method

would denote an automatic method for coming up with the motion equations as long as they offer in the form of potential and kinetic energies of the function. There is a need to first characterize the dynamic system in a unified form before continuing with the Lagrangean equation. The amount of independent coordinates is the most relevant ideology, one should know to completely know the position and the configuration of the system. If n , coordinates entirely to describe the configuration, then we conclude that the system has n degrees. Evidence is seen on how the generalized coordinate method with the iteration method is most suitable to evaluate problems of aero-elasticity. In every step in the iteration method and the generalized coordinates, deformation elasticity is known. Therefore, the problem of aerodynamics could be evaluated earlier and the outcome can be tabulated. In Aerodynamics, most issues can be developed as boundary value issues in various formulae and equations, and are joined together with integral formulae in the Green's Integral function. It is noted that Green's function is an asymmetric function in case the boundary value factor is identified using the differential equations and known as Self- Adjoint i.e Collatz. This symmetry in operators of aero-elasticity is attached to the non-self-adjointness of the problem of the boundary value (Burger and Hartfield, 2006).

E. FACTORS OF FUSELAGE SCALING AND AERODYNAMICS

A summary of the forces of fuselage aerodynamic and moments associated to the baseline HLH configuration at twelve thousand pounds weight is stated in the appendix A, 2nd table up to the 7th. The table is according to the results obtained from the wind tunnel test in the solid model of the tandem- rotor heavy-lift helicopter, angle, α , and fuselage sideslip angle, β . Tabular forces with moment information are expressed in the body axis in the form: drag (D/q_d), side-force (Y/q_d), lift (L/q_d), pitch moments (M/q_d), rolling moments (L/q_d), yawing moment (N/q_d), and α from -90° to $+90^\circ$, and β from -90° to $+90^\circ$. From 90° to 180° , the curves are assumed to be mirror image values of 0° to 90° . Fuselage aerodynamic results indicated in the 1st appendix in 2nd table to VII are already corrected for the rotor hub drags, and are based on the summation of representative flat plate area of 138.0 sq ft. This covers closely the 120,000-pound configurations, with the figure could be employed directly in the configuration gross mass.

$$D/q_d = \frac{f_e}{f_{eREF}} (D/q_d) \quad \text{in 2nd table} = \left(\frac{R}{R_{REF}} \right)^2 (Y/q_d) \quad \text{in 4th table}$$

$$L/q_d = \left(\frac{R}{R_{REF}} \right)^2 (L/q_d) \quad \text{in 3rd table}$$

$$M/q_d = \left(\frac{R}{R_{REF}} \right)^3 (M/q_d) \quad \text{in 5th table}$$

$$L/q_d = \left(\frac{R}{R_{REF}} \right)^3 (L/q_d) \quad \text{in 6th table}$$

$$N/q_d = \left(\frac{R}{R_{REF}} \right)^3 (N/q_d) \quad \text{in 7th table}$$

therefore :

$$f_{eREF} = 138.0 ft^2 = 138.0 ft^2$$

f_e is put in Appendix A in 1st table

$$R_{REF} = 45.0 ft$$

The above scaling formulae are in accordance with the idea that the non-dimensional aerodynamic force and coefficients are constantly following each other on the configuration of the gross mass. The only thing required is the scaling of the length referrals with the area and must be in proportion to the radius of the total area of the square (RD^2) respectively.

i. Dynamic Characteristics

Derived stability ideologies presented are in accordance with the standard Vertol trim of Boeing and the digital program stability A- 97. The digital program denotes the helicopter trims using the iterative formulae to a 6 steady-state equation, which sums the entire force and moments around the body axes which is fixed. The following are the 3 basic assumptions made on the rotor analyses:

- The velocity distribution induction is constant
- All the freedom degree elasticity's and the Blade lag are neglected
- The spanwise flow impact with the non-steady Aerodynamic effects are neglected

The stability derivative with the control powers is got numerically through calculating the changes change of the helicopter force and moment from the trim value resulted from the minor perturbation is used. Stability data used for the evaluation of seal level conditions which is standard i.e midpoint (for example the position) in a hover derive the gross mass and the entire estimated empty grosses. Therefore, all the results are in accordance with the cockpit control-to-blade pitch angle mechanical points constant to the original tandem-rotor HLH configuration.

ii. Assertion of Steadiness Derivatives.

The explanations below show the scaling features of the main derivatives.

iii. Longitudinal Axis.

Some representatives show the derivatives that are considered very crucial in hover. The representatives are Z_w (vertical damping), M_q (pitch damping), and M_u (pitch acceleration caused by lengthwise speed). The derivatives in cooperation with the regulator sensitivities, these are, $Z_{\delta c}$ and $M_{\delta B}$ establish the feedback of the aircraft to the input of the pilot.

I. Vertical damping (Z_w).

The vertical damping is established based on how sensitive the rotor thrust of the aircraft is to vertical (perpendicular) velocity. The vertical damping of the hover is determined from the formula below;

$$Z_w = - \left[\frac{8}{V_T \left(\frac{2c_{TS}}{a\sigma} \right) \left(1 - \frac{a\sigma}{16\lambda_0} \right)} \right]$$

However, the disc loading, the blade-chord-to-rotor radius fraction, and the tip speed (VT) are constituent with the conformation gross mass, the vertical damping stays almost steady with the gross mass as illustrated below.

$$\left(\frac{2c_{TS}}{a\sigma} \right) \propto \frac{\text{Disc Loading}}{\frac{C}{R} Npa V_T^2}$$

When the disc loading is less, vertical damping upsurges for a particular conformation. The above equation shows how the mass of the jet is reduced with the reduction of the gross mass of a particular conformation. For weightier jets, a minor rise in the vertical damping for the vacant weight conformation and an increased gross mass results in a reduced fraction of vacant-to-design gross mass feature.

I. The pitch damping (M_q).

Pitch damping is equivalent to a derivative factor as shown in the equation below;

$$M_q \cong Z_w \left(\frac{l^2 m}{I_{yy}} \right)$$

Given that vertical damping is steady with conformation design gross mass, then pitch damping is a factor placed in the brackets. The scaling feature used in this case is a shown an upsurge pitch damping with conformation design gross mass. At the point when the disc loading is very small (vacant gross mass), M_q increases because of small pitch inertia.

II. The pitch acceleration is caused by onward velocity (M_u).

The pitch acceleration in the hover caused by forwarding velocity is given by the formula below.

$$M_u = \frac{8g}{V_T} \left(\frac{2c_{TS}}{a\sigma} \right) \left(\frac{h_{er}m}{I_{yy}} \right)$$

Thus, the pitch acceleration will scale regarding the element $(h_{er}m/I_{yy})$. Low pitch inertia and an empty gross weight (little disc loading) result in a minor reduction in pitch acceleration.

2.2.1. Lateral-Directional Axis

The directives of the lateral-directional directives are always indicated by L_p for roll damping, L_r for yaw damping, and L_v for side velocity. These directives when combined with control sensitivities indicated by $L_{\delta s}$ and $N_{\delta R}$, best explain the basic response of the aircraft to the pilot.

I. L_p (Roll damping).

This rolling moment functions as a result of the lateral tilting of the disc caused by the roll rate of the aircraft. It is expressed as the equation below;

$$L_p \cong - \left(\frac{4}{\gamma V_T} \right) R \left[\frac{h_{er}w_G}{I_{xx}} + \frac{N\sigma_\beta}{R I_{xx}} \left(\frac{e_\beta}{R} \right) V_T^2 \right]$$

γ is almost a constant and V_T is a constant for all the configurations of gross weight. L_p will gage and the radius of the rotor is multiplied with the expression which is in the brackets. The expression which is the brackets also can be expressed as the tilt contribution of the rotor thrust. L_{AIC} , and for the moment of the centrifugal part is, L_{AIC} and the sum $(L_{AIC} + L_{AIC})$, is the total acceleration sensitivity of roll. As it is assumed that the total sensitivity reduces together with the value of gross weight configuration and it is expected that decreases are very small compared to the inversed ratio for rotor

radius. The L_p will however rise together with the configuration gross weight. At null gross weights, higher L_p is taken as a reflection in the contribution of centrifugal forces about the value of a rolling moment, which then changes as an inverse ratio when it comes to rolling inertia.

II. N_r (the yaw damping)

This is connected to the tilting effect of the rotor disc caused as a result of lateral translational speeds at aft and the forward rotors. Because of such, it's a straight function for Y_v of every rotor, which is approximated by the function in hover as below;

$$Y_v \cong -\frac{8g}{V_T} \left(\frac{2c_{TS}}{a\sigma} \right)$$

Then;

$$N_r \propto Y_v \left(\frac{l^2 m}{I_{zz}} \right)$$

At the constant disc and constant (C/R) loading ratio, the Y_v remains unchanged in the gross weight calculations. At the lower disc loading like weight empty, the Y_v decreases respectively to disc loading effect. The yaw damping scales in accordance to the gross weight configuration as $\left(\frac{l^2 m}{I_{zz}} \right)$ ratio which is given by the definition of parametric aircraft which is indicated in Table I in the Appendix, which is equivalated to the design gross weight unity, and less than the unity of the empty gross weights. Therefore, N_r which is the yaw damping remains almost constant together with the weight of design gross and has a uniformity decrease on the lower disc loading.

L_v , which is roll acceleration as a result of sideward velocity.

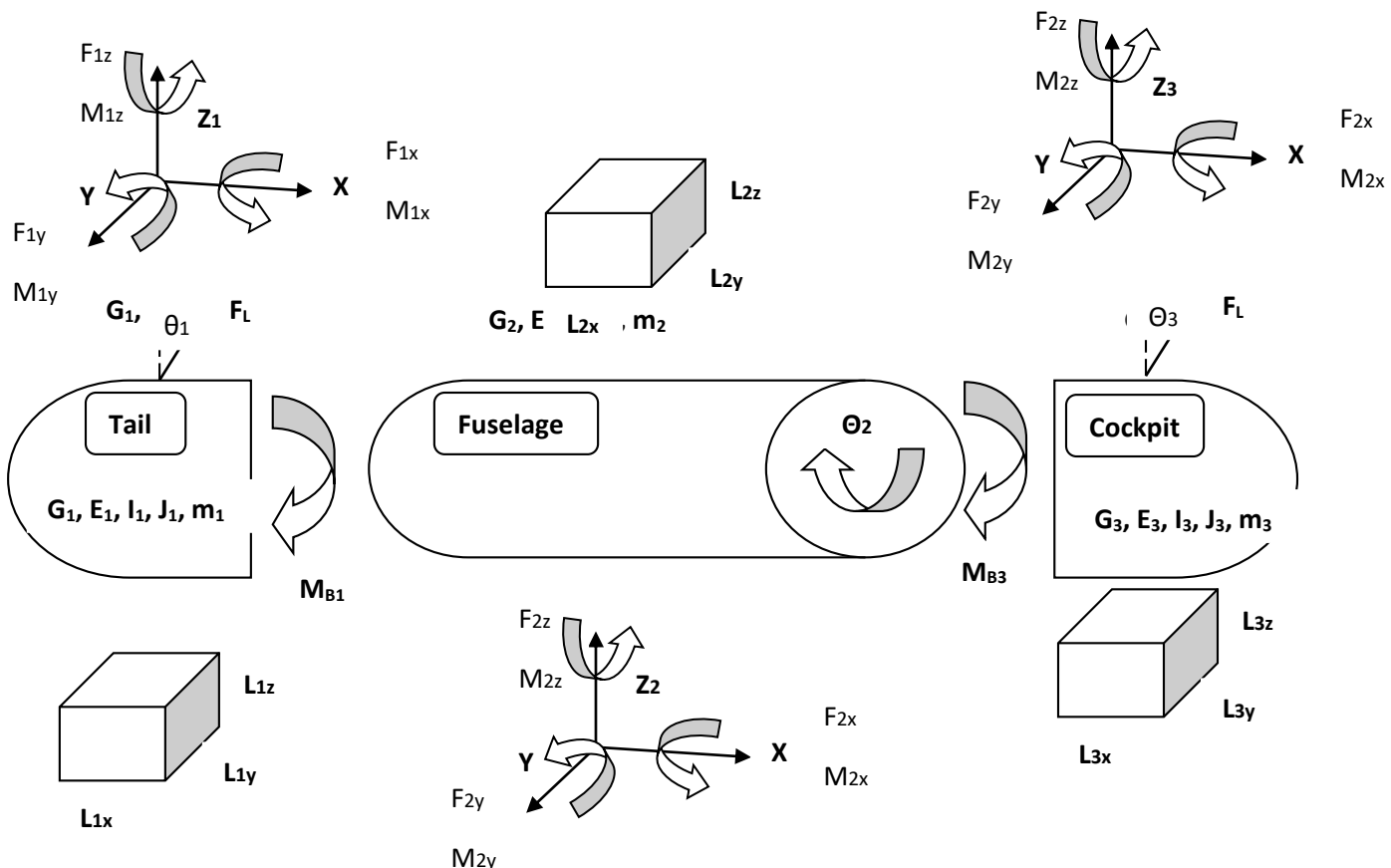
This is related directly to the tilt of the rotor disc which is a result of side velocity. Its dependence upon the configuration of design gross weight is associated to Y_v proportionally as below;

$$L_v \propto Y_v \left(\frac{h_{er} m}{I_{xx}} \right)$$

The factor of scaling $\left(\frac{h_{er} m}{I_{xx}} \right)$ declines together with the weight of design gross, and the Y_v remains a constant. The L_v derivative decrease with an increasing weight of the design gross. It reduces with decreasing disc loading.

F. THE PHYSICAL MODEL OF THE HELICOPTER TANDEM-ROTOR .

The physical dynamics of the helicopter tandem-rotor were formulated in balance for the 3 sectors, for the fuselage, the arena, and the tail as illustrated below



operator can be written in form of influence functions. An actual material ought to diverge from Hooke's law and portrays inelasticity as a given point. For instance, considering the ultimate association between strain and stress as linear and is not based on only the prompt quantities of strain and stress, but also depends on the degree of variability of strain and stress. With the linear postulation, there is no perpetual set that stays when all the stresses have been removed. Various other challenges can be figured out while the real importance is based on the nature of the conditions of flow and the structure¹. To categorize the general characteristics of a particular challenge or to establish the rate of the estimate of evaluation, it is necessary to possess the design as basic as possible during the start. After the classification, the features of the challenges faced are put into specialized cases through the introduction of additional assumptions. Using this strategy, the association between the different approaches used in solving the aircraft challenges becomes understandable and in case an adjustment on a given concept is required, the engineer can reposition the restrictive expectations and choose one that has to relax. The nature of the response obtained from the aeroelastic systems as well as their depiction by physical diagrams can be decreased and presented in pictorial depictions with the same meanings as the functional diagrams. The information is represented in an algebraic equation with the help of operational equations. The level of precision of the formulated problem is properly shown by the expectations utilized in the generation of the operators.

Overpowering the physical restrictions at an increased rate of the rotorcraft, new theories can consist of axial thrusters and raising the exteriors. The wings of the jet create a lift in the lateral flight and this causes the major rotor to become unloaded and its speed reduces. As a result of the lift, thrust is lost as the rotor is unloaded which is later compensated with further propulsive vigor created by the auxiliary propellers, thereby up surging the cruise velocity. Given this condition, the wings of the aircraft carry almost 75% of the total rotorcraft weight. Simplified wing models are being unified in this model formulation. Such wings comprise their main structure. The wings are therefore unified to form an airframe by either incorporation of the wing box or by major frame accessories. A proper organization of the gearbox, wing incorporation structure, and drive structure is therefore essential. Today, aircraft wings are installed on the fuselage assembly have immovable beam members which together form a simplified approach.

For the tail we have;

$$F_L \cos \theta_1 + \frac{E_1(A_1)_{yx}(s_1)_z}{(L_1)_z} + m_1(\ddot{s}_1)_z + \frac{2(M_{B1})_{zx}}{(L_1)_z} = 0 \quad \text{--- (i)}$$

$$F_L \sin \theta_1 + \frac{E_1(A_1)_{yz}(s_1)_x}{(L_1)_x} + m_1(\ddot{s}_1)_x = 0 \quad \text{--- (ii)}$$

$$(M_{r1})_y + \frac{G_1(J_1)_{xz}}{(L_1)_y}(\theta_1)_y + (J_1)_{xz}(\ddot{\theta}_1)_y = 0 \quad \text{--- (iii)}$$

$$(M_{r1})_x + \frac{G_1(J_1)_{zy}}{(L_1)_x}(\theta_1)_x + (J_1)_{zy}(\ddot{\theta}_1)_x = 0 \quad \text{--- (iv)}$$

The equations for reduction of the order of the system of equations for the tail structure to the first order for computational compatibility with the MATLAB ODE45 solver are thus;

$${}^2(\dot{s}_1)_z = (\ddot{s}_1)_z$$

$${}^2(\dot{s}_1)_x = (\ddot{s}_1)_x$$

$${}^2(\dot{\theta}_1)_y = (\ddot{\theta}_1)_y$$

$${}^2(\dot{\theta}_1)_x = (\ddot{\theta}_1)_x$$

For the cockpit we have;

$$F_L \cos \theta_3 + \frac{E_3(A_3)_{yx}(s_3)_z}{(L_3)_z} + m_3(\ddot{s}_3)_z + \frac{2(M_{B3})_{zx}}{(L_3)_z} = 0 \quad \text{--- (v)}$$

$$F_L \sin \theta_3 + \frac{E_3(A_3)_{yz}(s_3)_x}{(L_3)_x} + m_3(\ddot{s}_3)_x = 0 \quad \text{--- (vi)}$$

$$(M_{r3})_y + \frac{G_3(J_3)_{xz}}{(L_3)_y}(\theta_3)_y + (J_3)_{xz}(\ddot{\theta}_3)_y = 0 \quad \text{--- (vii)}$$

¹ Light, J.S., "Tip Vortex Geometry of a Hovering Helicopter Rotor in Ground Effect," Journal of American Helicopter Society, Vol. 38, No. 2, 1993, pp. 34-42.

$$(M_{r3})_x + \frac{G_3(J_3)_{zy}}{(L_3)_x}(\theta_3)_x + (J_3)_{zy}(\ddot{\theta}_3)_x = 0 \text{ --- (viii)}$$

The equations for reduction of the order of the system of equations for the cockpit structure to the first order for computational compatibility with the MATLAB ODE45 solver are thus;

$${}^2(\dot{s}_3)_z = (\ddot{s}_3)_z$$

$${}^2(\dot{s}_3)_x = (\ddot{s}_3)_x$$

$${}^2(\dot{\theta}_3)_y = (\ddot{\theta}_3)_y$$

$${}^2(\dot{\theta}_3)_x = (\ddot{\theta}_3)_x$$

For the fuselage we have;

$$(F_2)_z + (F_1)_z + (F_3)_z + m_2(\ddot{s}_2)_z = 0 \text{ --- (ix)}$$

$$\frac{2(M_{B1})_{zx}}{(L_2)_z} + \frac{2(M_{B3})_{zx}}{(L_2)_z} + \frac{E_2(A_2)_{zx}}{(L_2)_x}(s_2)_x + 2m_2(\ddot{s}_2)_x = 0 \text{ --- (x)}$$

$$(M_{B1})_{zx} + (M_{B3})_{zx} + E_2(I_2)_{yz} \frac{dz}{dx} + \frac{G_2(J_2)_{zx}}{(L_2)_y}(\theta_2)_y + (J_2)_{zx}(\ddot{\theta}_2)_y + m_2(L_2)_x = 0 \text{ --- (xi)}$$

$$(M_{r1})_x + (M_{r3})_x + \frac{G_2(J_2)_{zy}}{(L_2)_x}(\theta_2)_x + (J_2)_{zy}(\ddot{\theta}_2)_x + m_2(L_2)_y = 0 \text{ --- (xii)}$$

The equations for reduction of the order of the system of equations for the tail structure to the first order for computational compatibility with the MATLAB ODE45 solver are thus;

$${}^2(\dot{s}_2)_z = (\ddot{s}_2)_z$$

$${}^2(\dot{s}_2)_x = (\ddot{s}_2)_x$$

$${}^2(\dot{\theta}_2)_y = (\ddot{\theta}_2)_y$$

$${}^2(\dot{\theta}_2)_x = (\ddot{\theta}_2)_x$$

Thus the non-equilibrium first order structural system model of the tandem-rotor helicopter can be written as;

For the tail we have;

$$-\frac{F_L \cos \theta_1}{m_1} - \frac{E_1(A_1)_{yx}(s_1)_z}{m_1(L_1)_z} - \frac{2(M_{B1})_{zx}}{m_1(L_1)_z} = {}^2(\dot{s}_1)_z \text{ --- (i)}$$

$${}^2(\dot{s}_1)_z = (\ddot{s}_1)_z \text{ --- (ii)}$$

$$-F_L \frac{\sin \theta_1}{m_1} - \frac{E_1(A_1)_{yz}(s_1)_x}{m_1(L_1)_x} = {}^2(\dot{s}_1)_x \text{ --- (iii)}$$

$${}^2(\dot{s}_1)_x = (\ddot{s}_1)_x \text{ --- (iv)}$$

$$-\frac{(M_{r1})_y}{(J_1)_{xz}} - \frac{G_1(J_1)_{xz}}{(J_1)_{xz}(L_1)_y}(\theta_1)_y = {}^2(\dot{\theta}_1)_y \text{ --- (v)}$$

$${}^2(\dot{\theta}_1)_y = (\ddot{\theta}_1)_y \text{ --- (vi)}$$

$$-\frac{(M_{r1})_x}{(J_1)_{zy}} - \frac{G_1(J_1)_{zy}}{(J_1)_{zy}(L_1)_x}(\theta_1)_x = {}^2(\dot{\theta}_1)_x \text{ --- (vii)}$$

$${}^2(\dot{\theta}_1)_x = (\ddot{\theta}_1)_x \text{ --- (viii)}$$

For the cockpit we have;

$$-\frac{F_L \cos \theta_3}{m_3} - \frac{E_3(A_3)_{yx}(s_3)_z}{m_3(L_3)_z} - \frac{2(M_{B3})_{zx}}{m_3(L_3)_z} = {}^2(\dot{s}_3)_z \text{ --- (ix)}$$

$${}^2(\dot{s}_3)_z = (\ddot{s}_3)_z \text{ --- (x)}$$

$$-\frac{F_L \sin \theta_3}{m_3} - \frac{E_3(A_3)_{yz}(s_3)_x}{m_3(L_3)_x} = {}^2(\dot{s}_3)_x \text{ --- (xi)}$$

$${}^2(\dot{s}_3)_x = (\ddot{s}_3)_x \text{ --- (xii)}$$

$$-\frac{(M_{r3})_y}{(J_3)_{xz}} - \frac{G_3(J_3)_{xz}}{(J_3)_{xz}(L_3)_y}(\theta_3)_y = {}^2(\dot{\theta}_3)_y \text{ --- (xiii)}$$

$${}^2(\dot{\theta}_3)_y = (\ddot{\theta}_3)_y \text{ --- (xiv)}$$

$$-\frac{(M_{r3})_x}{(J_3)_{zy}} - \frac{G_3(J_3)_{zy}}{(J_3)_{zy}(L_3)_x}(\theta_3)_x = {}^2(\dot{\theta}_3)_x \text{ --- (xv)}$$

$${}^2(\dot{\theta}_3)_x = (\ddot{\theta}_3)_x \text{ --- (xvi)}$$

For the fuselage we have;

$$-\frac{(F_2)_z}{m_2} - \frac{(F_1)_z}{m_2} - \frac{(F_3)_z}{m_2} = {}^2(\dot{s}_2)_z \text{ --- (xvii)}$$

$${}^2(\dot{s}_2)_z = (\ddot{s}_2)_z \text{ --- (xviii)}$$

$$-\frac{(M_{B1})_{zx}}{m_2(L_2)_z} - \frac{(M_{B3})_{zx}}{m_2(L_2)_z} - \frac{E_2(A_2)_{zx}}{2m_2(L_2)_x}(s_2)_x = {}^2(\dot{s}_2)_x \text{ --- (xix)}$$

$${}^2(\dot{s}_2)_x = (\ddot{s}_2)_x \text{ --- (xx)}$$

$$-\frac{(M_{B1})_{zx}}{(J_2)_{zx}} - \frac{(M_{B3})_{zx}}{(J_2)_{zx}} - \frac{E_2(I_2)_{yz}}{(J_2)_{zx}} \frac{dz}{dx} - \frac{G_2(J_2)_{zx}}{(J_2)_{zx}(L_2)_y}(\theta_2)_y - \frac{m_2(L_2)_x}{(J_2)_{zx}} = {}^2(\dot{\theta}_2)_y \text{ --- (xxi)}$$

$${}^2(\dot{\theta}_2)_y = (\ddot{\theta}_2)_y \text{ --- (xxii)}$$

$$-\frac{(M_{r1})_x}{(J_2)_{zy}} - \frac{(M_{r3})_x}{(J_2)_{zy}} - \frac{G_2(J_2)_{zy}}{(J_2)_{zy}(L_2)_x}(\theta_2)_x - \frac{m_2(L_2)_y}{(J_2)_{zy}} = {}^2(\dot{\theta}_2)_x \text{ --- (xxiii)}$$

$$^2(\dot{\theta}_2)_x = (\ddot{\theta}_2)_x \quad \text{--- (xxiv)}$$

G. THE AERODYNAMIC MODEL OF THE TANDEM-ROTOR HELICOPTER

The aerodynamics of the tandem-rotor helicopter were modelled for the holistic flight state of the tandem-rotor helicopter model that is for; the advance velocity V_x , the vertical velocity V_z the pitch angle θ , the pitch angular velocity ω_y , the longitudinal control angle of the main rotor β and the cyclic longitudinal input δ . The kinetic definition of aerodynamic model was thus written as shown below.

$$\dot{V}_x = X_u V_x + X_q \omega_y + X_\theta \theta + X_\beta \beta + X_w V_z + X_\delta \delta \quad \text{--- (xiii)}$$

$$\dot{\omega}_y = M_u V_x + M_q \omega_y + M_\beta \beta + M_w V_z + M_\delta \delta \quad \text{--- (xiv)}$$

$$\dot{\theta} = \omega_y \quad \text{--- (xv)}$$

$$\dot{\beta} = B_u V_x - \omega_y + B_\beta \beta + B_\delta \delta \quad \text{--- (xvi)}$$

$$\dot{V}_z = Z_u V_x + Z_q \omega_y + Z_\theta \theta + Z_\beta \beta + Z_w V_z + Z_\delta \delta \quad \text{--- (xvii)}$$

So we now consider the Multi Input Multi Output (MIMO) state space representation of the case of the non-linear dynamics of the tandem-rotor helicopter in matrix form as shown below;

$$\begin{bmatrix} \dot{V}_x \\ \dot{\omega}_y \\ \dot{\theta} \\ \dot{\beta} \\ \dot{V}_z \end{bmatrix} = \begin{bmatrix} X_u & X_q & X_\theta & X_\beta & X_w \\ M_u & M_q & 0 & M_\beta & M_w \\ 0 & 1 & 0 & 0 & 0 \\ B_u & -1 & 0 & B_\beta & 0 \\ Z_u & Z_q & Z_\theta & Z_\beta & Z_w \end{bmatrix} \begin{bmatrix} V_x \\ \omega_y \\ \theta \\ \beta \\ V_z \end{bmatrix} + \begin{bmatrix} X_\delta \\ M_\delta \\ 0 \\ B_\delta \\ Z_\delta \end{bmatrix} [\delta]$$

The Unaugmented Tandem-rotor Helicopter model

To represent the motion of the rigid-body helicopter, a system of small-perturbation differential equations was used. The equations, as shown in the system of equations below, represent the unaugmented helicopter, distinguished into longitudinal-vertical motion and lateral-directional motion. This notion of the axes was maintained throughout the study. In later Aeroservoelasticity section, this system of equations was connected to the structural dynamics model to make the complete aeroelasticity model of the tandem-rotor helicopter. The system of equations is in first-order form suitable for state space matrix evaluations and eigen-value analyses.

We have the Longitudinal -Vertical relations as;

$$\dot{u} = x_u u + x_w w + (x_q - w_o)q - g\theta \quad \text{--- (i)}$$

$$\dot{w} = z_u u + z_w w + (z_q - u_o)q \quad \text{--- (ii)}$$

$$\dot{q} = M_u u + M_w w + (M_q)q \quad \text{--- (iii)}$$

$$\dot{\theta} = q \quad \text{--- (iv)}$$

$$\begin{bmatrix} \dot{u} \\ \dot{w} \\ \dot{q} \\ \dot{\theta} \end{bmatrix} = \begin{bmatrix} x_u & x_w & (x_q - w_o) & -g \\ z_u & z_w & (z_q - u_o) & 0 \\ M_u & M_w & M_q & 0 \\ 0 & 0 & 1 & 0 \end{bmatrix} \begin{bmatrix} u \\ w \\ q \\ \theta \end{bmatrix}$$

So the Lateral- Longitudinal relations are;

$$\dot{V} = Y_v V + (Y_p + w_o)p + (Y_r - U_o)r + g\Phi \quad \text{---(v)}$$

$$\dot{p} = \left(\frac{I_{xx}I_{zz}}{I_{xx}I_{zz} - I_{xz}^2} \right) \left[\left(L_v + \frac{I_{xz}}{I_{xx}}N_v \right)V + \left(L_p + \frac{I_{xz}}{I_{xx}}N_p \right)p + \left(L_r + \frac{I_{xz}}{I_{xx}}N_r \right)r \right] \quad \text{---(vi)}$$

$$\dot{r} = \left(\frac{I_{xx}I_{zz}}{I_{xx}I_{zz} - I_{xz}^2} \right) \left[\left(N_v + \frac{I_{xz}}{I_{zz}}L_v \right)V + \left(N_p + \frac{I_{xz}}{I_{zz}}L_p \right)p + \left(N_r + \frac{I_{xz}}{I_{zz}}L_r \right)r \right] \quad \text{---(vii)}$$

$$\dot{\Phi} = p \quad \text{---(viii)}$$

$$\dot{\Psi} = r \quad \text{---(ix)}$$

$$\begin{bmatrix} \dot{V} \\ \dot{p} \\ \dot{r} \\ \dot{\Phi} \\ \dot{\Psi} \end{bmatrix} = \begin{bmatrix} Y_v & (Y_p + w_o) & (Y_r - U_o) & g & 0 \\ \left(L_v + \frac{I_{xz}}{I_{xx}}N_v \right)C_p & \left(L_p + \frac{I_{xz}}{I_{xx}}N_p \right)C_p & \left(L_r + \frac{I_{xz}}{I_{xx}}N_r \right)C_p & 0 & 0 \\ \left(N_v + \frac{I_{xz}}{I_{zz}}L_v \right)C_r & \left(N_p + \frac{I_{xz}}{I_{zz}}L_p \right)C_r & \left(N_r + \frac{I_{xz}}{I_{zz}}L_r \right)C_r & 0 & 0 \\ 0 & 1 & 0 & 0 & 0 \\ 0 & 0 & 1 & 0 & 0 \end{bmatrix} \cdot \begin{bmatrix} V \\ p \\ r \\ \Phi \\ \Psi \end{bmatrix}$$

Where;

$$C_p = \left(\frac{I_{xx}I_{zz}}{I_{xx}I_{zz} - I_{xz}^2} \right)$$

$$C_r = \left(\frac{I_{xx}I_{zz}}{I_{xx}I_{zz} - I_{xz}^2} \right)$$

Case Study: Simulation and Analysis of the open loop unaugmented Aerodynamic control model of the tandem-rotor helicopter using MATLAB and SIMULINK

The MATLAB code for numerical simulation and analysis of the aerodynamic model is shown in Appendix B. The figure below shows that a slight pitch displacement from the zero-pitch equilibrium will eventually steadily destabilise the helicopter and thus cause an accident if unattended to. A feasible solution to this problem would be the incorporation of a stabilising feedback controller such as a Potential Integrator Differential (PID) controller in parallel with the aerodynamic model. The incorporation of such behavioral feedback information of the aerodynamic model with that from the structural model will enable a more realistic and detailed analysis of the holistic aeroservoelasticity model of the tandem-rotor helicopter as we shall see further on.

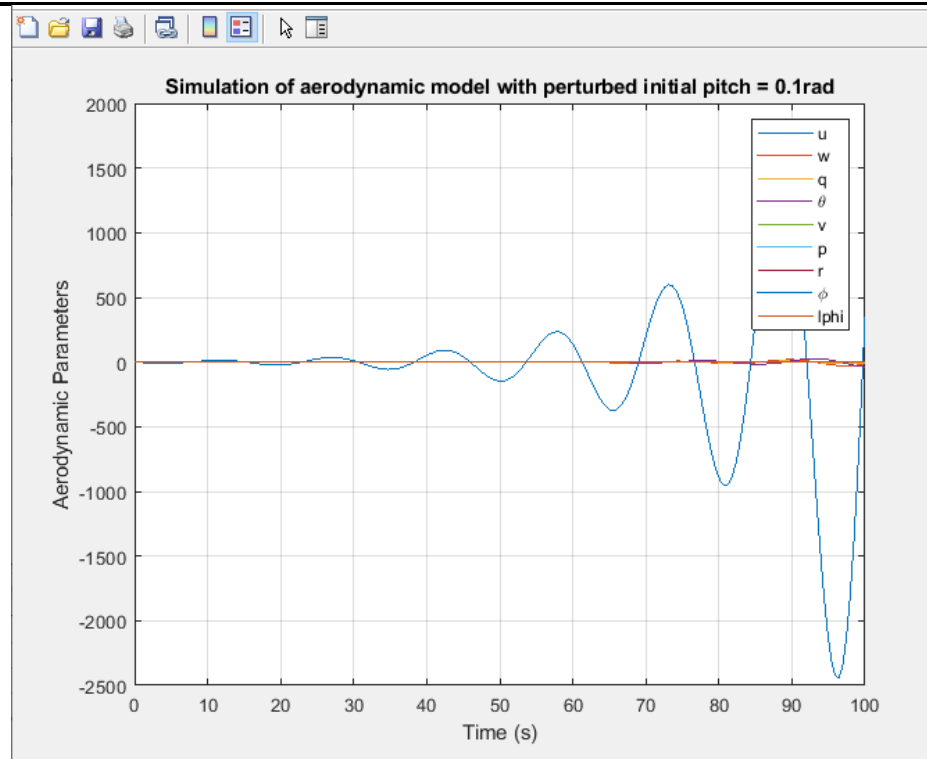


Figure 4: Effect of initial pitching perturbation on the aerodynamic stability of the tandem-rotor helicopter

3. Research Design

This chapter, discourses the aerodynamic and structural and thus the aeroelastic modeling, optimization and designing, and analysis of the feasible tandem-rotor helicopter model configurations and designs. The tandem-rotor helicopter models herein are appropriately manipulated and simulated on various static and dynamic and input environments and their corresponding responses are analyzed and evaluated using state-of-the-art engineering tools such as MATLAB and NX Nastran so as to obtain the optimal aeroelastic configurations of the models for various flight mode transitions. The structural model of the tandem helicopter considered here assumes the union at their boundaries, of three body segments of the helicopter, that is; the tail and cockpit which are at the extremities of the helicopter, and the fuselage which is the middle of the two, as the major structural components of the aircraft. The structural dynamics parameters such as the elastic and torsion stresses and strains were modeled and their model's setup in MATLAB for analysis of each system stability configuration using both the eigenvalue analysis SIMULINK simulations in order to obtain the most optimal configurations and to evaluate the influence of various actuation of the various aircraft's end effectors, especially the swashplate, on the aeroelasticity of the tandem-rotor helicopter model.

A. STATIC AEROELASTICITY

In this study, the field of static aeroelasticity is concerned with the study of the tandem-rotor helicopter phenomena associated with the interaction of aerodynamic loading induced by steady flow and the resulting elastic deformation of the helicopter's body structure. The tandem-rotor helicopter possesses "high aspect ratio" blades and employs composite objects that make static aeroelasticity more acute. There are important static aeroelastic implications existing on different occasions. Static aeroelasticity has a great effect on the tandem-rotor helicopter. They make reverse movements in a situation that does not favor the tandem-rotor helicopter. In this situation, the pilot may not be certain and ends up commanding wrong inputs (Paul, 2012). For example, the pilot uses the control stick to command the tandem-rotor to the right direction instead of the left. When the tandem-rotor helicopter is flying at a maximum speed, the big portion of the front blade undergoes a flow caused by a rise in the advance ratio. The disconnection of the flow at the sharpest point of the aerodynamic flow turns into a negative lift of the tandem-rotor helicopter. Kinematics of the blades of a tandem-rotor result in an increased stall in the reverse flow of the rotors. This worsens the situation by leading to unsteady loading of the tandem rotor. Such barriers have led to restricting the speed of the tandem-rotor helicopter to 250 kts.

Research indicates that these impacts can be reduced by deflecting the blades on both rotors in a different direction. The method is named trailing edge because it is similar to tying a camber to the last edge of any of the blades. Various controls have been established upon the sliding back and forward cantilevered models. All the edges of the blades provide an important fall of the flow of separation originating from the sharpest edges. It results in a fall in the wake volume. If the control surface of the tandem-rotor helicopter is deflected below, the front shift produces a downward pointing twist. When the tandem-rotor helicopter is in a total state of torsion, the reduction in the direction of flight leads to a loss in the level of lift. The result is a reduction in the control action and the tandem-rotor helicopter cannot

fly at that moment. The center of flight makes the tandem-rotor helicopter move forward in direction of the sound. This makes pilots believe that static aeroelasticity was a significant feature of the tandem-rotor helicopter flight. Nevertheless, it is a false belief since the hindrances in the torsion stiffness are significant with an increase in aerodynamic.

There is an obvious and rapid increase in terms of research relating to the flexible unmanned aerial vehicle (UAV). This could be down to the massive and extensive levels of attention associated with the high-altitude long-endurance and very flexible UAV aircraft. The attention could be because of their large flexibility and lightweight. It is common for the HALE wing to produce large deformations in the course of the flight. In the same manner, its structural stiffness behaves in a nonlinear manner and this is attributed to the changes in terms of the geometric stiffness. Consequently, a considerable wing elastic deformation will instigate significant alterations in the configurations related to aerodynamics and the airplane's stiffness characteristics. It is for that reason that problems of aeroelastic nature and especially for the huge flexible aircraft do arise. It should be noted that the old or traditional linear technique for static aeroelastic investigation hardly takes into account the effects associated with structural geometric or non-planar aerodynamic nonlinearity. In terms of the design requirement regarding HALE, It is suggested by Patil and Hodges,(1991) that the model of geometrical nonlinear aeroelasticity associated with the fixed-wing would suffice. There have been several research conducted over the years containing diverse content regarding geometrically nonlinear aeroelastic concepts. For all these investigations, the big flexible HALE has been the center of attention. In their investigation, Patil and Hodges did make use of the geometrically-exact beam concept. They used it to investigate the geometric nonlinearities impacts within a static or dynamic aeroelastic exploration where the structure was more like the large-aspect-ratio wing. Cesnik and Palacios did solve the nonlinear static aeroelastic reactions through the use of the CSD/ CFD/ coupled technique. Xie applied the generalized strips theorem as well as the structure nonlinear finite element technique (FEM) to undertake an analysis of the aeroelastic features associated with the flexible wing having a large deformation. In the same manner, the linearized technique was applied in the prediction of the characteristics associated with the flexible wing. Howcroft et al. examined five methods of aeroelastic modeling applicable to the aeroelastic investigation and these included the geometric nonlinearities carried out in the more research.

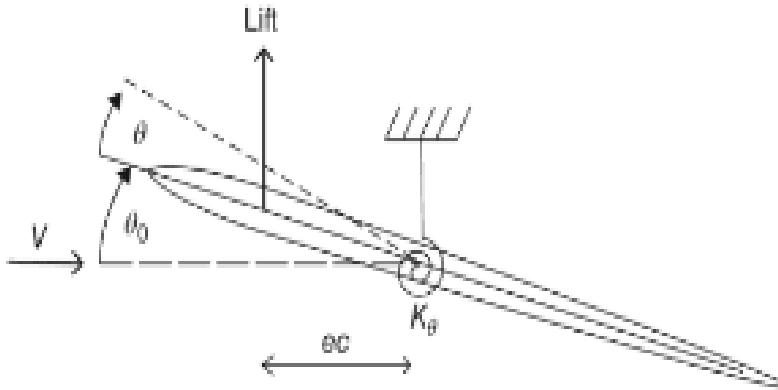
A comparison was undertaken between the static aeroelastic equilibrium predictions attained from the five modeling methods. Discussions related to the effects of aerodynamic modeling selections drag effect and aero forces orientations as established within their paper did have considerable impacts on the related investigations. An analysis of the trim has been established as a fundamental part of the overall progress of the design of the aircraft. When the structure is subjected to a huge deformation, there will be an emergence of the non-planar aerodynamic impact. Consequently, the huge deformation will have a massive impact on the overall structural stiffness. The linear aeroelastic technique has its basis on the supposition deformations of structural are nature is merely an indication of the infinitesimal failures when it comes to the analysis of aeroelastic characteristics associated with the very flexible airplane. Patil and Zhang et al. constructed a technique through the combination of the model of the ONERA aerodynamics and the nonlinear beam. Wang et al. did propose a method including the combination of the nonplanar vortex lattice technique (VLM) and nonlinear FEM. They did through iterative progress within the aeroelastic trim exploration entailing geometrical nonlinearity. The results attained from the analysis of the longitudinal trim were presented and they included both the linear nonlinear methods as proposed. The linear technique developed in this study has its major basis on the MSC. Flight loads. To calculate the model stiffness and the related displacement, Nonlinear FEM is applied. That is particularly under aerodynamics within the aeroelastic analysis especially when geometric nonlinearities are rendered into consideration. There is a need for expensive computation to ensure that the attainment of the geometrical nonlinearity simulation (Newton Raphson technique). It is important that there is a huge amount of freedom when providing solutions to problems of aeroelastic nature. This is especially so when the problems include coupling of structure and geometrical nonlinearity. In the same manner, dynamics do necessitate a huge amount of iterative progress. The aim for that is to ensure that there is a severe limitation of the application of nonlinear FEM within the aeroelastic problem and this includes the geometrical nonlinearity. In comparison to FEM, the reduced-order model (ROM) has the capability of reducing the problem scale. In the same manner, it has the potential or capability to be useful in the analysis of the features of the geometrics nonlinearity associated with large and flexible aircraft. It illustrates to us the computational economical mathematical representation for the structural analysis in regard to the problems of nonlinear aeroelasticity. It consequently provides the potential for approximate real-time examination. Demasi and Palacios did reconduct the function of load step with structural tangent modes via the procedure of proper orthogonal decomposition (POD) to reduce freedom of structure with planar and non-planar structural configurations. For this case study, the focus is attempting to solve static aeroelastic problems. It is important to note that huge deformations relating to flexible aircraft do change the aerodynamics loads as well as the structural dynamic structures. There is a possibility for all of these to massively influence the response analysis or the dynamic stability features. By solving the static aeroelastic nonlinear symmetry state, it becomes possible to reveal the changes within the structural dynamic structures. That provides the basis through which dynamic aeroelastic problems such as geometric nonlinearity are solved. In the same manner, the computation of the aerodynamic derivatives, as well as the dynamic/static stability or the flexible helicopter, necessitates the confirmation of buckled configuring of the airplane. It is henceforth evident that the analysis of the static aeroelastic trim must form the basis of the calculation of aerodynamic derivatives as well as the research for aircraft stability.

Static aeroelasticity of helicopter refers to as the study of helicopter structural deflection (the structure are normally flexible), when dealing with aerodynamic weights or loads, given the forces and movements are time-independent for instance aerodynamic upward force or lift and motion toward a wing rely on the occurrence of every chord-wise flight strip. These two heavy loads make the wing flex and turn, therefore altering the occurrence, and as a result, the aerodynamic moves and alters the loads or forces applied on the wing, and the result deflections till an equilibrium state is normally attained. The contact between deflections of the wing structure and aerodynamic forces influences the bending of wings and turns at every flight state, therefore it must be regarded for aeroelastic manner modeling. The contortion of static aeroelastic is vital in the stable flight state because it controls the lift distribution, control surface effectuality, and behavior of helicopter trim, forces of drag, and control aspects, and stableness. Divergence is defined as a state or condition that happens if the moments or the turning forces as a result of aerodynamic forces conquer the reinstating forces because of stiffness of the structure, therefore leading to failure of the structure. The common kind of divergence is a torsional divergence of wings. It is important to note that the first helicopter made by the Wright brothers failed because of the divergence onset.

Static Aeroelastic Action of a 2-D Stiff Airfoil attached with a Spring

At first, the aeroelastic action is regarded with a help of the iterative method, and a direct or single-step method is used after.

Iterative method



Assume that the above 2 D airfoil has a chord denoted as c and unit span, and the slope of lift as σ . The stiff airfoil part doesn't have *inherent camber* with a spring attachment of stiffness K_θ with a length ec from the centre of aerodynamic to the $1/4$ chord. The initial angle of incidence is denoted as θ_0 and turns via a certain angle that is not known (denoted as θ). The incidence is a result of the aerodynamic forces. When the aerodynamic effect decreases the stiffness, kinetic pressure also rises. The unknown angle θ can be expressed as follows;

$$\theta = \frac{qec^2\sigma}{K_\theta - qec^2\sigma} \theta_0 = \frac{q^R}{1 - q^R} \theta_0$$

Where, q represents kinetic pressure. The elastic turn is not finite as q tends to reach $1/R$ hence definition of the term known as speed of divergence which is expressed as

$$q_{div} = \frac{1}{R} = \frac{K_\theta}{qec^2\sigma}$$

And this is represented in the equation below;

$$\theta = \frac{(q/q_{div})}{(1 - q/q_{div})} \theta_0$$

The above analysis shows that the divergence physical state takes place when dynamic lurching forces conquer the recovering moment of the structure. Practically the structure will definitely fail because deflections are infinite and hence infeasible. It is important to note that the direct method that is illustrated above is only possible when dynamic moments are mathematically associated with the bends or deflections. The above approach is also known as 'strongly coupled' and it is widely known and traditional as well when dealing with aeroelastic calculations.

Static Aero-elastic Action of a flexile wing situated at the root

A more naturalistic illustration of Static Aero-elastic action of a flexile wing situated at the wing root is assessed. Here a *rectangular wing* containing chord denoted as c , *semi span* which is denoted as s , airfoil part that is symmetric and no initial turn is considered. The axis of elasticity that is denoted as GJ is situated at a length ec from the centre of aerodynamic to the $1/4$ chord and the stiffness of wing, assuming the incidence of the root (denoted as θ_0) is unchanged, however the helicopter trim in stable flight is disregarded. For easy understanding, the change in elastic turn of wing containing span is described or explained by the following linear equation

$$\theta = \frac{y}{s} \theta_r$$

θ_r is the turn at the tip of wing and the wing turn rises away from the root in a linear manner.

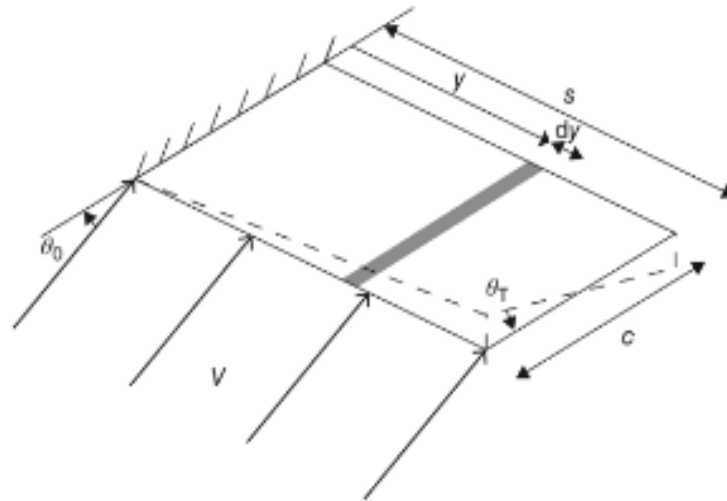
Divergency and turn of the wing which is flexible and with an unmovable root

The aerodynamic lift is opposed at the Centre due to symmetricity of the part and no lurching forces. Therefore use lift equation that considers wing turn and the root occurrence; the following is the equation where dy represents a strip and a_w represents curve gradient of the lift

$$dL = qca_w \left(\theta_0 + \frac{y}{s} \theta_r \right) dy$$

When the aerodynamic lift rises, the length from the root also rises or increases and the overall wing lift is determined through integration

Rectangular wing having an unmovable root



$$L = \int_0^y qca_w \left(\theta_0 + \frac{y}{s} \theta_r \right) dy = qca_w \left(s\theta_0 + \frac{s}{2} \theta_T \right)$$

The dynamic energy is zero that is T is equal to zero because there is no wing movement. The energies of strain and elasticity are consistent because of wing turn. This is provided by the following equation

$$U = \frac{1}{2} \int_0^y GJ \left(\frac{d\theta}{dy} \right)^2 dy = \frac{1}{2} \int_0^y GJ \left(\frac{\theta_T}{s} \right)^2 dy = \frac{GJ}{2s} \theta_T^2$$

The turn angle with an increment is expressed in form of a co-ordinate (incremental) such that;

$$\delta\theta = \frac{y}{s} \delta\theta_T$$

The work done by kinetic forces is calculated by regarding the lurching forces imposed on every strip operating by the wing turn angle by increment. The change in the overall work done δW is got through integration, therefore the work done can be expressed as follows.

$$\begin{aligned} \delta W &= \int_0^y dL e c \delta\theta = \int_0^y qca_w \left(\theta_0 + \frac{y}{s} \theta_T \right) e c \delta\theta dy \\ &= \int_0^y qc^2 a_w \left(\theta_0 + \frac{y}{s} \theta_T \right) e \frac{y}{s} \delta\theta_T dy = qec^2 a_w \left(\frac{s\theta_0}{2} + \frac{s\theta_T}{3} \right) \delta\theta_T \end{aligned}$$

θ_T can also be got by the help of equations of Lagrange as follows

$$\frac{GJ\theta_T}{s} = qec^2 a_w \left(\frac{s\theta_0}{2} + \frac{s\theta_T}{3} \right), \text{ therefore } \left(\frac{GJ}{s} - qec^2 a_w \frac{s}{3} \right) \theta_T = qec^2 a_w \frac{s\theta_0}{2}$$

In general, the equation above can be written in the following form

$$\rho V^2 C(\theta + \theta_0) + E\theta = 0$$

Now, the aerodynamic effect decreases toughness or stiffness of the structure therefore the *elastic tip turn* is derived from Equation below

$$\theta_T = \frac{3qec^2s^2a_w}{6GJ - 2qec^2s^2a_w} \theta_0$$

When the tip wing turn rises, the kinetic pressure also increases and it acts with the same behaviors of that typical turn for 2 D airfoil connected with spring. If the divergence state is attained, the wing turn has infinity, however, in real life, the structure will first fail. For this case of the wing which is flexible and with an unmovable root, the kinetic pressure at the point of divergence which is denoted by q_w is as follows

$$q_w = \frac{3GJ}{ec^2s^2a_w}$$

Regarding the equation above, it is feasible to make implications in order to raise the speed of divergence so as not to take place inside the helicopter. When the distance from the axis of elasticity to the point of aerodynamic is small, the GJ that is the inflexibility of Flexure becomes big and the speed of divergence also becomes great. When the axis of elasticity is on the line of the 1/4 chord, turning doesn't occur because of aerodynamic forces and hence there will be no divergence. When the axis of elasticity is in front of the point of aerodynamic, the moment of the aerodynamic will be negative, the tip turns nose dive and there will be no divergence as well.

Change in lift along the wing (Flexible)

After finding the turn of the wing, the respective dispersion of lift along the wing may as well be found. The lift of each unit of wing span is determined as follows

$$\frac{dL}{dy} = qca_w \left(\theta_0 + \frac{y}{s} \theta_r \right) = qca_w \left(1 + \frac{3qec^2s^2a_w}{6GJ - 2qec^2s^2a_w} \frac{y}{s} \right) \theta_0$$

This can be expressed in form of the Kinetic pressure at the point of divergence i.e

$$\frac{dL}{dy} = qca_w \left(1 + \frac{3(q/q_w)}{2(1 - (q/q_w))} \frac{y}{s} \right) \theta_0$$

Figure 1

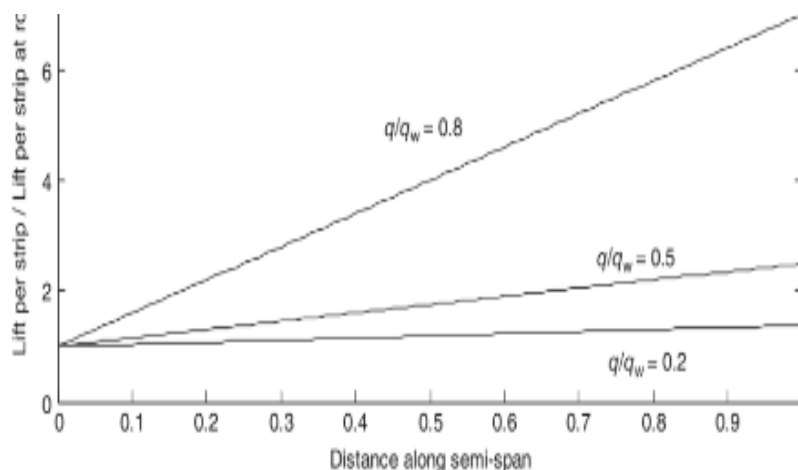


Figure 1 shows Lift of each unit of wing span for various kinetic energy.

When the speed of air rises, there is a generation of more lift and therefore kinetic energy rises. When the kinetic pressure q reaches the state of divergence for the wing situated at the root, the sum of lift gets to infinity.

Impact of Helicopter attitude/Trim on Static Air-elastic Action

The illustration above indicates that an increase in the speed will lead to an increase in the turn of the wing and therefore the lift will also increase. However, practically, a variation in the speed of air will need the attitude or the trim of the helicopter to be changed through the elevator such that aerodynamic, propelling forces, and inertia equilibrium are retained.

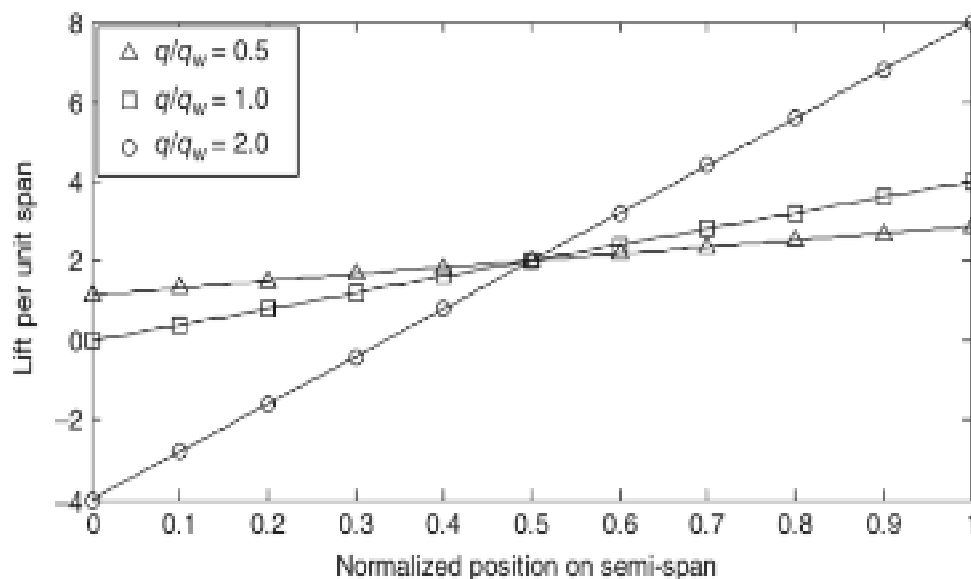
Impact of Helicopter trim on change in lift along the blade/wing

Considering θ_0 and θ_r as elements of the kinetic pressure. If the equations of θ_0 and θ_r are substituted into equation below for the distribution of lift that is Lift of every unit of wing span, the following expression is as follows;

$$\frac{dL}{dy} = \frac{w[2+q/q_w(3y/s-2)]}{4s[1-q/(4q_w)]}$$

Figure 2 shows how lift is distributed along the wing span for helicopter with trim at different normalized kinetic pressures.

The lift rises in linear form from the bottom (the root) to the top (the Tip). The lift is negative near the bottom above the speed of divergence. Because the trim of helicopter has to be retained, the overall lift must be unchanged and hence the area below every line in the illustration above is unchanged.



2.3. Aeroelastic behavior of the tandem helicopter model in Hover Flight mode

The reaction of the tandem helicopter to the differences in a gust is a bit different from others (helicopters). This is common if the staggering aerodynamic force of the rotors of the tandem helicopter creates a coupling impact. The role of the rotors in the staggered aerodynamic model which is in a dissimilar state makes the rotors move at a large angle of flight. Nevertheless, the different aerodynamics create collaborations with the changes in the flap of the rotor blades. As a result of the load and non-linear aerodynamics forced by the movement of the blade, the interior dynamic stress of the blades goes to the maximum. The stress damages the performance of the rotors which later affects the tandem-rotor helicopter as a whole. If gust is present, it (pressure) may lead to increased deflections of the blades due to disturbances imparted to the rotors hence leading to their (blades) failure. A tandem-rotor helicopter faces a large number of flight conditions with different roles and aims namely; maximum hover and a great maneuvering pace. The hover situation is such a significant design since it controls power requirements with the aid of the pilot. Correct value estimations of the rotor aerodynamics like thrust require the best gust modeling signs. The front rotor of the tandem-rotor helicopter is employed to critically analyze the signs of the helicopter caused by dissimilarities in the gust shapes. The effect of the gust and its shape towards the response of the rotor tandem are very strong.

The rotors function using the interchanging stall flow. These pass through the rotors and are quite difficult for flight. They are located near the root of the blades of the tandem helicopter. Additionally, dynamics make up some of the broadest aeroelastic phenomena also it should also be noted that static aeroelastic occurrences are equally fundamental. It is possible for aeroelastic as well as structural-dynamic occurrences to result in what can easily be hazardous static as well as dynamic instabilities and deformations (Brown and Leishman, 2002). It is for that reason that their importance in terms of the applicable consequences with major aspects of technology can hardly be ignored. The nonlinear aerial pressure and the temporary inertia force the blades to deflect in large directions. Therefore, the quasi aerodynamics are not reliable to the fullest to be used in the dynamic gust. In reference to the differing aerodynamic model, an appropriate model for the rotors was formed by Chopra. He (Chopra) continued to calculate the shear force to find out the gust effect on the tandem-rotor helicopter (Cao, et al. 2002). Given the design of the rotor tandem helicopter, creating a correct estimation of the dynamic load as a result of gust provides a reference to its stability. The rotor damage as a result of gust changes the load on the rotor in the hover flight mode. The rigid model doesn't consider the rotor damage impact.

B. EFFECT OF STRUCTURAL FLEXIBILITY ON THE DISTRIBUTION OF LOADS IN THE HELICOPTER

BODY

Case Study: Analysis of the variation of the Structural Flexibility and the distribution of loads in the helicopter body using MATLAB and SIMULINK

This analysis involved the appropriate variation, that is, the decrement and increment of the structural stiffness properties of the various segments of the structural model and a subsequent simulation of each configuration for the distribution of the force and moment loads in the structural model of the tandem-rotor helicopter performed with MATLAB as shown in the figure below.

C. EFFECT OF STRUCTURAL FLEXIBILITY ON CONTROLLABILITY OF THE TANDEM-ROTOR HELICOPTER

Case Study: Analysis of the variation of the Structural Flexibility and the Control Effectiveness of the helicopter body using MATLAB and SIMULINK

This analysis involved the appropriate variation, that is, the decrement and increment of the structural stiffness properties of the various segments of the structural model and a subsequent simulation of each configuration for the change in the kinematic parameters such as the change in the pitching rate, in the aerodynamics model of the tandem-rotor helicopter performed with MATLAB as shown in the figure below.

D. ANALYSIS OF STRUCTURAL DEFORMATIONS OF THE TANDEM-ROTOR HELICOPTER

The deformations setup in the tandem-rotor helicopter's body structure is purely a result of the aeroelastic behavior of the helicopter mechanical system which involves the mutual interaction of both the aerodynamic and the structural loads. Such deformations must be carefully analyzed and evaluated in the design process of the tandem-rotor helicopter so that they never exceed certain safe limits. Deformation of the tandem-rotor helicopter occurs in its rotors most especially when the meantime to failure is if ranging between 350 to 650 hours. It occurs in the blades between 0.5 to 0.8 radius and in between their faces. The deformation amount is determined by the profile gauge and doesn't exceed 7.8 mm for the case of the tandem-rotor helicopter. The rotors of the tandem helicopter are made using a sandwich material that incorporates a carbon beam. It contains polyurethane a material that makes the rotors weight and boosts their strength. By use of the deformed blade, cracks are formed in the working face of the rotors and the downside. Cracks are formed near the interface together with the cracks. As a result of behaviors of vitality, the landing material is employed as an energy absorber. The challenge is worsened when the material of the rotors has joints and related nonlinearities. This is a real problem for the tandem-rotor helicopter since there may be a large volume of the riveted joints to facilitate further modeling. The joints on the rotors that are based on contact pressure to keep the assembly of other helicopter parts are not modeled

E. ANALYSIS OF THE DOWNWASH DRAG EFFECT ON THE TANDEM HELICOPTER

The effect of the downwash drag on the aeroelasticity of the tandem helicopter was neglected in the analysis in this study since its magnitude is relatively low as compared to the heavy-duty design payloads for the helicopter. However, an effort was made in this section to find the possible most efficient and optimal shape of the helicopter's body for a minimum downwash drag on the helicopter by use of the NX NASTRAN Aeroelasticity Computational Fluid Dynamics (CFD) software tool as discoursed further.

F. DYNAMIC AEROELASTICITY

i. The effect of Pitching

Here, the study investigates the implication of pitching on the structural dynamics of the tandem-rotor helicopter and also establishes the safe pitching velocity boundaries for a given helicopter system configuration. Due to the speed trap of the tandem helicopter, pilots and

engineers identify pitching as the solution to controlling the upward and downward movement of the tandem-rotor helicopter. Pilots rotate the rotor in different directions by unloading cargo for it to go upwards while on the flight, or by applying a little lift when it is accelerating at a high speed. This is executed by the rotor which aids the blades to rotate differently hence facilitating the movement of the helicopter in different directions. The process of unloading the rotor to move the helicopter in different directions was mimicked from the autogiros planes. The tandem-rotor helicopter features have been improved and unloading doesn't look to be a common practice in the present manufactured helicopters. The helicopter has two coaxial rotors placed in front and behind that facilitate its pitching processes in different directions. The pilot makes use of the rotor flight controls to attain momentum and maintain the rate of acceleration at which the rotor is flying.

The variations to the tandem-rotor system provide effects to the blades that make the helicopter move in different ways. For the helicopter to pitch, it needs the controls to determine the direction of flight when the pilot is rotating it (the helicopter). This creates different forces and amounts of lifts at certain points of flight (Konstanzer, et al., 2008). To raise or reduce the level of lift of the helicopter needs the controls to provide the pilot's desired direction by use of the blades. When the helicopter flies at the same amount at the time of flight, the pilot becomes able to accelerate, ascend, decelerate, or even descent the helicopter. The tandem-rotor helicopter has three major flight control parts, namely; the pedals placed at the base of the pilot seat, the lever, and the cyclic stick placed on the motherboard of the rotor tandem helicopter. Depending on the decision of the pilot, all the above parts of a tandem-rotor helicopter can be utilized together to facilitate pitching in all directions. The governors of the rotor tandem helicopter succor the pilot to gain balance while pitching. The process of pitching leads to three main effects on the rotor tandem helicopter, namely; hovering, forward flight, and autorotation.

In hovering, a few pilots consider this effect as the most challenging during a flight. It is because the tandem-rotor helicopter becomes unstable in the process of hovering. It implies that deviations attained by the tandem-rotor helicopter at any given level of flight are not controlled by the pilot. The pilot is forced to apply rapidly control efforts and measures to keep the tandem-rotor helicopter at the required level and speed of flight. The pilot uses the controls in the hover mode. The cyclic is employed to reduce the drifting of the tandem-rotor helicopter in a different direction. The collective mode is used to regain the required level of flight by the pilot and the pedals are employed to control the forward flight of the tandem-rotor helicopter. The interaction of these controls makes hovering difficult in a way that the application of one, requires the employment of the other two. Therefore, it becomes a necessity for the pilot to become familiar with their use to have a smooth flight of the tandem-rotor helicopter.

The second effect is the forward flight. It involves the tandem-rotor helicopter to behave like a "fixed-wing aircraft" while flying. It makes movements in a cyclic way with its nose pointing forward and downwards at a high level of acceleration. It involves a reduction in the altitude, while an increase in the altitude is brought about by the tandem-rotor helicopter moving its nose up and making it climb up at a slow pace. The increase of the tandem-rotor helicopter's power on the flight while maintaining a constant speed forces it to go upwards while reducing its power makes it descend. The pedals are employed to keep a balanced flight. They are used to maintain the tandem-rotor helicopter in one direction at the desired speed.

Autorotation being the third effect involves the two rotors turn due to force from air moving upwards imparting a force on them (rotors). It involves the tandem-rotor helicopter moving without the application of the engine. It is not a common scenario but it is evidenced in circumstances when the tandem-rotor helicopter fails to land safely in case one or both of the rotors fail or the engine. In the normal flight of the tandem-rotor helicopter, air draws into its rotors from above and it is exhausted in the descending motion. Nevertheless, in auto rotation, air moves up into the two rotors from below as the tandem-rotor helicopter falls. Autorotation is a safe process in some cases since it incorporates the two rotors to continue rotating even when the engine ceases its functions. Pilots employ it for safe landing when the engine fails to respond.

G. THE EFFECT OF ROLLING

Here, the study investigates the implication of rolling on the structural dynamics of the tandem-rotor helicopter and also establishes the safe rolling velocity boundaries for a given helicopter system configuration. Rolling on the tandem-rotor helicopter appears in two ways, namely; the dynamic rolling and the static rolling. Dynamic rolling occurs when the tandem-rotor helicopter is near the landing area while starting a flight or landing. In dynamic rolling, a couple of factors have to influence the tandem-rotor helicopter to make a roll in the desired critical angle of the pilot. When the rotor tandem exceeds the pilot's desired angle of rolling, its rotors proceed with the rolling process and make the recovery of the normal speed and altitude impossible. This makes the tandem rotor fly sideways with the cyclic control having no control over it. The dynamic control initiates when the pilot pivots the tandem-rotor in the area of the wheels. It also occurs when the landing was not appropriate landing or take-off of the tandem-rotor helicopter. The process of dynamic rolling becomes evident when the gear becomes the pivot place and no alternative procedure is being carried out by the pilot. When the rolling initiates, it cannot be ceased by employing the cyclic control measure(Su and Cao, 2002).

Static rolling occurs when the tandem-rotor helicopter blades are not rotating. When the blades cease rolling, the rotor tandem possesses similar principles to all other objects in the static mode. However, it will not roll when it flies beyond the critical angle. For the tandem to roll, the pilot moves its cyclic to the left or right. This applies force to the front and aft rotors hence making them make tilts in opposite directions. The rolling control is incorporated in the cyclic stick of the tandem rotor.

H. THE EFFECT OF YAWING

Here, the study investigates the implication of yawing on the structural dynamics of the tandem-rotor helicopter and also establishes the safe yawing velocity boundaries for a given helicopter system configuration.

Case Study: Analysis of the Effect of yawing on the structural dynamics of the tandem-rotor Helicopter model using MATLAB and SIMULINK

The analysis thus involved the appropriate variety of the yawing value and yaw rate values of the aerodynamic model and a subsequent simulation of each configuration for the corresponding variation of the distribution of the force and moment loads in the structural model of the tandem-rotor helicopter performed with MATLAB as shown in the figure below.

I. THE EFFECT OF ECCENTRICITY OF THE PAYLOAD IN THE FUSELAGE

Here, this analysis investigates the effect of the variation of the eccentricity of the payload in the fuselage on the structural dynamics and the degree of controllability of the aerodynamics model of the tandem-rotor helicopter and also establishes the safe yawing velocity boundaries for a given helicopter system configuration.

Case Study: Analysis of the Effect of variation of the eccentricity of the payload in the fuselage on the structural dynamics the degree of controllability of the tandem-rotor Helicopter model using MATLAB and SIMULINK

The analysis, therefore, involved the appropriate variety of the eccentricity of the payload in the fuselage in the structural model and a subsequent simulation of the aeroelastic model for each configuration for the corresponding change in the kinematic parameters such as the change in the yawing rate, in the aerodynamics model of the tandem-rotor helicopter performed with MATLAB as shown in the figure below.

4. Results

3. Aeroservoelastic solutions

Active Control of Aeroelastic Stability and Response (that is, Vibration) in Rotorcraft

Quite possibly the most exhaustive investigations on air reverberation concealment, in float and forward flight, utilizing cutting edge pitch control was done by Takahashi and Friedmann. The model comprised of a coupled rotor-fuselage framework addressing a four-bladed hingeless rotor appended to an unbending fuselage with pitch and roll levels of opportunity. The regulator worked through an ordinary swash plate that acquainted a similar pitch contribution with every one of the cutting edges. The regulator configuration depended on an ideal state assessor joined with ideal input gains. Ideal circle shapes were planned to utilize the circle move recuperation approach. The result of this plan interaction brought about a basic regulator that utilized a solitary roll rate estimation in the body (non-pivoting outline), and smothered air reverberation by utilizing a sine and a cosine swashplate input. In this examination, we will frequently utilize the swashplate to stifle aeroelastic conduct impacts in the underlying elements of the pair rotor helicopter by controlling the rolling and pitching second contribution to the primary elements control framework. The undertaking to create rotorcraft having a "stream smooth" ride has moved the accentuation in the space of vibration lightening (that is, a decrease of aeroelastic reaction) from the less dependable common aloof method for vibration decreases like vibration safeguards and isolators to dynamic control techniques. Severe prerequisites on vibration levels take a stab at vertical speed increases beneath 0.05g at most fuselage areas. These prerequisites imply that the couple rotor helicopter producers might endure the cost related to a functioning control framework that works in the pivoting outline, that is, the rotor. When such a control framework is available, it can likewise be utilized for extra destinations, for example, clamor decrease, execution upgrades, and adjustment of aeroelastic conduct. This segment talks about the solid servomechanical framework control systems in the two regions, adjustment of aeroelastic and aeromechanical conduct, and vibration decrease in rotorcraft utilizing dynamic controls with circled criticism instruments.

Automatic control systems have been demonstrated to help prevent or limit flutter-related structural vibration.

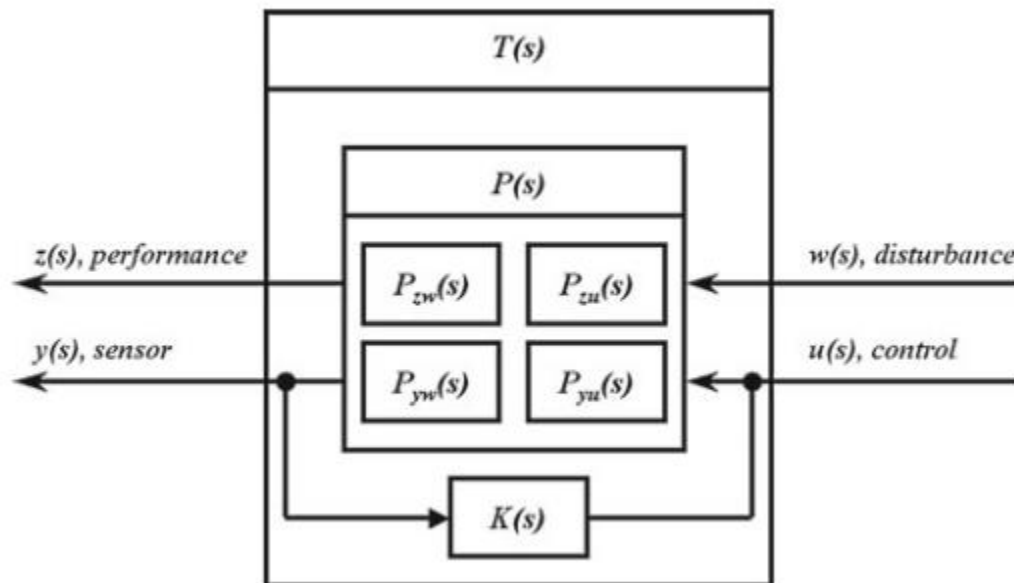


Figure 5 : General schematic of the Tandem-rotor helicopter's control system model

A. STATE SPACE MODELS

Situations happen, rather often, where a portion of the properties of a powerful framework can't be communicated straightforwardly as steady coefficients in a mass, damping, or solidness network. On the off chance that the issue is figured in the recurrence space, as are numerous issues in aeroelasticity and hydroelectricity, terms might happen that have other than steady, direct, or quadratic reliance on the base recurrence. These terms may, nonetheless, be communicated as recurrence subordinate coefficients in the mass, damping, or firmness lattices. This presents some level of ungainliness in the Eigen-esteem extraction, yet it's anything but a significant burden in recurrence reaction examination. In order to efficiently solve such challenges, we have to use the state-space representation of the aeroelastic model of the tandem-rotor helicopter that is, state-space representations of both the aerodynamic and structural dynamic models of the helicopter. The figure below shows the step response of the unaugmented open-loop aerodynamic model of the tandem-rotor helicopter. The figure shows that in the open-loop aerodynamic model, all the output parameters take too (up to 300 seconds) to attain a steady-state, thus the model itself is steady as the different output parameters, such as advance velocity V_x , pitch angular velocity ω_y , pitch angle Θ , longitudinal control angle of the rotor β and vertical velocity V_z respectively, eventually achieve steady-state values, given that the input is a step signal of the cyclic longitudinal input.

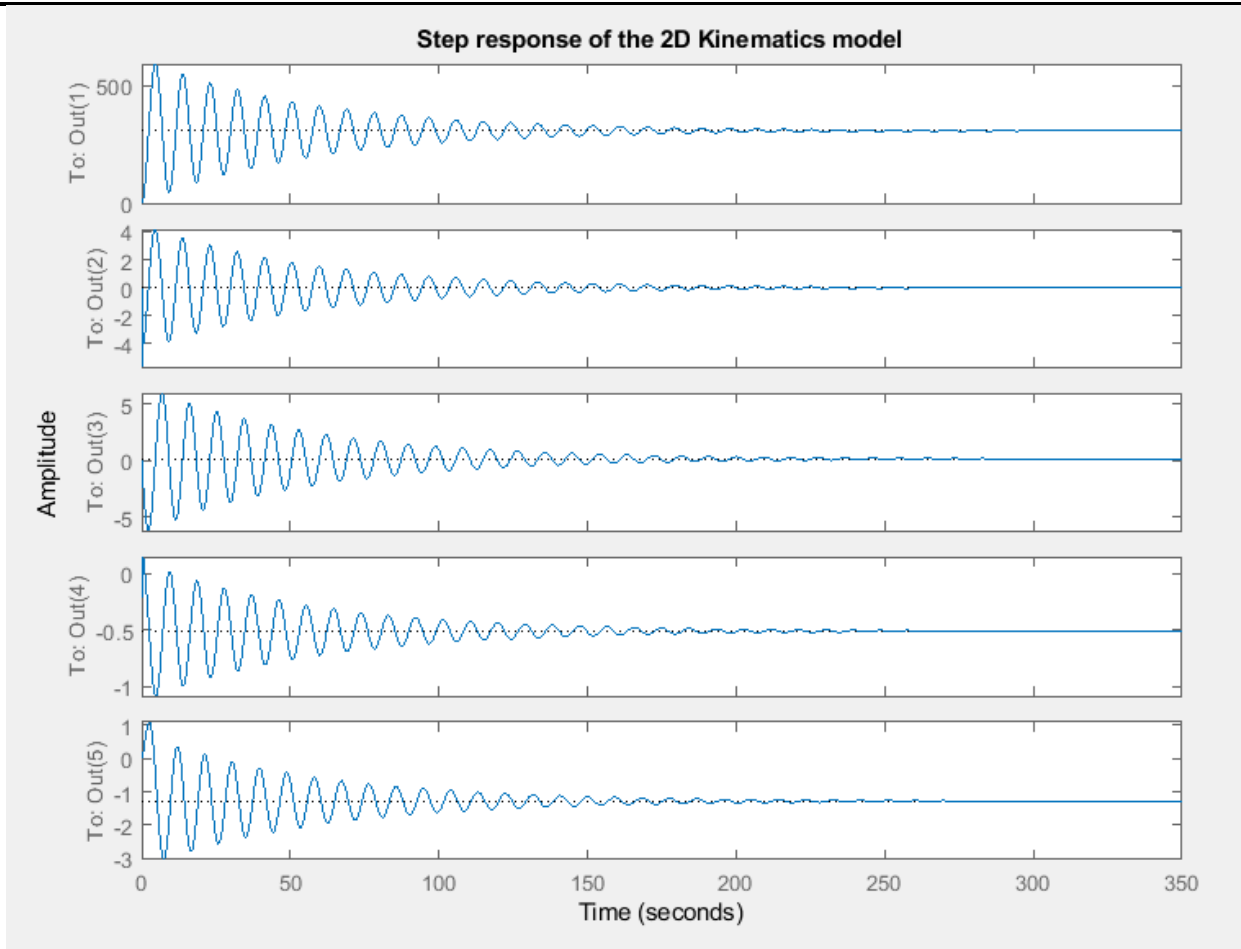


Figure 6: Step response of the unaugmented open loop aerodynamic model of the tandem-rotor helicopter

The figure below shows the continuous *ramp* response of the unaugmented open loop aerodynamic model of the tandem-rotor helicopter. However, unlike for the case of step signal input, here the figure shows that in the open loop aerodynamic model, all the output parameters never attain a steady state and the system is persistently unstable, thus the model itself is unsteady as the different output parameters, such as, advance velocity V_x , pitch angular velocity ω_y , pitch angle Θ , longitudinal control angle of the rotor β and vertical velocity V_z respectively, never achieve steady state values with a continuous ramp input of the cyclic longitudinal signals.

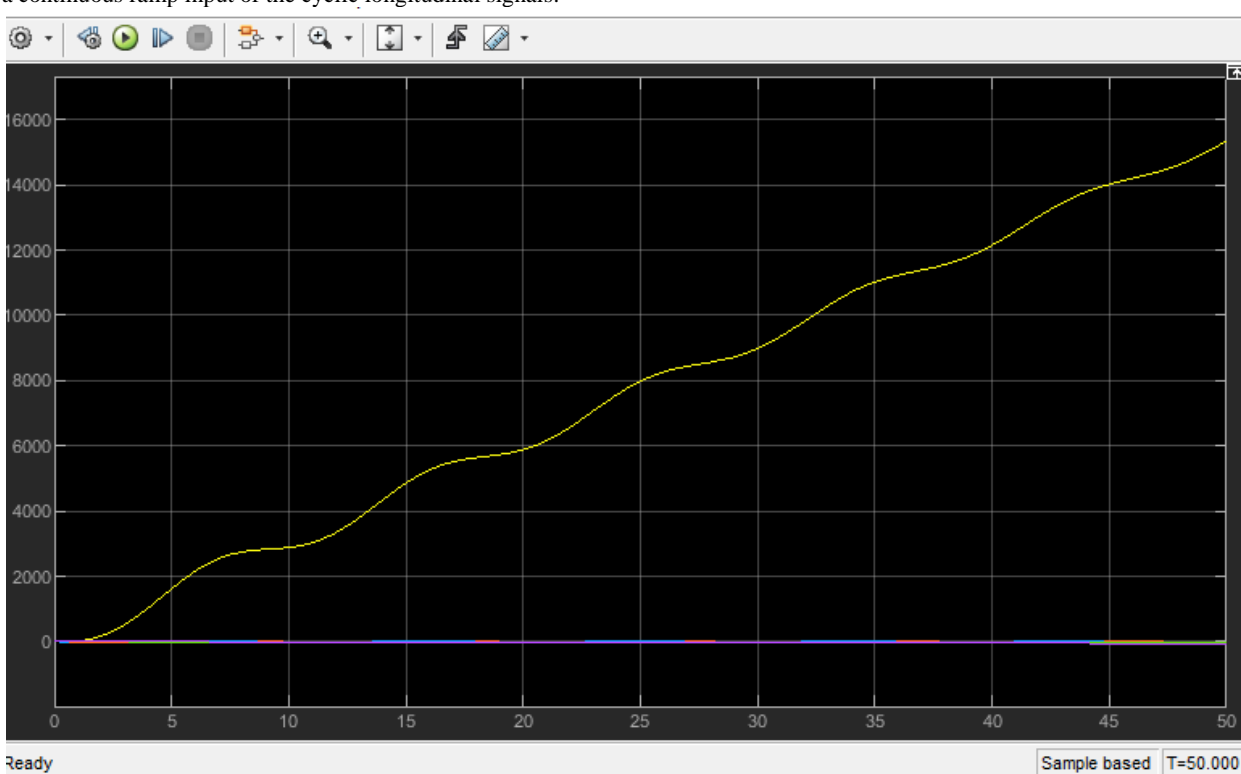


Figure 7: Ramp response of the unaugmented open loop aerodynamic model of the tandem-rotor helicopter

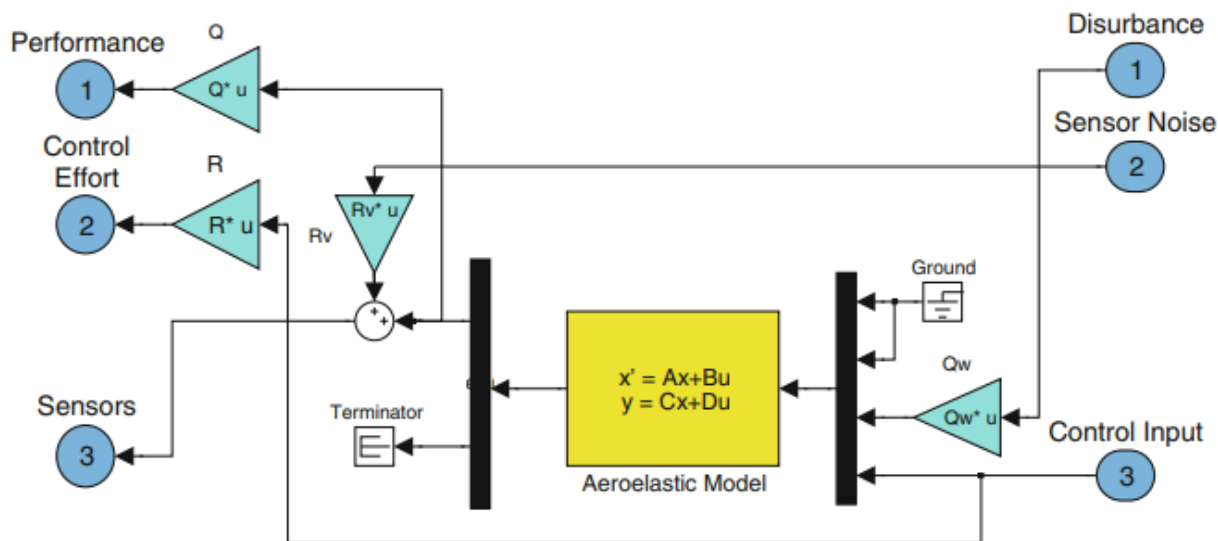


Figure 8 : System augmentation for H-infinity controller of the tandem-rotor helicopter feedback control

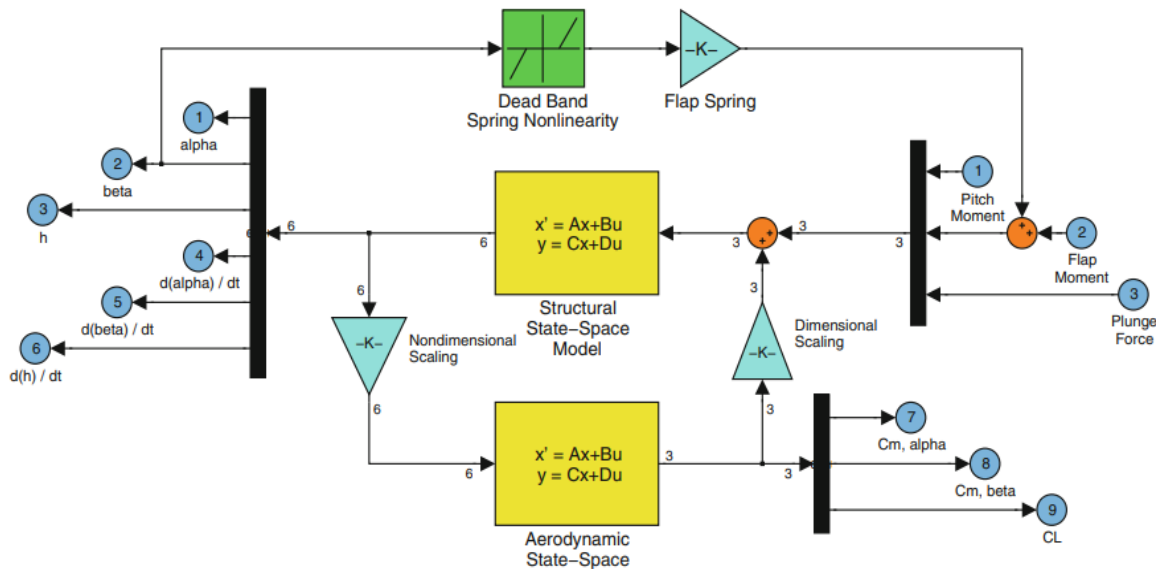


Figure 9 : Chosen model design of the state space representation of the tandem-rotor helicopter closed loop feedback control system with dead band nonlinearity

3.2. System Stability characteristics from Eigen-value Analysis

Problems of stability as far as aeroelasticity is concerned are Eigenvalue in nature. When subjected to a specific set of conditions such as the Hermitian symmetry of the kernel or Hermitian self-adjointness, it is always evident that there is an existence of eigenvalues. It is also always shown that they don't just exist but are subject to real valuation. It is further indicated that these eigenfunctions do form what is referred to as a "complete" form of functions and that these functions form the basis for the conclusion that the iteration procedure associated with the calculation of the eigenfunctions and values is valid. In the same manner, it forms a solid basis from which to prove that the bounds to the values of the eigen can indeed be projected. Notably, though, this cannot be said when it comes to non-self-adjoint complications. It is worth noting that the eigenvalues are generally complex and might not exist most of the time. It is therefore questionable how complete the eigenfunctions are and because of such doubts, there is a need for the reexamination of the ordinary proofs regarding the convergence of the procedure of iteration. It is also not yet known if there are simple approximation eigenvalues bounds. It could equally be asserted though that some of the more recent studies undertaken have already demonstrated a significant amount of results. Wielandt's proof 1124 which asserts that it is possible to make use of the classical iteration technique is one of the most highly sought-after discoveries. It is essential, especially when making attempts to find the eigenvalues if at all they do exist. In the same manner, it is essential in terms of figuring out the eigenfunctions relating to non-self-adjoint equations. In terms of the practical calculation methods, Lanczos's "minimized iterations" method has proven itself as highly powerful and labor-saving as possible. This is especially so when there is a desire for various

eigenfunctions and values. On the other hand, Wielandt's "iterative revolution" technique [11-24-11-26] has proven its usefulness in terms of its applicability to the structural deformation failure criteria complications especially for a tandem-rotor helicopter as well as other related eigenvalue complications. By simply applying for a slight extension, Wielandt does provide gebrochene iteration as demonstrated by procedures 11-24. This can be useful especially when it comes to the correction of a particular approximation regarding any random greater eigenvalue as well as the conforming eigenfunctions and this can be done without necessarily having to know the preceding values eigen. The methods developed by Wielandt and Lanczos are highly applicable when it comes to algebraic (matrix), integral operators as well as differentials. These are of greater importance especially when it comes to the study of the fundamental questions within the field of aeroelasticity as well as in the investigation of the approximate solutions. In contrast, though, solutions concerning the non-homogeneous equations which have their basis on the expansion of arbitrary function have been developed by Flax [7-1 A]. Some of these solutions include a series of the biorthogonal functions, the "adjoint energy function concept as well as the variational standard which has a relationship with the Rayleigh-Ritz type procedure.

3.2.1. Eigen value analysis for the two space dimensional kinematic model of the tandem-rotor helicopter

$$\begin{bmatrix} \dot{V}_x \\ \dot{\omega}_y \\ \dot{\theta} \\ \dot{\beta} \\ \dot{V}_z \end{bmatrix} = \begin{bmatrix} X_u & X_q & X_\theta & X_\beta & X_w \\ M_u & M_q & 0 & M_\beta & M_w \\ 0 & 1 & 0 & 0 & 0 \\ B_u & -1 & 0 & B_\beta & 0 \\ Z_u & Z_q & Z_\theta & Z_\beta & Z_w \end{bmatrix} \cdot \begin{bmatrix} V_x \\ \omega_y \\ \theta \\ \beta \\ V_z \end{bmatrix} + \begin{bmatrix} X_\delta \\ M_\delta \\ 0 \\ B_\delta \\ Z_\delta \end{bmatrix} [\delta]$$

For non-trivial solutions, the eigen-value problem would be such that;

$$\begin{bmatrix} \dot{V}_x \\ \dot{\omega}_y \\ \dot{\theta} \\ \dot{\beta} \\ \dot{V}_z \end{bmatrix} - \begin{bmatrix} X_\delta \\ M_\delta \\ 0 \\ B_\delta \\ Z_\delta \end{bmatrix} [\delta] = \begin{bmatrix} 0 \\ 0 \\ 0 \\ 0 \\ 0 \end{bmatrix} = \begin{bmatrix} X_u & X_q & X_\theta & X_\beta & X_w \\ M_u & M_q & 0 & M_\beta & M_w \\ 0 & 1 & 0 & 0 & 0 \\ B_u & -1 & 0 & B_\beta & 0 \\ Z_u & Z_q & Z_\theta & Z_\beta & Z_w \end{bmatrix} \cdot \begin{bmatrix} V_x \\ \omega_y \\ \theta \\ \beta \\ V_z \end{bmatrix}$$

So, we need to find a solution of $\begin{bmatrix} V_x \\ \omega_y \\ \theta \\ \beta \\ V_z \end{bmatrix}$ that satisfies the above relation as shown below.

The eigen-vector solution for the stability analysis of the two dimensional tandem-rotor helicopter kinematic model computed with MATLAB is shown below while the MATLAB code used to compute the eigen-value solution is shown in Appendix B

```
>> A = [X_u, X_q, X_theta, X_beta, X_w;
        M_u, M_q, 0, M_beta, M_w;
        0, 1, 0, 0, 0;
        B_u, -1, 0, B_beta, 0;
        Z_u, Z_q, Z_theta, Z_beta, Z_w];
eig(A)
ans =
-4.5627 + 7.8783i
-4.5627 - 7.8783i
-0.0178 + 0.6832i
-0.0178 - 0.6832i
-0.5727 + 0.0000i
```

3.2.2. Eigen value analysis for the Unaugmented kinematic model of the tandem-rotor helicopter

$$\begin{bmatrix} \dot{u} \\ \dot{w} \\ \dot{q} \\ \dot{\theta} \\ \dot{V} \\ \dot{p} \\ \dot{r} \\ \dot{\Phi} \\ \dot{\Psi} \end{bmatrix} = \begin{bmatrix} x_u & x_w & (x_q - W_o) & -g & 0 & 0 & 0 & 0 & 0 \\ z_u & z_w & (z_q - U_o) & 0 & 0 & 0 & 0 & 0 & 0 \\ M_u & M_w & M_q & 0 & 0 & 0 & 0 & 0 & 0 \\ \overline{0} & \overline{0} & 1 & 0 & 0 & 0 & 0 & 0 & 0 \\ 0 & 0 & 0 & 0 & Y_v & (Y_p + W_o) & (Y_r - U_o) & g & 0 \\ 0 & 0 & 0 & 0 & \left(L_v + \frac{I_{xz}}{I_{xx}} N_v\right) C_p & \left(L_p + \frac{I_{xz}}{I_{xx}} N_p\right) C_p & \left(L_r + \frac{I_{xz}}{I_{xx}} N_r\right) C_p & \frac{0}{-} & \frac{0}{-} \\ 0 & 0 & 0 & 0 & \left(N_v + \frac{I_{xz}}{I_{zz}} L_v\right) C_r & \left(N_p + \frac{I_{xz}}{I_{zz}} L_p\right) C_r & \left(N_r + \frac{I_{xz}}{I_{zz}} L_r\right) C_r & \frac{0}{-} & \frac{0}{-} \\ 0 & 0 & 0 & 0 & 0 & 1 & 0 & 0 & 0 \\ 0 & 0 & 0 & 0 & 0 & 0 & 1 & 0 & 0 \end{bmatrix} \begin{bmatrix} u \\ w \\ q \\ \theta \\ V \\ p \\ r \\ \Phi \\ \Psi \end{bmatrix}$$

Where;

$$C_p = \left(\frac{I_{xx} I_{zz}}{I_{xx} I_{zz} - I_{xz}^2} \right)$$

$$C_r = \left(\frac{I_{xx} I_{zz}}{I_{xx} I_{zz} - I_{xz}^2} \right)$$

The eigen-value problem for the unaugmented kinematic system above would be easily finding a solution of $\begin{bmatrix} u \\ w \\ q \\ \theta \\ V \\ p \\ r \\ \Phi \\ \Psi \end{bmatrix}$ that satisfies the equation below.

$$\begin{bmatrix} 0 \\ 0 \\ 0 \\ 0 \\ 0 \\ 0 \\ 0 \\ 0 \\ 0 \end{bmatrix} = \begin{bmatrix} x_u & x_w & (x_q - w_o) & -g & 0 & 0 & 0 & 0 & 0 \\ z_u & z_w & (z_q - u_o) & 0 & 0 & 0 & 0 & 0 & 0 \\ M_u & M_w & M_q & 0 & 0 & 0 & 0 & 0 & 0 \\ \overline{0} & \overline{0} & 1 & 0 & 0 & 0 & 0 & 0 & 0 \\ 0 & 0 & 0 & 0 & Y_v & (Y_p + w_o) & (Y_r - U_o) & g & 0 \\ 0 & 0 & 0 & 0 & \left(L_v + \frac{I_{xz}}{I_{xx}} N_v\right) C_p & \left(L_p + \frac{I_{xz}}{I_{xx}} N_p\right) C_p & \left(L_r + \frac{I_{xz}}{I_{xx}} N_r\right) C_p & \frac{0}{-} & \frac{0}{-} \\ 0 & 0 & 0 & 0 & \left(N_v + \frac{I_{xz}}{I_{zz}} L_v\right) C_r & \left(N_p + \frac{I_{xz}}{I_{zz}} L_p\right) C_r & \left(N_r + \frac{I_{xz}}{I_{zz}} L_r\right) C_r & \frac{0}{-} & \frac{0}{-} \\ 0 & 0 & 0 & 0 & 0 & 1 & 0 & 0 & 0 \\ 0 & 0 & 0 & 0 & 0 & 0 & 1 & 0 & 0 \end{bmatrix} \begin{bmatrix} u \\ w \\ q \\ \theta \\ V \\ p \\ r \\ \Phi \\ \Psi \end{bmatrix}$$

The eigen-vector solution for the stability analysis of the unaugmented tandem-rotor helicopter kinematic model computed with MATLAB is shown below whereas the MATLAB code used to compute the eigen-value solution is shown in Appendix B

I. For hover mode

eig(B)

ans =

0.0000 + 0.0000i

-0.9520 + 0.0000i

-0.2146 + 0.0000i

0.0804 + 0.3969i

0.0804 - 0.3969i

0.5033 + 0.0000i

-0.3220 + 0.0000i

-0.0560 + 0.3594i

-0.0560 - 0.3594i

II. For trimmed continuous longitudinal motion mode

eig(B)

ans =

0.0000 + 0.0000i

-0.9910 + 0.0000i

0.0953 + 0.3944i

0.0953 - 0.3944i

-0.2054 + 0.0000i

0.5569 + 0.0000i

-0.3764 + 0.0000i

-0.0556 + 0.3150i

-0.0556 - 0.3150i

III. For trimmed continuous motion mode

% non longitudinal continuous trimmed motion flight mode

eig(B)

ans =

0.0000 + 0.0000i

-0.9133 + 0.0000i

$$-0.2146 + 0.0000i$$

$$0.0611 + 0.4089i$$

$$0.0611 - 0.4089i$$

$$0.5212 + 0.0000i$$

$$-0.3170 + 0.0000i$$

$$-0.0675 + 0.3538i$$

$$-0.0675 - 0.3538i$$

There has been significant progress made particularly in attempts to model and understand nonlinear aeroelastic phenomena. Both theoretical and experimental investigations have demonstrated good correlation for several nonlinear physical instruments. From a general point of view, it could be contended that our comprehension of as well as the correlation between alternate hypothetical models and experiments needs further advancement, especially for the nonlinear mechanical mechanisms. Some of these mechanisms include free play as well as huge deflection symmetrical nonlinearities of plates and beams. This is quite different especially when related to the nonlinear fluid mechanisms like the large separated flows and the shock motions. Nonetheless, it is quite clear that there are now more precise and equally more computationally proficient theoretical models present for nonlinear aerodynamic flows. Moreover, there is reason to be positive especially when dealing with these kinds of issues moving forward. As has been underscored throughout the previous chapters, it is quite evident that several physical mechanisms have the potential or capability to lead to nonlinear aeroelastic responses. These include the impact associated with static structural nonlinearities or solid flow fluid when changing the flutter boundary for an aeroelastic system. It is quite clear though that dynamic nonlinearities are highly critical in terms of their role in the development of limit cycle oscillations, LCO response as well as the hysteresis in a flutter, and finally the sensitivity associated with both the external and initial disturbances. The most positive aspect regarding the flight vehicle designers relates to the fact that nonlinear aeroelastic impacts can cause a replacement of what in some situations be rapidly emerging and equally destructive oscillations with finite amplitude oscillations. Given the thorough and meticulous consideration as well as design devoted to the aeroelastic processes and the associated nonlinearities, there is a new possibility for enhanced performance as well as safety for the valuable models of the wind tunnel, the flight vehicles as well as the passengers and the operators. It is also noted that as soon as the nonlinear aeroelastic simulations have attained a maturity level that is sufficient enough for the consideration within the design process, the adaptive and active control mechanisms would then be able to potentially facilitate and even allow for greater performance of the flight vehicle. Reduction in the model demonstrated a capacity to cause and make it possible to achieve substantial simplification. What's even more interesting is that this is possible to achieve without suffering a critical loss in terms of accuracy. This is possible because the majority of the focus is put on the physically pertinent input/output paths as well as the bandwidth of concern. Such a reduction in the model was not shown to just be important in terms of the design for the compensators, but also demonstrated a high level of usefulness in terms of the system's physical design especially when determining the sensor placement and optimal actuator. The models analyzed above were also subjected to extensions with the major purpose of ensuring that they encompass parameter varying classifications while they could also be in a position of permitting explicit designs for gain scheduled control regulations. There has been significant progress achieved especially in terms of the modeling as well as comprehension of the nonlinear aeroelastic phenomena. There have been good correlations shown by both the theoretical and experimental investigations and this has been consistent for several of the nonlinear physical instruments.

In terms of broad generalizations, it is possible for one to assert that the general understanding of, as well as the correlation between alternate theoretical and experimental models, is much more advanced for nonlinear mechanical mechanisms than it is for nonlinear fluid mechanisms. Nonetheless, it is now more apparent that more computationally accurate and equally efficient theoretical models have become and are continuing to become readily obtainable for nonlinear aerodynamic flows. In that sense, there is the reason for the positivity principally when it comes to dealing with such issues when moving forward. Just like it has been highlighted all through this paper, various physical mechanisms have the potential to cause nonlinear aeroelastic reactions and this includes the impact of steady flow fluid or static structural nonlinearities when changing the flutter boundary relating to an aeroelastic system. It is not in doubt that dynamic nonlinearities contribute significantly towards the development of limit cycle oscillations, LCO response, hysteresis in a flutter as well as the sensitivity of both initial as well as external disturbances. On a better note though particularly for the designers of the flight vehicles is the fact that the nonlinear aeroelastic effects do ensure that the finite-amplitude oscillations do in some instances replace what would in some cases be the destructive and equally rapidly growing oscillations normally attached to the classical flutter compartment vibration deformations of the fuselage. In this sense, undertaking a careful consideration as well as the design of satisfactory nonlinearities makes it possible for the emergence of new opportunities to ensure the improvement in performance. In the same manner, it creates opportunities for the safety of the flight vehicles, the passengers as well as their operators. This study has also demonstrated that the problem of failure by structural deformations of the tandem-rotor helicopter can be effectively suppressed only by the appropriate aeroservoelastic control of the helicopter system for example, by manipulating the swash plates, unlike most other kinds of aircraft that have significant wingspans and control surfaces.

i. Eigen value analysis for the Structural dynamics model of the tandem-rotor helicopter

ii. Closed-loop Feedback Control Remedies

It can be seen that unlike most other kinds of aircraft that have significant wingspans and control surfaces, the problem of failure by structural deformations of the tandem-rotor helicopter can be effectively mitigated only by aeroservoelastically controlling the helicopter for example, by manipulating the swash plates. A reduced-order aerodynamic model was developed based upon the vortex lattice approach⁶. Thus, assumptions include subsonic, inviscid, incompressible, and irrotational flow.

5. Analysis and findings

The figure below summarises the behavior of the open-loop aerodynamic model of the tandem-rotor helicopter under various initial conditions. This clearly shows that substantial initial perturbation of the aerodynamic parameters such as the pitch, roll, and yaw angles and the advanced flight velocity all generally result in persistently destabilized aerodynamics of the tandem-rotor helicopter

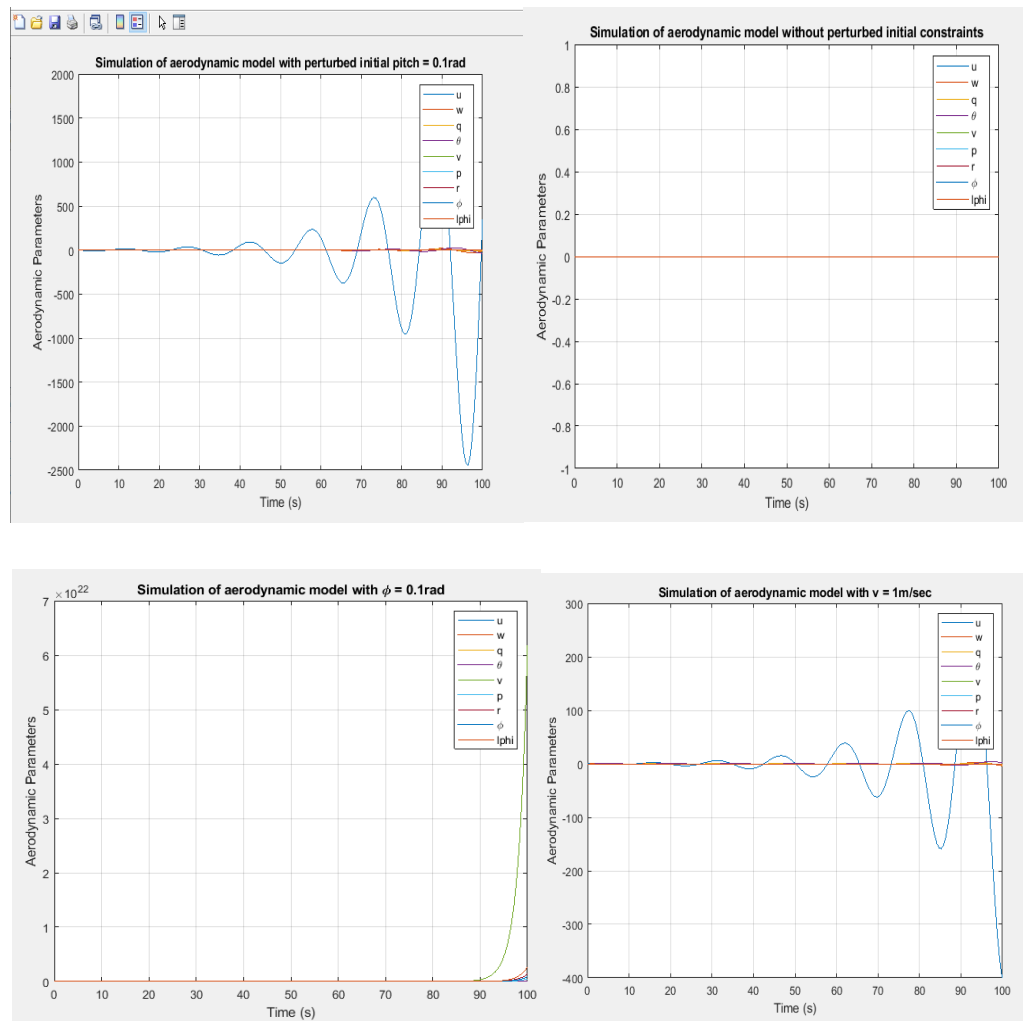


Figure 10: The behavior of the open-loop aerodynamic model of the tandem-rotor helicopter under various initial conditions.

A. COMPUTATIONAL FLUID DYNAMICS (CFD) SIMULATIONS

The aeroelastic Computational Fluid Dynamics simulations in this study were done with NX Nastran software tool using the Doublet Lattice Method which is most reliable for the subsonic compressible atmospheric environment which is characteristic of the operational environment of a tandem-rotor helicopter. The rotors of the tandem-rotor helicopter provide it with the ability to ascend. The performance of the rotors incorporates with the dynamic features of the whole tandem-rotor helicopter. In the forward movement, a compound rocky environment forms in the flow field of the tandem rotor. The situation incorporates the effects of hard vortices with one another and with the blades. This results in variations on the blades and the creation of a hard spiral wake in the rotors. These aerodynamic challenges require a couple of methods and solutions to stabilize the performance of the tandem-rotor helicopter basing on its rotors. In this study, experimental methods were executed with the NX Nastran software tool using the Doublet Lattice Method which is most reliable for the subsonic compressible atmospheric environment. This is aimed at studying the aerodynamic production from the two rotors of the tandem-rotor helicopter. These provide a reliable way for the causes and effects of aerodynamics. Today, CFD methods are increasing in number due to the increase in technology and have provided a way for increased aerodynamic simulations. These are determined and performed in a limited number of short turnarounds. The CFD methods are significant in the aerodynamic presentation of the tandem-rotor helicopter and provide a couple of numerical equations to the doublet lattice method. A number of CFD technologies are employed in the simulations of the blades. Since it provides a number of merits, the double lattice method has been employed in CDF simulation of the rotors of the tandem-rotor helicopter. The Doublet Lattice Method is appropriate for all kinds of flights and is appropriate for the aerodynamic simulation of the tandem-rotor helicopter. This method was employed in this study and will be critically analyzed in the following sections. The Double Lattice method (DLM) was initially employed in the 1970s by the United States air force. The improved version of the method is known as N5KQ and has a few upgrades in the concept of lifting surfaces. The behavior of the rotor is constant as the N5KA method that was used in the 1970s. The N5KA formula presented a numerator variation along with each rotor that helped the normal wash characteristics to be recessed.

The N5KQ replaces the NK5A with an additional quartic approximation. A great improvement in the accuracy of the new formula is got from an upgraded approximation to the integrand. The integrand is portrayed in the integral expression of the kernel equation. In the forward flight motion, the rotors of the tandem helicopter have a circular aerodynamic load. This leads to unwanted situations with consideration of the rotor hub. Consequently, rotor trimming is significant to give an improved decision between the CFD value and the real test values. The main rotor must provide a sufficient force to the trimming situations at a given moment. This means that the “rotor thrust is equivalent to the target thrust”.

$$(C_T = C_T^{\text{desired}}),$$

In the Double Lattice method situation, Pitching and Rolling = 0.

$$C_{M_z} = C_{M_z}^{\text{desired}} = 0, C_{M_x} = C_{M_x}^{\text{desired}} = 0$$

Nevertheless, the rotor parameters achieved from testing the level of speed during the setting off of the tandem-rotor plane possess a few errors. It is difficult for the situations of the CFD boundary and the parameters to be calculated accurately in the flight test. Consequently, to improve the values of the CDF simulation, the double lattice method is appropriate.

B. TANDEM-ROTOR HELICOPTER AERODYNAMIC MODEL

The aeroelastic model of the tandem-rotor helicopter was set up with NX Nastran software as shown in the figure below.

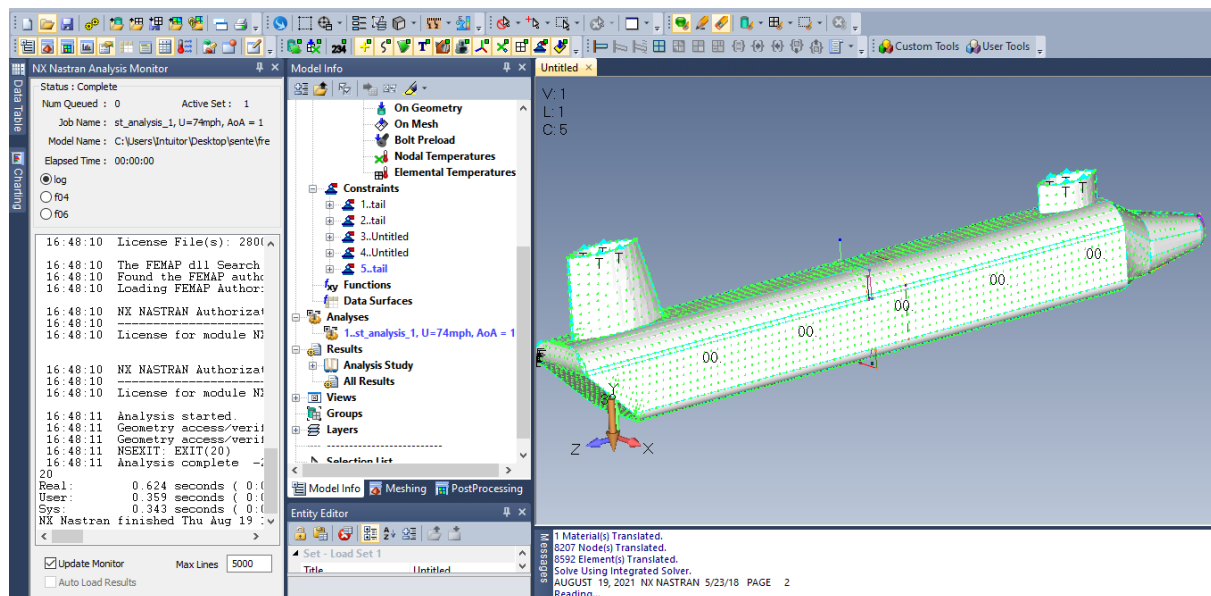


Figure 11: The aeroelastic model of the first configuration of the tandem-rotor helicopter

C. SIMULATIONS AND ANALYSIS

It is clear that as opposed to most different sorts of airplanes that have critical wingspans as well as control surfaces, failure due to structural defamations of the pair rotor helicopter do not pose a huge threat since they can be adequately moderated. This is exclusively possible by aero servoelastically managing the helicopter for instance, through the control of the swash plates

D. AEROELASTIC EFFECT OF THE DOWNWASH DRAG

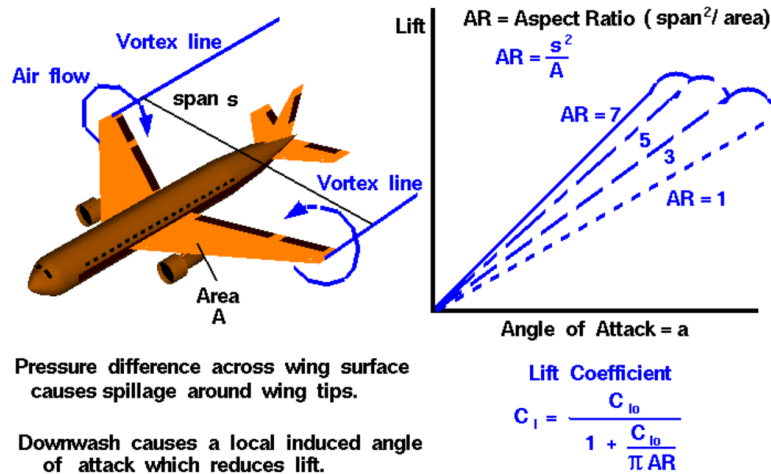


Figure 12: Aeroelastic Effect Of The Downwash Drag

For what is considered the lifting wing, the air pressure that exists on the wing top is much lower when compared to the air pressure found below the lifting wing. Near the wingtips, there is a free movement of the air from a high-pressure region to a low-pressure region. The flow that results is indicated in the left-hand figure above. The two blue lines in circular shape containing arrowheads are illustrative of the directional flow. While the aircraft takes a lower left direction, there is a formation of a pair of counter-rotating vortices. These vortices are formed at the tip of the wings. The lines which mark the vortices center are indicated as the blue vortex lines which lead from the tips of the wing. In the event that the atmosphere contains very high humidity levels, it is possible to occasionally witness the vortex lines on an aircraft at the time of landing as long and yet thin "clouds" departing from the tips of the wing. The tip of the wing vortices generates a downwash of air. This is generated behind the wing and it's quite strong especially near the tips of the wing while it reduces towards the root of the wing. The wing's effective angle of attack is reduced as a consequence of the downwash-induced flow. This, therefore, provides an additional and also downstream-facing element to the aerodynamic forces which act across the whole wing.

6. CONCLUSIONS

1. It is possible to configure the tandem-rotor helicopter configurations within the VHLH class to ensure that their hover holds action/performance has similarities with the current MLH class. More particularly, these configurations are possible with the control systems which are necessary to create a possibility for the precise automatic position for hover hold as well as pilot control. These can be fused from the applicable designs of the MLH and the associated experience. The only exception to this particular rule could be within the blade lead-lag approaches and the rotor-made coupled elastic fuselage. There might be a requirement or need for special filtering to help prohibit an unwanted exacerbation for such low damping modes through the cyclic control responses.
2. The acceptance level/ rating of the pilot is principally a function associated with or relating to the automatic control as well as hover hold mechanisms. Moreover, it hardly appears to have a strong dependence on the overall or gross weight configuration for the augmented solidity tandem-rotor helicopter.
3. The most effective hover performance capabilities in terms of the scope for the control augmentation categories considered within this study are provided by the stick control for the longitudinal cyclic pitch (LCP). That is done in combination with the conformist roll control necessary to facilitate mainly a system of velocity control within the horizontal axes. The workload of the pilot and ultimately their ratings are improved in the event that inertial velocity response has been included within the stability augmentation system. It should be noted though that systems of such nature are characteristically sensitive when exposed to turbulence. When exposed, their overall position hold proficiencies will vitiate with the level of the turbulence. By improving the system of velocity control especially for tasks concerning the precise hover hold, a positive position for the command system shall be achieved.
4. The least operational and desirable control capabilities include those that make use of pure attitude control. Some of these include those which are characteristic of the tandem-rotor controlled differential collective pitch helicopters or in some instances the conformist single-rotor airplane.
5. The model for simulation which is currently applicable within the HLH model work has been known to produce enhanced response fidelity. This response is achieved for all normal operational flight conditions as shown through the response compared with the flight response data for Model 347. The model comprising of the simplified depiction of the exterior load equations should be exclusively adequate for the simulator calculation tasks for this particular contract.
6. The directed test system assessment results identifying with the drift execution task overall affirm the legitimacy of the insightful methodology for characterizing the relative presentation ability of different control expansion modes. In supreme execution terms (RMS, or standard deviation of the pair rotor helicopter's position mistake), the investigation predicts well the best pilot execution ability for a particular increase framework. On the test system, the genuine pilot will move toward this exhibition level just with adequate practice. By and large, the pilot appears to pick an exhibition point in which the aggregate (pilot-airplane) framework damping level is almost steady with pilot acquire, instead of the "ideal" point (characterized by 0.35 damping proportion at least position blunder).

References

- Alpman, E.; Long, Lyle N. (2004). Understanding Ducted-Rotor Antitorque and Directional Control: Characteristics Part II: Unsteady Simulations. Archived 2015-04-02 at the Way back Machine Journal of Aircraft Vol. 41, No. 6, November–December 2004.
- Brown, R.E., and Leishman, R.G. (2002). Blade Twist Effect on Rotor Behavior in the Vortex Ring State, European Rotorcraft Forum. Bristol, England, September 17-20, 2002.
- Brown, R.E., and Line, A.J., (2005) Efficient High-Resolution Wake Modeling Using the Vorticity Transport Equation, AIAA Journal, Vol. 43, No. 7, July 2005.
- Burger, C, and Hartfield, R., (2006). Wind Turbine Airfoil Performance Optimization using the Vortex Lattice Method and a Genetic Algorithm, AIAA 2006-4051, 4 th AIAA Energy Conversion Engineering Conference 26-29, June 2006, San Diego, CA.

- Cao, Y., Yu, Z., and Su, Y. (2002). A Coupled Free Wake-CFD Method for the Simulation of Helicopter Rotor Flow, Canadian Aeronautics and Space Journal, Vol. 48, No. 4, December 2002.
- Cribbs, R. C., Friedmann, P. P., and Chiu, T., (2000). Coupled Helicopter Rotor/Flexible Fuselage Aeroelastic Model for Control of Structural Response, AIAA Journal, Vol. 38, No. 10, 2000, pp. 1777–1788.
- Datta, A. (2014). Experimental Investigation and Fundamental Understanding of a Slowed UH-60A Rotor at High Advance Ratios page 2. NASA ARC-E-DAA-TN3233, 2011. Header Accessed: May 2014.
- Franchesca F., Guiseppe, Q. Alberto, G.; Pietro, C. (2015). Robust aerodynamic optimization of morphing airfoils for helicopter rotor blades, AIAA, 2015.
- Ganesh, B., Komerath, N.M., Pulla, D.P., Conlisk, A.T., (2005). Unsteady Aerodynamics of Rotorcraft in Ground Effect, 43rd AIAA Aerospace Sciences Meeting, Reno, Nevada AIAA 2005-1407, January 10-13 2005.
- Hahn, S., Ananthan, S., Iaccarino, G., Baeder, J.D., and Moin, P., (2007). Coupled URANS Simulation For The MDART Rotor In Forward Flight, Center for Turbulence Research Annual Research Briefs 2007.
- Hahn, S., Duraisamy, K., and Iaccarino, G., (2006). Coupled High—Fidelity URANS Simulation for Helicopter Applications, Center for Turbulence Research Annual Research Briefs 2006.
- Harris, F. D. (2008). Rotor Performance at High Advance Ratio: Theory versus Test Archived 2013-02-18 at the Wayback Machine page 119 NASA/CR—2008–215370, October 2008. Accessed: 13 April 2014.
- Head, E. (2015). A better track and balance. Vertical Magazine. p. 38. Archived from the original on 11 April 2015. Retrieved 11 April 2015.
- I. Goulos, V. Pachidis, R. D'Ippolito, J. Stevens, and C. Smith, (2012). An Integrated Approach for the Multidisciplinary Design of Optimum Rotorcraft Operations, Journal of Engineering for Gas Turbines and Power, vol. 134, no. 9, p. 091701, 2012.
- J. S. Bendat and A. G. Piersol, (2011). Random data: analysis and measurement procedures, vol. 729. John Wiley and Sons, 2011
- Leishman, J. G. (2006). Principles of Helicopter Aerodynamics. Cambridge aerospace series, 18. Cambridge: Cambridge University Press, 2006. ISBN 978-0-521-85860-1. pp. 7-9. Web extract Archived 2014-07-13 at the Wayback Machine
- Light, J.S., (1993). Tip Vortex Geometry of a Hovering Helicopter Rotor in Ground Effect, Journal of American Helicopter Society, Vol. 38, No. 2, pp. 34-42.
- Loewy, R. G., (1984). Helicopter Vibrations: A Technological Perspective, Journal of the American Helicopter Society, Vol. 29, No. 4, pp. 4–30.
- Mestrinho, J., Gamboa, P., Santos, P., (2011). Design Optimization of a Variable Span Morphing Wing for a Small UAV, AIAA/ASME/AHS Structures, Structural Dynamics and Materials Conference.
- Nirmit, P. (2014). Design and Dynamic Analysis of a variable sweep, variable span morphing UAV.
- P. Konstanzer, B. Enenkl, P. Aubourg, and P. Cranga, (2008). Recent Advances in Eurocopter's Passive and Active Vibration Control, in American Helicopter Society 64th Annual Forum, 2008
- Paul, B. (2012). The shaft driven Lift Fan propulsion system for the Joint Strike Fighter Archived 2011-06-05 at the Wayback Machine page 3. Presented May 1, 1997.
- Ramaswamy, M., Johnson, B., and Leishman, J.G., (2007). Toward Understanding the Aerodynamic Efficiency of a Hovering Micro-Rotor, American Helicopter Society International Specialists Meeting on Unmanned Rotorcraft.
- Seddon, J. Newman, S. (2011). Basic Helicopter Aerodynamics. John Wiley and Sons. p. 216. ISBN 1-119-99410-1. 2011.
- Shinoda, P.M., Yeo, H., and Norman, T.R., (2002). Rotor Performance of a UH-60 Rotor System in the NASA Ames 80- by 120-Foot Wind Tunnel, American Helicopter Society 58th Annual Forum, Montreal, Canada.
- Smith, E. C., Govindswamy, K., Beale, M. R., Vascinec, M., and Lesieutre, G. A., (1996). Aeroelastic Response and Stability of Helicopters with Elastomeric Lag Dampers, Journal of the American Helicopter Society, Vol. 41, No. 3, 1996, pp. 257–266
- Su, Y., and Cao, Y., (2002). A Nonlinear Inverse Simulation Technique Applied to Coaxial Rotor Helicopter Maneuvers, Journal of Aircraft Engineering and Aerospace Technology, 2002, Vol.74, issue:6, Page:525-533.
- Vassberg, J., Gopinath, A. K., and Jameson, A., (2005). Revisiting the Vertical-Axis Wind-Turbine Design Using Advanced Computational Fluid Dynamics, AIAA 43rd Aerospace Sciences Meeting & Exhibit, Reno, NV, AIAA Paper.
- Wachspress, D.A., and Quackenbush, T.R., (2006). Impact of Rotor Design on Coaxial Rotor Performance, Wake Geometry and Noise, American Helicopter Society 62nd Annual Forum, Phoenix, AZ.
- Whittle, R. (2015). It's A Bird! It's A Plane! No, It's Aircraft That Fly Like A Bird! Archived 2015-05-01 at the Wayback Machine Breaking Defense, 12 January 2015. Accessed: 17 January 2015.
- Wieslaw, Zenon Stepniewski, C. N. Keys. (2004). Rotary-wing aerodynamics p3, Courier Dover Publications, 1979. Accessed: 25 February 2012. ISBN 0-486-64647-5
- Yagiz, B., and Asian, A.R., (2004). Effect of Rotor Tip Shape on Helicopter Main Rotor Performance, 11th International Symposium on Flow Visualization, August 9-12, 2004, University of Notre Dame, Notre Dame, Indiana, USA.

7. Appendices

A. APPENDIX A: DYNAMIC PROPERTIES OF BASIC AIRCRAFT CONFIGURATIONS

The dynamic features discoursed within this particular section have their basis on the helicopter rigid-body performance. This is as per the definition of the uncoupled longitudinal as well as lateral-directional permanence derivatives as illustrated in Table VIII. To elucidate the variations within the roots, an approximation of the typical roots associated with hovers is used. This is configured to consistently match the disc loading as well as the gross weight. The complete dynamic features, without oversimplifications, are presented in Table IX.

Table 1. ADVANCED TANDEM-ROTOR HELICOPTER CONFIGURATION PARAMETERS					
Item	Units	Value			
Design Gross Weight	Lb	50,000.000	130,000.000	120,000.000	200,000'
Equiv. Flat Plate Area (Airframe)	sq Ft	82.100	110.000	141.700	195.100
Disc Loading	Lb/5q	8.900	8.900	8.900	8.900
Rotor Radius, R	Ft	29.900	37.820	46.320	59.800
Rotor Chord	Ft	2.167	2.741		4.333
Blades per Rotor	-	4.000	4.000	4.000	4.000
Flap Hinge Offset	Ft	1.408	1.781	2.182	2.817
Blade Twist	Deg	-12.000	-12.000	-12.000	-12.000
Blade Airfoil Cutout	-	0.164	0.164	0.164	0.164
Tip Speed	Ft/Sec	750.000	750.000	750.000	750.000
Dist. Between Rotors (Waterline)	Ft	45.570	57.640	70.590	91.140
Vertical Hub Separation	Ft	6.825	8.633	10.573	13.650
C _a (Ratio)	Ft	1.943	2.457	3.100	3.986
I _β - Flapping Moment	Slug-Ft	1,828 1,828	5,945.000	16,932.000	63,724.000
σ _β - Weight Moment	Pt-Lb	3,099.000	7,969.000	18,587.000	54,026.000
	2				
I _{xx}	Slug-Ft	67,120.000	118,950.000	266.820	622,250.000
I _{yy}		384,350.000	929,340.000		5,400,340.000
	Slug-Ft,				
I _{zz}	Slug-Ft'	1,331,930.000	849,670.000	1,911,530.000	5,310,230.000
Fuselage Width - Constant Section	Ft	R 6.5	8.235	10,1	13.000
Fuselage Height - Constant Section	Ft	6.000	7.600	9.350	12.100
Fwd. Shaft Angle	Deg	6.000	6.000	6.000	6.000

Aft Shaft Angle	Deg	3.000	3.000	3.000	3.000
4					
Blade Lock No. = 1/2 pac R^4/I_B	-	5.790	5.780	5,58	5.320
I_F, I_R - Horiz. Dist. from A/C c.g.	Ft	22.790	28.820	35.290	45.570
to Rotor	Ft	7.500	7.800	8.200	9.000
h_F (Vert. Dist. from A/C c.g. to					
Fwd. Rotor)	Ft	14.330	16.430	18.770	22.650
h_R (Vert. Dist. from A/C c.g. to					
Rear Rotor)					
Estimated Empty Cross Weight (TOGW)	Lb	29,000.000	43,000.000	62,000.000	101,000.000
I_c (midpoint c.g.	Ft	2.000	2.000	2.000	2.000
h_c (midpoint c.g. location)	Ft	0.000	0.000	0.000	0.000
--					

Table 2. ADVANCED TANDEM-ROTOR HELICOPTER CONFIGURATION PARAMETERS

TABLE II. BASELINE TANDEM-ROTOR RLH FUSELAGE DRAG TABLES, D/qd													
REFERENCE: STA. 596", WATER LINE 164"													
120,000-POUND GROSS WEIGHT													

α „													
	90.0	-	-	-	-9.30	-4.30	0.70	5.70	10.70	20.70	30.70	50.7	90.0
β r													
-	10.0 0	-	-	-	-	-	-	-	-	-	-	-	-
-		35.0	35.0	35.00	35.00	35.00	35.00	35.00	35.00	35.00	35.00	35.0	10.0
60.0 0		0	0	0	0	0	0	0	0	0	0	0	0

-50.00													
-40.00	0.00	10.00	50.00	55.00	60.00	60.00	60.00	65.00	75.00	75.00	65.00	10.00	0.00
-30.00	0.00	-30.00	50.00	70.00	75.00	80.00	RO	85.00	90.00	90.00	65.00	-35.00	0.00
-20.00	0.00	-45.00	20.00	45.00	55.00	60.00	60.00	65.00	75.00	70.00	40.00	-45.00	0.00
-15.00	0.00	-35.00	15.00	35.00	45.00	50.00	50.00	55.00	70.00	70.00	40.00	-35.00	0.00
-10.00	0.00	-20.00	50.00	65.00	75.00	80.00	80.00	85.00	105.00	110.00	75.00	-20.00	0.00
-6.00	0.00	-15.00	65.00	91.00	104.00	108.00	111.00	120.00	136.00	139.00	95.00	-35.00	0.00
-2.00	0.00	15.00	75.00	106.00	120.00	124.00	128.00	136.00	153.00	154.00	110.00	-15.00	0.00
0.00	0.00	-10.00	80.00	113.00	127.00	131.00	134.00	142.00	160.00	161.00	115.00	-10.00	0.00
2.00	0.00	-10.00	BO	116.00	130.00	134.00	137.00	145.00	164.00	164.00	115.00	-10.00	0.00
6.00	0.00	-10.00	80.00	117.00	131.00	135.00	139.00	145.00	164.00	164.00	115.00	-10.00	0.00

10.0 0	0.00	- 10.0 0	90.0 0	116.0 0	130.0 0	134.0 0	137.0 0	145.0 0	164.0 0	164.0 0	115.0 0	- 10.0 0	0.00
15.0 0	0.00	- 10.0 0	90.0 0	113.0 0	127.0 0	131.0 0	134.0 0	142.0 0	160.0 0	161.0 0	115.0 0	- 10.0 0	0.00
	0.00	- 15.0 0	75.0 0	106.0 0	120.0 0	124.0 0	128.0 0	136.0 0	153.0 0	154.0 0	110.0 0	- 15.0 0	0.00
20.0 0	0.00	-1\$	65.0 0	91.00	104.0 0	108.0 0	111.0 0	120.0 0	136.0 0	139.0 0	95.00	- 15.0 0	0.00
	0.00	- 20.0 0	50.0 0	65.00	75.00	80.00	80.00	85.00	105.0 0	110.0 0	75.00	- 20.0 0	0.00
30.0 0	0.00	- 35.0 0	15.0 0	35.00	45.00	50.00	50.00	55.00	70.00	70.00	40.00	- 35.0 0	0.00
40.0 0	0.00	- 45.0 0	20.0 0	45.00	55.00	60.00	60.00	65.00	75.00	70.00	40.00	- 45.0 0	0.00
50.0 0	0.00	- 35.0 0	50.0 0	70.00	75.00	80.00	80.00	85.00	90.00	90.00	65.00	- 35.0 0	0.00
60.0 0	0.00	10.0 0	50.0 0	55.00	60.00	60.00	60.00	65.00	75.00	75.00	65.00	10.0 0	0.00
90.0 0	10.0 0	- 35.0 0	- 35.0 0	- 15.00	- 35.00	- 35.00	- 35.00	- 35.00	- 35.00	- 35.00	- 35.00	- 35.0 0	10.0 0

Table 3: BASELINE TANDEM-ROTOR RLH FUSELAGE DRAG TABLES, D/qd

TABLE III. BASELINE TANDEM- 120,000-FOUND GROSS WEIGHT				FUSELAGE				TABLES,					
α , deg B ,	-	-	-	-	-9.30	-4.30	0.70	5.70	10.7	20.7	30.7	50.7	90.0 I
--		-	--	--		-							
-90.00	-	-	-	-	-	-15D	-	-	-	-	-	-	390.0

-60.00													
-50.00													
-40.00													
-30.00													
-20.00	- 750. 00	- 720. 00	- 595. 00	- 465. 00	- 355. 00	- 115. 00	- 290. 00	- 235. 00	- 190. 00	- 95.0 0	- 20.0 0	240. 00	950.0 0
-15.00	- 750. 00	- 615. 00	- 565. 00	- 475. 00	- 345. 00	- 300. 00	- 250. 00	- 195. 00	- 120. 00	10.0 0	135. 00	490. 00	850.0 0
-10.00	- 750. 00	- 555. 00	- 435. 00	- 335. 00	- 185. 00	- 125. 00	- 80.0 0	- 15.0 0	65.0 0	230. 00	31L5	645. 00	650.0 0
-6.00	- 750. 00	- 560. 00	- 380. 00	- 240. 00	- 50.0 0	- 15.0 0	65.0 0	135. 00	225. 00	390. 00	495. 00	710. 00	950.0 0
-2.00	- 750. 00	- 605. 00	- 400. 00	- 235. 00	- 20.0 0	- 55.0 0	105. 00	185. 00	270. 00	425. 00	535. 00	730. 00	950.0 0
0.00	- 750. 00	- 620. 00	- 420. 00	- 255. 00	- 36.0 0	- 42.0 0	96.0 0	181. 00	265. 00	424. 00	535. 00	735. 00	950.0 0
2.00	- 750. 00	- 635. 00	- 435. 00	- -0.28	- 57.0 0	- 19.0 0	75.0 0	165. 00	252	417. 00	530. 00	730. 00	850.0 0
6.00	- 750. 00	- 640. 00	- 445. 00	- 286. 00	- 70.0 0	- 5.00	60.0 0	151. 00	242. 00	410. 00	530. 00	730. 00	950.0 0
10.00	- 750. 00	- 640. 00	- 450. 00	- 291. 00	- 77.0 0	- -3.00	51.0 0	142. 00	236. 00	406. 00	530. 00	730. 00	850.0 0

		-	-	-	-		50.0	140.	235.	405.	530.	730.	950.0
	..750	640. 00	450. 00	292. 00	79.0 0	-5.00	0	00	00	00	00	00	0
15.00	- 750. 00	- 640. 00	- 450. 00	- 291. 00	- 77.0 0	-3.00	51.0 0	142. 00	236. 00	406. 00	530. 00	730. 00	8501. 00
	- 750. 00	- 640. 00	- 445. 00	- 266. 00	- 70.0 0	5.00	60.0 0] 51	242. 00	410. 00	530. 00	730. 00	950.0 0
20.00	- 750. 00	- 635. 00	- 0.44	- 276. 00	- 57.0 0	19.0 0	75.0 0	165. 00	252. 00	417. 00	530. 00	710. 00	850.0 0
	- 750. 00	- 620. 00	- 420. 00	- 255. 00	- 36.0 0	42.0 0	96.0 0	181. 00	265. 00	424. 00	535. 00	735. 00	950.0 0
30.00	- 750. 00	- 505. 00	- 400. 00	- 235. 00	- 20.0 0	55.0 0	105. 00	185. 00	270. 00	425. 00	535. 00	710. 00	950.0 0
40.00	- 750. 00	- 560. 00	- 320. 00	- 240. 00	- 90.0 0	15.0 0	65.0 0	135. 00	225. 00	390. 00	495. 00	710. 00	950.0 0
50.00	- 750. 00	- 555. 00	- 435. 00	- 335. 00	- 18.18 5	125. 00	80.0 0	15.0 0	65.0 0	230. 00	355. 00	645. 00	852.0 0
60.00	- 750. 00	- 615. 00	- 565. 00	- 475. 00	- 345. 00	300. 00	250. 00	195. 00	120. 00	10.0 0	135. 00	490. 00	B5D
	- 750. 00	- 720. 00	- 595. 00	- 485. 00	- 355. 00	315. 00	280. 00	235. 00	190. 00	95.0 0	20.0 0	240. 00	850.0 0
90.00	- 780. 00	- 150. 00	- 150. 00	- 150. 00	- 150. 00	150. 00	150. 00	150. 00	150. 00	150. 00	150. 00	150. 00	390.0 0

Table 4: TABLE III. BASELINE TANDEM-ROTGR HLHFUSELAGE LIFTTABLES, L./qd

TABLE IV. BASELINE TANDEM-ROTOR HLH FUSELAGE SIDEFORCE TABLES, Y/qd 120,000-POUND GROSS WEIGHT

B , α „	90.0	-	-	-	-9.30	-4.30	0.70	5.70	10.7	20.7	30.7	50.7	90.
-	790.	1030	1030	1030	1030	1030	1030	1030	1030	1030	1030	1030	790
-													
60.00													
-													
50.00													
-													
40.00													
-													
30.00													
-													
20.00		855.00	995.00	1030.00	1040.00	1045.00	1050.00	1045.00	1040.00	1025.00	905.00	40.00	0.00
-													
15.00		660.00	810.00	855.00	870.00	875.00	1080.00	75.00	870.00	50.00		645.00	0.00
-													
10.00		470.00	620.00	665.00	685.00	690.00	695.00	690.00	685.00	665.00	615.00	460.00	0.00
-													
6.00		315.00	425.00	470.00	490.00	495.00	500.00	495.00	490.00	470.00	425.00	310.00	0.00
-													
2.00		2135.00	270.00	290.00	300.00	305.00	310.00	305.00	300.00	290.00	270.00	200.00	0.00
0.00		150.00	205.00	217.00	226.00	228.00	230.00	228.00	226.00	215.00	205.00	145.00	0.00

2.0			100.	130.	142.	152.	153.	153.	153.	152.	140.	130.	100.	0.0
0		0.00	00	00	00	00	00	00	00	00	00	00	00	0
6.0			65.0	80.0	90.0	92.0	93.0	93.0	93.0	92.0	89.0		65.0	0.0
0		0.00	0	0	0	0	0	0	0	0	0	BO	0	0
			25.0	30.0	33.0	35.0	35.0	35.0	35.0	35.0	33.0	30.0	25.0	0.0
		0.00	0	0	0	0	0	0	0	0	0	0	0	0
10.														0.0
00		0.00	0.00	0.00	0.00	0.00	0.00	0.00	0.00	0.00	0.00	0.00	0.00	0
			-	-	-	-	-	-	-	-	-	-	-	
			25.0	30.0	33.0	35.0	35.0	35.0	35.0	35.0	33.0	30.0	25.0	0.0
		0.00	0	0	0	0	0	0	0	0	0	0	0	0
15.			-	-	-	-	-	-	-	-	-	-	-	
00		0.00	65.0	80.0	90.0	92.0	93.0	93.0	93.0	92.0	89.0	80.0	65.0	0.0
			0	0	0	0	0	0	0	0	0	0	0	0
			-	-	-	-	-	-	-	-	-	-	-	
		13.0	100.	130.	142.	152.	153.	153.	153.	152.	140.	130.	100.	0.0
		0	00	00	00	00	00	00	00	00	00	00	00	0
20.			-	-	-	-	-	-	-	-	-	-	-	
00		0.00	150.	205.	217.	226.	228.	230.	228.	226.	215.	205.	145.	0.0
			00	00	00	00	00	00	00	00	00	00	00	0
			-	-	-	-	-	-	-	-	-	-	-	
			205.	270.	290.	300.	305.	310.	305.	300.	290.	270.	200.	0.0
		0.00	00	00	00	00	00	00	00	00	00	00	00	0
30.			-	-	-	-	-	-	-	-	-	-	-	
00		0.00	315.	425.	470.	490.	495.	500.	495.	490.	470.	425.	310.	0.0
			00	00	00	00	00	00	00	00	00	00	00	0
40.			-	-	-	-	-	-	-	-	-	-	-	
00		0.00	470.	620.	665.	685.	690.	695.	690.	605.	665.	615.	460.	0.0
			00	00	00	00	00	00	00	00	00	00	00	0
50.			-	-		-	-	-	-	-	-	-	-	
00		0.00	660.	10.0	-r=d	870.	875.	880.	875.	870.	50.0	805.	645.	0.0
			00	0		00	00	00	00	00	0	00	00	0

60.			-	-	-	-	-	-	-	-	-	-	-	
00		0.00	855.	995.	1030	1040	1045	1050	1045	1040	1025	985.	840.	0.0
			00	00	.00	.00	.00	.00	.00	.00	.00	00	00	0
90.		-	-	-	-	-	-	-	-	-	-	-	-	
00		790.	1030	1030	1030	1030	1030	1030	1030	1030	1030	1030	790.	0.0
		00	.00	.00	.00	.00	.00	.00	.00	.00	.00	.00	00	0

Table 5: BASELINE TANDEM-ROTOR HLH FUSELAGE SIDEFORCE TABLES, Y/qd 120,000-POUND GROSS WEIGHT

TABLE V. BASELINE TANDEM-ROTOR HLH FUSELAGE PITCH MOMENT

TABLES, M / qd													
120,000-FOUND													
GROSS WEIGHT													
	-90	-49.3	-29.3	-19.3	-9.3	-4.3	0.7	5.7	10.7	20.7	30.7	50.7	90
-90.0	1,00 0.0	(500. 0)	(500. 0)	(500. 0)	(500. 0)	(500. 0)	(500. 0)	(500. 0)	(500. 0)	(500. 0)	(500. 0)	(500. 0)	(4,30 0.0)
-60.0	3,50 0.0	(2,80 0.0)	(3,80 0.0)	(4,00 0.0)	(3,90 0.0)	(3,80 0.0)	(3,60 0.0)	(3,50 0.0)	(3,40 0.0)	(2,90 0.0)	(2,00 0.0)	(700. 0)	(4,00 0.0)
-50.0	3,50 0.0	(2,70 0.0)	(3,20 0.0)	(3,20 0.0)	(3,00 0.0)	(2,80 0.0)	(2,60 0.0)	(2,50 0.0)	(2,30 0.0)	(1,70 0.0)	(1,00 0.0)	(500. 0)	(4,00 0.0)
-40.0	3,50 0.0	(3,90 0.0)	(3,50 0.0)	(3,20 0.0)	(2,90 0.0)	(2,60 0.0)	(2,40 0.0)	(2,10 0.0)	(2,00 0.0)	(1,50 0.0)	(900. 0)	(1,50 0.0)	(4,00 0.0)
-30.0	3,50 0.0	(4,00 0.0)	(4,90 0.0)	(4,50 0.0)	(4,00 0.0)	(3,50 0.0)	(3,20 0.0)	(3,00 0.0)	(3,00 0.0)	(2,50 0.0)	(2,00 0.0)	(1,10 0.0)	(4,00 0.0)

-20.0	3,50 0.0	(2,80 0.0)	(4,20 0.0)	(4,20 0.0)	(4,00 0.0)	(3,80 0.0)	(3,50 0.0)	(3,20 0.0)	(3,00 0.0)	(2,20 0.0)	(1,10 0.0)	200.0	(4,00 0.0)
-15.0	3,50 0.0	(2,30 0.0)	(3,60 0.0)	(3,40 0.0)	(3,15 0.0)	(2,95 0.0)	(2,25 0.0)	(2,30 0.0)	(2,15 0.0)	(1,35 0.0)	200.0	600.0	(4,00 0.0)
-10.0	3,50 0.0	(2,00 0.0)	(3,00 0.0)	(2,85 0.0)	(2,50 0.0)	(2,30 0.0)	(1,95 0.0)	(1,60 0.0)	(1,45 0.0)	(700. 0)	300.0	900.0	(4,00 0.0)
-6.0	3,50 0.0	(1,80 0.0)	(2,70 0.0)	(2,50 0.0)	(2,20 0.0)	(1,95 0.0)	(1,60 0.0)	(1,30 0.0)	(1,15 0.0)	(350. 0)	600.0	1,000 .0	(4,00 0.0)
-2.0	3,50 0.0	(1,70 0.0)	(2,50 0.0)	(2,35 0.0)	(2,00 0.0)	(1,75 0.0)	(1,40 0.0)	(1,10 0.0)	(950. 0)	(200. 0)	700.0	1,100 .0	(4,00 0.0)
0.0	3,50 0.0	(1,70 0.0)	(2,50 0.0)	(2,30 0.0)	(1,95 0.0)	(1,70 0.0)	(1,35 0.0)	(1,05 0.0)	(900. 0)	(150. 0)	800.0	1,200 .0	(4,00 0.0)
2.0	3,50 0.0	(1,70 0.0)	(2,50 0.0)	(2,35 0.0)	(2,00 0.0)	(1,75 0.0)	(1,40 0.0)	(1,10 0.0)	(950. 0)	(200. 0)	700.0	1,100 .0	(4,00 0.0)
6.0	3,50 0.0	(1,80 0.0)	(2,70 0.0)	(2,50 0.0)	(2,20 0.0)	(1,95 0.0)	(1,60 0.0)	(1,30 0.0)	(1,15 0.0)	(350. 0)	600.0	1,000 .0	(4,00 0.0)
10.0	3,50 0.0	(2,00 0.0)	(3,00 0.0)	(2,85 0.0)	(2,50 0.0)	(2,30 0.0)	(1,95 0.0)	(1,60 0.0)	(1,45 0.0)	(700. 0)	300.0	900.0	(4,00 0.0)
15.0	3,50 0.0	(2,30 0.0)	(3,60 0.0)	(3,40 0.0)	(3,15 0.0)	(2,95 0.0)	(2,55 0.0)	(2,30 0.0)	(2,15 0.0)	(1,35 0.0)	(200. 0)	600.0	(4,00 0.0)
20.0	3,50 0.0	(2,80 0.0)	(4,20 0.0)	(4,20 0.0)	(4,00 0.0)	(3,80 0.0)	(3,50 0.0)	(3,20 0.0)	3,000 .0	(2,20 0.0)	(1,10 0.0)	200.0	(4,00 0.0)

30.0	3,50 0.0	(4,00 0.0)	(4,90 0.0)	(4,50 0.0)	(4,00 0.0)	(3,50 0.0)	(3,20 0.0)	(3,30 0.0)	(3,00 0.0)	(2,50 0.0)	(2,00 0.0)	(1,10 0.0)	(4,00 0.0)
40.0	3,50 0.0	(3,90 0.0)	(3,50 0.0)	(3,20 0.0)	(2,90 0.0)	(2,60 0.0)	(2,40 0.0)	(2,10 0.0)	(2,00 0.0)	(1,50 0.0)	(900. 0)	(1,50 0.0)	(4,00 0.0)
50.0	3,50 0.0	(2,70 0.0)	(3,20 0.0)	(3,20 0.0)	(3,00 0.0)	(2,80 0.0)	(2,60 0.0)	(2,50 0.0)	(2,30 0.0)	(1,70 0.0)	(1,00 0.0)	(500. 0)	(4,00 0.0)
60.0	3,50 0.0	(2,80 0.0)	(3,80 0.0)	(4,00 0.0)	(3,90 0.0)	(3,80 0.0)	(3,60 0.0)	(3,50 0.0)	(3,40 0.0)	(2,90 0.0)	(2,00 0.0)	(700. 0)	(4,00 0.0)
90.0	1,00 0.0	(500. 0)	(500. 0)	(500. 0)	(500. 0)	(500. 0)	(500. 0)	(500. 0)	(500. 0)	(500. 0)	(500. 0)	(500. 0)	(4,30 0.0)

Table 6: BASELINE TANDEM-ROTOR HLH FUSELAGE PITCH MOMENT

TABLE VI. BASELINE TANDEM-ROTOR HLH FUSELAGE ROLL MOMENT TABLES, L / qd
120,000-POUND GROSS WEIGHT

B ,	α ,	80.0	-	-	-	-9.30	-4.30	0.70	5.70	10.7	20.7	30.7	50.7	90.0
-		230	2500	2500	2500	2500	2500.	2500	2500	2500	2500	2500	2500	1250
-														
60.														
0														
-														
50.														
0														
-														
40.														
0														

-30.0														
-20.0														
-15.0														
-10.0														
-6.0		0.00	2200.00	2100.00	2200.00	2300.00	2200.00	2200.00	20.04	1000.00	1500.00	1100.00	1200.00	0.00
		0.00	3000.00	2200.00	2200.00	2200.00	2100.00	2000.00	1000.00	1500.00	1200.00	1200.00	180D	0.00
-2.0		0.00	3000.00	3200.00	3000.00	2900.00	2700.00	2500.00	2400.00	2100.00	1700.00	1900.00	1000.00	0.00
0.0		0.00	2200.00	2800.00	3000.00	3000.00	3000.00	2900.00	2800.00	2200.00	1800.00	1700.00	1200.00	0.00
		0.00	1300.00	1700.00	1900.00	2000.00	2000.00	1800.00	1500.00	1200.00	1000.00	900.00	ID	
2.0		0.00	1000.00	1200.00	1350.00	1400.00	1150.00	1300.00	1250.00	1000.00	850.00	800.00	600.00	0.00
		0.00	700.00	900.00	950.00	900.00	900.00	850.00	800.00	750.00	500.00	500.00	400.00	0.00
6.0		0.00	400.00	500.00	550.00	500.00	550.00	550.00	500.00	450.00	400.00	100.00	300.00	0.00
		0.00	100.00	200.00	200.00	200.00	200.00	200.00	200.00	150.00	150.00	100.00	100.00	0.00

10. 0		0.00	0.00	0.00	0.00	0.00	0.00	0.00	0.00	0.00	0.00	0.00	0.00	0.00
			- 100. 00	- 200. 00	- 200. 00	- 200. 00	- 2191 1.00	- 200. 00	- 200. 00	- 150. 00	- 150. 00	- 100. 00	- 100. 00	0.00
15. 0		0.00	- 400. 00	- 500. 00	- -55A 00	- 600. 00	- 550.0 0	- 550. 00	- 500. 00	- 450. 00	- 400. 00	- 300. 00	- 300. 00	0.00
		0.00	- 700. 00	- 900. 00	- 950. 00	- 950. 00	- 900.0 0	- 850. 00	- 0.00 00	- 150. 00	- 600. 00	- 500. 00	- 400. 00	3.00
20. 0		0.00	- 1000 .00	- 1200 .00	- 1350 .00	- 1400 .00	- 1350. 00	- 1300 .00	- 1250 .00	- 1000 .00	- 850. 00	- 800. 00	- 500. 00	0.00
		0.00	- 1300 .00	- 1700 .00	- 1500 .00	- 2000 .00	- 2000. 00	- 2000 .00	- 1800 .00	- 1500 .00	- 1200 .00	- 1000 .00	- -BOO	0.00
30. 0		0.00	- 2200 .00	- 2800 .00	- 3000 .00	- 3000 .00	- 3000. 00	- 2900 .00	- 2600 .00	- 2200 .00	- 1800 .00	- 1700 .00	- 1200 .00	0.00
40. 0		0.00	- 3000 .00	- 1200 .00	- 3000 .00	- 2900 .00	- 2700. 00	- 2600 .00	- 2400 .00	- 2100 .00	- 1700 .00	- 1900 .00	- 1800 .00	0'
50. 0		0.00	- 1000 .00	- 2200 .00	- 2200 .00	- 2200 .00	- 2100. 00	- 2000 .00	- 1800 .00	- 1500 .00	- 1200 .00	- 1200 .00	- 1800 .00	0.00
60. 0		0.00	- 2200 .00	- 2100 .00	- 2200 .00	- 2300 .00	- 2200. 00	- 2200 .00	- 2000 .00	- 1000 .00	- 1500 .00	- 1300 .00	- 1200 .00	0.00
90. 0		230 0.00	- 2500 .00	- 2500 .00	- 2500 .00	- 2500 .00	- 2500. 00	- 2500 .00	- 2500 .00	- 2500 .00	- 2500 .00	- 2500 .00	- 2500 .00	- 1250 .00

Table 7: BASELINE TANDEM-ROTOR HLH FUSELAGE ROLL MOMENT TABLES, L / qd 120,000-POUND GROSS WEIGHT

TABLE VII. BASELINE TANDEM-ROTOR HMI FUSELAGE

Text Box: B ,				YAW MOMENT TABLES, N/qd									
α „	90.0	-	-	-19.2..	-9.30	-4.30	0.70	5.70	1D.7	20.7	30.7	50.7	90.
-	-	-	-	-9000.0	-	-	-	-	-	-	-	-	-
-	0.0	-	-	-2300.0	-	-	-	-	-	-	-	-	0.0
-	0.0	-	-	-2500.0	-	-	-	-	-	-	-	-	0.0
-	0.0	-	-	-6000.0	-	-	-	-	-	0.0	100.	200.	0.0
-	0.0	-	-	-4600.0	-	-	-	-	-	100.	200.	400.	0.0
-	0.0	-	-	-2600.0	-	-:800	-	-	-	400.	500.	500.	0.0
-/5	0.0	-	-	-1950.0	-	-	-	-	100.	500	600.	600.	0.0
-	0.0	-	-	-1300.0	-	-	-	-	250.	550.	600.	500.	0.0
-6.0	0.0	-	-	-800.0	-	-	-50.0	150.	300.	450.	500.	400.	0.0
-2.0	0.0	-	-	-300.0	-	0.0	50.0	100.	150.	200.	200.	200.	0.0
0.0	0.0	0.0	0.0	0.0	0.0	0.0	0.0	0.0	0.0	0.0	0.0	0.0	0.0
2.0	0.0	200.	200.	300.0	100.	0.0	-50.0	-	-	-	-	-	0.0
6.0	0.0	600.	700.	800.0	5130	300.	50.0	-	-	-	-	-	0.0
10.0	0.0	900.	1200	1300.0	1050	750.	450.	100.	-	-	-	-	0.0
15.0	0.0	1400	1900	1950.0	1700	1250	850.	350.	-	-	-	-	0.0
20.0	0.0	1900	2400	2600.0	2200	1800	1200	600.	100.	-	-	-	0.0
30.0	0.0	2900	4100	4600.0	4000	3300	2400	1400	500.	-	-	-	0.0
40.0	0.0	4600	6000	6000.0	5000	3900	2800	1800	800.	0.0	-	-	0.0
50.0	0.0	6000	3100	2500.0	2000	1600	1200	800.	500.	100.	100.	-	0.0
60.0	0.0	2500	2100	2300.0	2000	1800	1500	1000	700.	400.	300.	100.	0.0

Table 8: BASELINE TANDEM-ROTOR HMI FUSELAGE

TABLE IX. LATERAL-DIRECTIONAL AND LONGITUDINAL										
onfiguration		50,0010 Lb		910'000 Lb		220,000 Lb		200,000 Lb		
		'Fun , Wt		Full GrWt		'ul1 Crwt		Full CrWt		
Mode										
	Lateral-Directional									
	Roll Subsidence	-.891 '	-.900	-.920	-.957	-.975	-1.042	-1.074	-1.223	
	Spiral	-.0871	+.0472	-.0R57	-.0415	-.0848	-.0386	-.0640	-0.0385	
	Dutch Roll	Frequency	+501	.455	.468	.411	.417	.370	.394	+0.322
		Real Part	+152	.119	.125	.11176	.0998	.0623	.0708	+0.0374
	Longitudinal									
	pitch Sub51dence	-.945	.976	-.952	-.970	-.967	-.987	-.985	-1.005	
	Vertical	-.222 '	-.352	-.228	-.372		-.364	-.225!	-.392	
		Frequency	.390	.375	.353	.336	.323	.307	.288:	.273

Oscillatory	Real	Part	.0806	.0715	.0639	.0565	.0510	.0451	.03631	.0337
---	I/Sec									

Table 9: LATERAL-DIRECTIONAL AND LONGITUDINAL

Table XX: Configurations that were considered for the Simulation of the Tandem-rotor Helicopter

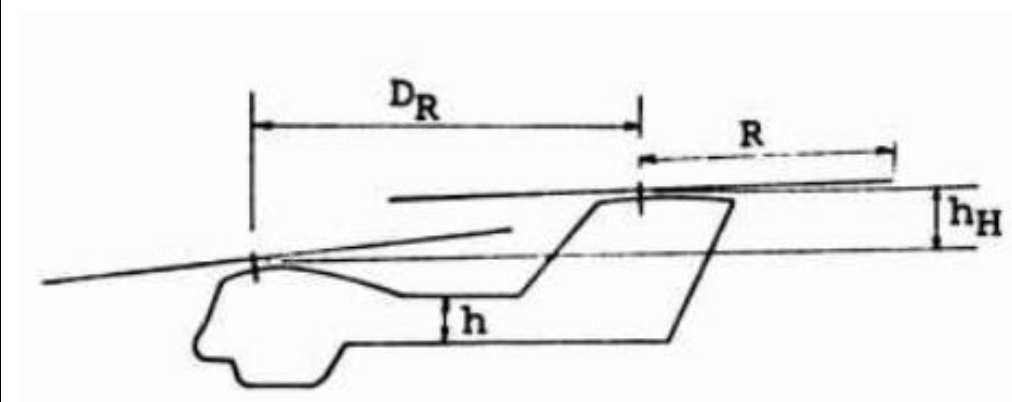
NORMAL GROSS WHEIGHT (Lbs)	
	
Advanced Tandem-Rotor Helicopter Configuration Data.	
Configuration 1 <u>50,000 LB</u> $R = 29.90 \text{ FT}$ $D_R = 45.57 \text{ FT}$ $h = 6.0 \text{ FT}$ $h_H = 6.83 \text{ FT}$	Configuration 2 <u>80,000 LB</u> $R = 37.82 \text{ FT}$ $D_R = 57.64 \text{ FT}$ $h = 7.6 \text{ FT}$ $h_H = 8.63 \text{ FT}$
Configuration 3 <u>120,000 LB</u> $R = 46.32 \text{ FT}$ $D_R = 70.59 \text{ FT}$ $h = 9.35 \text{ FT}$ $h_H = 10.57 \text{ FT}$	Configuration 4 <u>200,000 LB</u> $R = 59.80 \text{ FT}$ $D_R = 91.14 \text{ FT}$ $h = 12.1 \text{ FT}$ $h_H = 13.65 \text{ FT}$

Table 10: Configurations that were considered for the Simulation of the Tandem-rotor Helicopter

B. APPENDIX B: MATLAB CODE FOR SOLVING THE EIGEN-VECTOR PROBLEM FOR THE TWO DIMENSIONAL KINEMATICS MODEL

```

clear all
X_u = -0.0553;
X_q = 1.413;
X_theta = -32.1731;
X_beta = -19.9033;
X_w = 0.0039;
X_delta = 11.2579;
M_u = 0.2373;
M_q = -6.9424;
M_beta = 68.2896;
M_w = 0.002;
B_u = 0.0101;
B_beta = -2.1633;
Z_u = -0.0027;
Z_q = -0.0236;
Z_theta = -0.2358;
Z_beta = -0.1233;
Z_w = -0.5727;
B_delta = -4.2184;
Z_delta = -0.0698;
A = [X_u, X_q, X_theta, X_beta, X_w;
     M_u, M_q, 0, M_beta, M_w;
     0, 1, 0, 0, 0;
     B_u, -1, 0, B_beta, 0;
     Z_u, Z_q, Z_theta, Z_beta, Z_w;];
eig(A)

```

C. APPENDIX C: MATLAB CODE FOR SOLVING THE EIGEN-VECTOR PROBLEM FOR THE UNAUGMENTED TANDEM-ROTOR HELICOPTER KINEMATICS MODEL

```

clear all
% declare variables
% case for light duty load (50,000 lbs)
g = 32.2;
X_u = -0.01802;
X_q = .6444;
X_w = .00791;
% stedy trim longitudinal velocity, hover mode
U_o = 0.0;
% stedy trim velocity, hover mode
W_o = 0.0;
M_u = .00485;
M_q = -.7648;
M_w = -.00406;
% B_u = ;
Z_u = .0101;
Z_q = -1.0901;
Z_w = -.223;
Y_p = -.9316;
Y_v = -.01939;
Y_r = -.03489;
L_v = -.00761;
L_p = -.5681;
L_r = .02801;
N_v = .0000528;
N_p = -.000647;
N_r = -.08745;
I_xx = 67120;
I_xz = 384350;
I_zz = 331930;
C_p = I_xx*I_zz/(I_xx*I_zz - I_xz^2);
C_r = I_xx*I_zz/(I_xx*I_zz - I_xz^2);
% eigen matrix
B = [X_u, X_w, (X_q - W_o), -g, 0, 0, 0, 0, 0;
     Z_u, Z_w, (Z_q - U_o), 0, 0, 0, 0, 0, 0;
     M_u, M_w, M_q, 0, 0, 0, 0, 0, 0;
     0, 0, 1, 0, 0, 0, 0, 0, 0;
     0, 0, 0, 0, Y_v, (Y_p + W_o), (Y_r + U_o), g, 0;
     0, 0, 0, 0, C_p*(L_v + I_xz/I_xx*N_v), C_p*(L_p + I_xz/I_xx*N_p), C_p*(L_r + I_xz/I_xx*N_r), 0, 0;
     0, 0, 0, 0, C_r*(N_v + I_xz/I_xx*L_v), C_r*(N_p + I_xz/I_xx*L_p), C_r*(N_r + I_xz/I_xx*L_r), 0, 0;
     0, 0, 0, 0, 0, 1, 0, 0, 0;
     0, 0, 0, 0, 0, 0, 1, 0, 0;];
eig(B)

```


D. APPENDIX D: MATLAB CODE FOR NUMERICAL SIMULATION OF THE UNAUGMENTED TANDEM-ROTOR HELICOPTER KINEMATICS MODEL

a). The MATLAB ODE object handle function

```
function dydt = unaug_ki(t, v)
% declare variables
% case for light duty load (50,000 lbs)
g = 32.2;
X_u = -0.01802;
X_q = .6444;
X_w = .00791;
% stedy trim longitudinal velocity, hover mode
U_o = 0.0;
% stedy trim velocity, hover mode
W_o = 10.0;
M_u = .00485;
M_q = -.7648;
M_w = -.00406;
% B_u = ;
Z_u = .0101;
Z_q = -1.0901;
Z_w = -.223;
Y_p = -.9316;
Y_v = -.01939;
Y_r = -.03489;
L_v = -.00761;
L_p = -.5681;
L_r = .02801;
N_v = .0000528;
N_p = -.000647;
N_r = -.08745;
I_xx = 67120;
I_xz = 384350;
I_zz = 331930;
C_p = I_xx*I_zz/(I_xx*I_zz - I_xz^2);
C_r = I_xx*I_zz/(I_xx*I_zz - I_xz^2);
% mapping
% v(1) = u, v(2) = w, v(3) = q, v(4) = theta, v(5) = v, v(6) = p, v(7) = r,...
% v(8) = phi, v(9) = lphi

dydt = [X_u*v(1) + X_w*v(2) + (X_q - W_o)*v(3) - g*v(4);
        Z_u*v(1) + Z_w*v(2) + (Z_q - U_o)*v(3);
        M_u*v(1) + M_w*v(2) + M_q*v(3);
        v(3);
        Y_v*v(5) + (Y_p + W_o)*v(6) + (Y_r + U_o)*v(7) + g*v(8);
        C_p*(L_v + I_xz/I_xx*N_v)*v(5) + C_p*(L_p + I_xz/I_xx*N_p)*v(6) + C_p*(L_r +
        I_xz/I_xx*N_r)*v(7);
        C_r*(N_v + I_xz/I_xx*L_v)*v(5) + C_r*(N_p + I_xz/I_xx*L_p)*v(6) + C_r*(N_r +
        I_xz/I_xx*L_r)*v(7);
        v(6);
```

```
v(7);];
end
```

b). The MATLAB simulation code

```
[t,y] = ode45(@unaug_ki, [0 100], [1; 0.5; 0.5; 0.1; 0; 0; 0; 0; 0]);
plot(t,y(:,1),t,y(:,2),t,y(:,3),t,y(:,4),t,y(:,5),t,y(:,6),t,y(:,7),t,y(:,8),t,y(:,9))
title('Simulation of aerodynamic model with perturbed initial velocities');
xlabel('Time t');
ylabel('Aerodynamic Parameters');
legend('u','w','q','\theta','v','p','r','\phi','lphi')
grid on;
```

E. APPENDIX E: MATLAB CODE FOR NUMERICAL SIMULATION OF THE 24 X 24 ODE SYSTEM OF THE TANDEM-ROTOR HELICOPTER STRUCTURAL MODEL

a). The MATLAB ODE object handle function

```
function dydts = struct_M(ts, vs)
% declare variables
% case for light duty load (50,000 lbs)
g = 32.2;
I_xx = 67120;
I_xz = 384350;
I_zx = I_xz;
I_zz = 331930;
F_L = 30000;
theta_1 = 0.1;
E_1 = 200000000;
m_1 = 8000;
A_1yx = 10000;
L_1z = 10;
M_B1zx = 100;
A_1yz = 10000;
L_1x = 10;
M_r1y = 100;
J_1xz = 100000;
G_1 = 50000000;
L_1y = 10;
M_r1x = 100;
J_1zy = 100000;
L_1x = 10;
theta_3 = 0.05;
m_3 = 8000;
E_3 = 190000000;
A_3yx = 10000;
L_3z = 10;
M_B3zx = 100;
A_3yz = 10000;
L_3x = 10;
```

```

M_r3y = 100;
J_3xz = 120000;
G_3 = 40000000;
L_3y = 8;
M_r3x = 80;
J_3zy = 80000;
L_3x = 12;
F_2z = 20000;
m_2 = 15000;
F_1z = 180000;
F_3z = 20000;
M_B1zx = 200;
L_2z = 10;
M_B3zx = 300;
E_2 = 300000000;
A_2zx = 40000;
L_2x = 45;
J_2zx = 80000;
M_B3zx = 500;
I_2yz = 200000;
G_2 = 40000000;
L_2y = 10;
M_r1x = 300;
J_2zy = 20000;
M_r3x = 600;
% mapping
% output vector vs;
% vs = [2dots_1z, 2dots_1x, 2dottheta_1y,
% 2dottheta_1x, 2dots_3z, 2dots_3x,
% 2dottheta_3y, 2dottheta_3x,
% 2dots_2z, 2dots_2x,
% 2dottheta_2y, 2dottheta_2x,]
% for tail
% vs(2) = 2dots_1z, vs(4) = 2dots_1x,
% vs(6) = 2dottheta_1y, vs(8) = 2dottheta_1x,
% linear dims (zero order)
% vs(1) = s_1z,
% vs(3) = s_1x,
% angular vars (zero order)
% vs(5) = theta_1y,
% vs(7) = theta_1x,
% for cockpit
% vs(10) = 2dots_3z, vs(12) = 2dots_3x,
% vs(14) = 2dottheta_3y, vs(16) = 2dottheta_3x,
% linear dims (zero order)
% vs(9) = s_3z,
% vs(11) = s_3x,
% angular vars (zero order)
% vs(13) = theta_3y,
% vs(15) = theta_3x,
% for fuselage

```

b). MATLAB simulation code for the Structural model

IJRAR21D1084

International Journal of Research and Analytical Reviews (IJRAR) www.ijrar.org

```

ylabel('Structural Model Parameters');
legend('_2dotS_1_z', 'dodotS_1_z', '_2dotS_1_x', 'dodotS_1_x',
'_2dot\theta_1_y', 'dodot\theta_1_y', '_2dot\theta_1_x', 'dodot\theta_1_x',
'_2dotS_3_z', 'dodotS_3_z', '_2dotS_3_x', 'dodotS_3_x', '_2dot\theta_3_y',
'dodot\theta_3_y', '_2dot\theta_3_x', 'dodot\theta_3_x', '_2dotS_2_z',
'dodotS_2_z', '_2dotS_2_x', 'dodotS_2_x', '_2dot\theta_2_y',
'dodot\theta_2_y', '_2dot\theta_2_x', 'dodot\theta_2_x');
grid on;
hold off;

```

List of Figures

Figure 1: the use of the geometry of the problem.....	5
Figure 2: A tandem-rotor helicopter.....	7
Figure 3: Schematic of the interdisciplinary of the field of aeroelasticity.....	8
Figure 4: Effect of initial pitching perturbation on the aerodynamic stability of the tandem-rotor helicopter	23
Figure 5 : General schematic of the Tandem-rotor helicopter's control system model.....	34
Figure 6: Step response of the unaugmented open loop aerodynamic model of the tandem-rotor helicopter	35
Figure 7: Ramp response of the unaugmented open loop aerodynamic model of the tandem-rotor helicopter	36
Figure 8 : System augmentation for H-infinity controller of the tandem-rotor helicopter feedback control	36
Figure 9 : Chosen model design of the state space representation of the tandem-rotor helicopter closed loop feedback control system with dead band nonlinearity	37
Figure 10 : The behavior of the open loop aerodynamic model of the tandem-rotor helicopter under various initial conditions.....	44
Figure 11: The aeroelastic model of the first configuration of the tandem-rotor helicopter	46
Figure 12: Aeroelastic Effect Of The Downwash Drag.....	46

List of Tables

Table 1. ADVANCED TANDEM-ROTOR HELICOPTER CONFIGURATION PARAMETERS	785
Table 2. ADVANCED TANDEM-ROTOR HELICOPTER CONFIGURATION PARAMETERS	53
Table 3: BASELINE TANDEM-ROTOR RLH FUSELAGE DRAG TABLES, D/qd	788
Table 4: TABLE III. BASELINE TANDEM-ROTOR HLH FUSELAGE LIFT TABLES, L/qd	791
Table 5: BASELINE TANDEM-ROTOR HLH FUSELAGE SIDEFORCE TABLES, Y/qd 120,000-POUND GROSS WEIGHT	793
Table 6: BASELINE TANDEM-ROTOR HLH FUSELAGE PITCH MOMENT	795
Table 7: BASELINE TANDEM-ROTOR HLH FUSELAGE ROLL MOMENT TABLES, L / qd 120,000-POUND GROSS WEIGHT	797
Table 8: BASELINE TANDEM-ROTOR HMI FUSELAGE	798
Table 9: LATERAL-DIRECTIONAL AND LONGITUDINAL	799
Table 10: Configurations that were considered for the Simulation of the Tandem-rotor Helicopter	799

List of Symbols

A_{IC}	lateral cyclic pitch in body axis (rad)
A_{ICF}	lateral cyclic pitch control input in body axes - forward rotor
A_{ICR}	lateral cyclic pitch control input in body axes - aft rotor
a	blade airfoil lift curve slope
a_0	rotor coning angle
a_1	longitudinal first harmonic flapping coefficient
$a_{XCG}, a_{YCG}, a_{ZCG}$	acceleration of aircraft center of gravity in the three body axes
a_{YP}, a_{ZP}	lateral and vertical acceleration at the cockpit pilot station, respectively
B_{IC}	longitudinal cyclic pitch in body axis (rad)
B_{ICFR}, B_{ICRR}	longitudinal cyclic pitch in the shaft normal plane (S.N.P.) wind axes, forward and aft rotor respectively
B_{ITF}, B_{ITR}	longitudinal cyclic trim in the body axes, forward and aft rotor respectively
b_1	lateral first harmonic flapping coefficient
c_a	equivalent blade chord length for non-uniform downwash power correction (input for digital trim calculation)
C_{TS}	rotor thrust coefficient
c	blade chord length (ft)
D	fuselage aerodynamic drag force (lbs)
D_R	distance between forward and aft rotor hubs (ft)
d	separation distance between external load hooks on the aircraft (ft)
e	natural exponential base
e_β	blade flapping hinge offset (ft)
f_e	equivalent flat plate drag area (ft ²)
f_{eREF}	reference configuration equivalent flat plate area (ft ²)
G_{Bpo}	longitudinal control pickoff gain setting on the ground test simulator
G_h	altitude error feedback gain (in/ft)
\dot{G}_h	altitude rate feedback gain (in/ft/sec)
G_p	roll rate feedback gain (in/rad/sec)
G_q	pitch rate feedback gain (in/rad/sec)
G_r, G_R	yaw rate feedback gain (in/rad/sec)

G_{spo}	roll quickening gain setting on the simulator
G_x	longitudinal ground position error feedback gain (in/ft)
\dot{G}_x	longitudinal ground speed feedback gain (in/ft/sec)
G_y	lateral ground position error feedback gain (in/ft)
\dot{G}_y	lateral ground speed feedback gain (in/ft/ sec)
G_{YWO}	\dot{G}_y
G_θ	pitch attitude feedback gain (in/rad)
G_ϕ	roll attitude feedback gain (in/rad)
G_ψ	yaw attitude feedback gain (in/rad)
g	gravity constant, 32.2 (ft/sec ²)
H_F, H_R	longitudinal (in plane of rotation) rotor 1 ' forces, forward and aft rotor respectively
H_D	density altitude (ft)
h	fuselage midsection height (ft)
h_c	model's center of gravity vertical position for scaling wind tunnel test data relating to fuselage aerodynamic moments
h_e	altitude position error (ft)
h_{er}	average vertical distance from aircraft center of gravity to rotor hubs
h_F, h_R	vertical distance from aircraft center of gravity to forward and aft rotor hub, respectively
h_H	differential height between forward and aft rotor hubs
\dot{h}	altitude rate (ft/sec)
I_{xx}, I_{yy}, I_{zz}	aircraft moment of inertia about the roll, pitch, and yaw body axes, respectively (slug-ft ²)
I_{xz}	aircraft product of inertia (slug-ft ²)
I_β	blade flapping moment of inertia (slug-ft ²)
K_{LCP}	lateral cyclic stick pickoff gain factor
K_P	pilot control feedback gain
K_{SLV}	lateral ground speed gain setting on simulator
K_{XLD}	longitudinal ground position gain setting on simulator
K_{XLV}	longitudinal ground speed gain setting on simulator
K_{YLD}	lateral position gain setting on the simulator
K_{ZLD}	vertical displacement gain setting on the simulator
K_{ZLV}	vertical velocity gain setting on the simulator

$K_{\delta B}$	longitudinal DCP control gain factor
$K_{X\delta BP}$	differential collective pitch control gain setting on the simulator
K_{XBP}	longitudinal cyclic pitch control gain setting on the simulator
$K_{X\delta BICF}$	forward rotor gain setting for longitudinal BICF cyclic pitch control on the simulator
$K_{X\delta BICR}$	aft rotor gain setting for longitudinal cyclic pitch control on the simulator
$K_{\delta BIC}$	longitudinal cyclic pitch control gain factor
L	fuselage aerodynamic lift force
L_{AIC}	total roll acceleration per unit lateral rotor disc tilt angle $L_{AIC} + \dot{L}_{AIC} + L_{AIC}^{\ddot{}}$
$\dot{L}_{AIC}, L_{AIC}^{\ddot{}}$	thrust tilt and centrifugal force contribution to L_{AIC}
L_t	integral scale of turbulence wave (gust)
L_v, L_p, L_r	roll acceleration per unit lateral velocity, roll rate, and yaw rate, respectively
$L_{\delta S}, L_{\delta R}$	roll acceleration per inch of cockpit lateral stick and pedal controls, respectively
I	average horizontal distance from aircraft center of gravity to rotor hubs
I_c	model center of gravity horizontal position for sealing wind tunnel test data relating to fuselage aerodynamic moments
I_F, I_R	horizontal distance from aircraft center of gravity to the forward and aft rotor hubs, respectively
L	fuselage aerodynamic roll moment
M	fuselage aerodynamic pitch moment
M_u, M_v, M_q	pitch acceleration per unit longitudinal velocity, vertical velocity, and pitch rate, respectively
$M_{\delta B}, M_{\delta C}$	pitch acceleration per inch of cockpit control - longitudinal and vertical control velocity
m	total aircraft mass (slugs)
N	number of blades per rotor
N_v, N_p, N_r	yaw acceleration per unit lateral velocity, roll rate, and yaw rate, respectively
$N_{\delta S}, N_{\delta R}$	yaw acceleration per inch of cockpit lateral stick and pedal controls, respectively

$N_{\delta R}$	$N_{\delta r}$
N_{AIC}	yaw acceleration per unit lateral rotor disc tilt angle
p	aircraft body axes oriented roll rate (rad/sec)
q	aircraft body axes oriented pitch rate (rad/sec)
q_d	dynamic pressure (lb/ft ²)
R	rotor radius (ft)
R_{REF}	reference configuration rotor radius (ft)
R	aircraft body oriented yaw rate (rad/sec)
r_{rs}, r_{sp}, r_{dr}	characteristic roots of lateral-directional aircraft dynamics
r_w, r_q, r_{qu}	characteristic roots of longitudinal-vertical aircraft dynamics
s	complex (Laplace) variable
T	rotor thrust force (lb)
T_i	pilot model adjustable lag time constant (sec)
T_L	pilot model adjustable lead time constant (sec)
T_{L2}	lateral stick control pickoff washout time constant (sec)
T_{L3}	lateral stick control pickoff lag time constant (sec)
T_N	pilot model constant neuromuscular lag time (sec)
U	longitudinal aircraft velocity
U_o	steady (trim) longitudinal aircraft velocity
u_g, \bar{u}_g	longitudinal gust velocities, instantaneous and average, respectively
v	Airspeed
v_{as}	characteristic turbulence airspeed (for hover, V_{as} = average wind speed) (ft/sec)
V_T	blade tip speed(ft/sec)
v	lateral aircraft velocity (ft/sec)
v_g, \bar{v}_g	lateral gust velocities, instantaneous and average, respectively
W_G	aircraft gross weight (lb)
w	vertical aircraft velocity
w_o	steady (trim) aircraft velocity
w_g	vertical gust velocity
x	longitudinal aircraft displacement response signal
x_c	longitudinal displacement command signal
x_e	longitudinal hover position error due to turbulence

x_i	North-South aircraft position with respect to a fixed ground reference point
\dot{x}_I	longitudinal aircraft ground speed
x_{Ie}	longitudinal aircraft ground position error (ft)
x_{sc}	longitudinal scope position display driving variable
x_U, x_W, x_q	longitudinal acceleration per unit longitudinal and vertical velocity and pitch rate, respectively
$x_{\delta B}, x_{\delta c}$	longitudinal acceleration per inch of cockpit control, longitudinal and collective stick, respectively
x	aircraft body oriented longitudinal axis
\bar{x}	aircraft average longitudinal ground position error in turbulence
x_{LOAD}	longitudinal axis of external load
y	lateral aircraft displacement response signal
y_c	lateral displacement command signal
y_e	lateral hover position error due to turbulence (ft)
y_I	East-West aircraft position error with respect to a fixed ground reference point (ft)
y_{Ie}	lateral aircraft ground position error (ft)
\dot{y}_I	lateral aircraft ground speed (ft/sec)
y_{sc}	lateral scope position display driving variable
y_p	pilot model transfer function
y_v, y_p, y_r	lateral acceleration per unit lateral velocity, roll rate, and yaw rate, respectively
$y_{\delta S}, y_{\delta R}$	lateral acceleration per inch of lateral stick and pedal control, respectively
$y_{\delta r}$	$y_{\delta R}$
y	aircraft body oriented lateral axis
\bar{y}	aircraft average lateral ground position error in turbulence
y_{LOAD}	lateral external load body oriented axis
z_U, z_W, z_q	vertical acceleration per unit longitudinal and vertical velocity, and pitch rate, respectively
$z_{\delta B}, z_{\delta c}$	vertical acceleration per inch of longitudinal and collective stick control, respectively

$z_{\theta c}$	vertical aircraft acceleration per unit of blade collective pitch angle
z	aircraft body oriented vertical axis
z_{LOAD}	vertical external load body oriented axis
α	fuselage aerodynamic angle of attack
α_{CA}	angle of attack of rotor control axis
β	fuselage angle of sideslip
γ	Locke number = $\frac{1}{2} \rho c_a R^4 / I_{\beta}$
δ_3	blade pitch-flap coupling angle
δ_B	longitudinal stick control (inches)
δ_C	collective control, inches of equivalent stick
δ_{BIC}	longitudinal cyclic control due to pilot input
δ_r (or δ_R)	pedal control (inches)
δ_s	lateral stick control (inches)
θ	aircraft pitch attitude
θ_{AS}, θ_{AP}	total control signals at aft rotor swiveling and pivoting actuators, respectively
θ_{BF}, θ_{BR}	longitudinal blade pitch angles due to cockpit BR pit DCP input
θ_{CF}, θ_{CR}	collective blade pitch angles due to cockpit collective stick input
θ_e	aircraft pitch attitude error feedback
θ_{FS}, θ_{FP}	total control signals at forward rotor swiveling and pivoting actuators, respectively
θ_o	steady (trim) aircraft pitch attitude
θ_{OF}, θ_{OR}	blade root collective pitch angles at forward and aft rotors
θ_{RF}, θ_{RR}	directional blade cyclic pitch angles due to cockpit control inputs
θ_{SF}, θ_{SR}	blade lateral cyclic pitch angles due to lateral stick control, forward and aft rotor, respectively
θ_{TF}, θ_{TR}	root collective pitch angles at full down position of collective stick, forward and aft rotor, respectively
λ	instantaneous rotor inflow ratio
λ_o	steady (trim) rotor inflow ratio
$\lambda_{SL}, \dot{\lambda}_{SL}, \ddot{\lambda}_{SL}$	lateral cable angle, angular rate and acceleration, respectively
μ	rotor advance ratio
$\mu_{SL}, \dot{\mu}_{SL}, \ddot{\mu}_{SL}$	longitudinal cable angle, angular rate and acceleration, respectively

$v_{SL}, \dot{v}_{SL}, \ddot{v}_{SL}$	lateral differential cable angle, angular rate and acceleration, respectively
ρ	air density at HQ (slugs/ft ³)
ρ_o	sea level air density (slugs/ft ³)
σ	rotor solidity ratio
σ_g	turbulence intensity RMS (ft/sec)
σ_{ug}	longitudinal gust magnitude, RMS or standard deviation
σ_{vg}	lateral gust magnitude, RMS or standard deviation
σ_{wg}	vertical gust magnitude, RMS or standard
σ_x	deviation a aircraft longitudinal position error, RMS or standard deviation
σ_y	aircraft lateral position error, RMS or standard deviation
σ_β	blade mass moment about the flapping hinge
τ	inherent pilot model reaction time delay (sec)
τ_h	PHS altitude rate feedback time constant (sec)
τ_{QL}	pitch rate feedback lag time constant (sec)
τ_{QWO}	pitch rate feedback washout time constant (sec)
τ_P	roll rate feedback time constant in SAS (sec)
τ_R	yaw rate feedback time constant in SAS (sec)
τ_W	vertical aircraft response time constant (sec)
τ_x	PHS longitudinal velocity feedback time x constant (sec)
τ_{yWO}	PHS lateral velocity feedback time constant (sec)
$\tau_{\delta B}$	longitudinal DCP control shaping time constant (sec)
$\tau_{\delta BIC}$	longitudinal cyclic control shaping time constant (sec)
$\tau_{\Phi WO}$	roll attitude feedback time constant (wash-out) (sec)
Φ_{aYP}	power spectral density of lateral acceleration at the pilot station due to turbulence
Φ_{aZP}	power spectral density of vertical acceleration at the pilot station due to turbulence
Φ_g	general expression for power spectral density of turbulence
$\Phi_{ug}, \Phi_{vg}, \Phi_{wg}$	power spectral densities of longitudinal, lateral, and vertical gust
Φ_x, Φ_y	power spectral density of longitudinal and lateral aircraft position error due to turbulence
Φ	aircraft roll attitude

Φ_e	aircraft roll attitude feedback error
Ψ	aircraft yaw attitude
Ψ_e	aircraft yaw attitude error feedback
Ψ_{sc}	scope display driving variable for yaw position
Ω	rotor rotational frequency (rad/sec)
ω	angular frequency (rad/sec)
ω_g	characteristic turbulence frequency, $w_g = 1.5 V_{as}/L_t$
ω_{CUTOFF}	cutoff frequency for gust spectral integration (rad/sec)